A Thesis for the Degree of Ph.D. in Science

Increased functional connectivity in human sensorimotor cortex induced by brain-computer interface aided motor exercises

October 2019

Graduate School of Science and Technology

Keio University

Shohei Tsuchimoto

Table of Contents

List of Figures

List of Tables

Abbreviations

AAL	automated anatomical labeling
ANOVA	analysis of variance
BCI	brain-computer interface
BOLD	blood-oxygen-level dependent
CI	constraint-induced movement
CONSORT	consolidated standards of reporting trials
CSF	cerebrospinal fluid
ECG	electrocardiogram
ECoG	electrocorticogram
EEG	electroencephalogram
EMG	electromyogram
FFT	fast Fourier transform
fMRI	functional magnetic resonance imaging
FOV	field of view
FWE	family-wise error
FWHM	full width at half maximum
GABA	γ-aminobutyric acid
GLM	general linear model
Hb	hemoglobin
HRF	hemodynamic response function
LFP	local field potential
LTD	long-term depression
LTP	long-term potentiation
M1	motor cortex
MEG	magnetoencephalogram
MNI	Montreal Neurological Institute
MRI	magnetic resonance imaging
MUA	multi-unit activity
NMES	neuromuscular electrical stimulation
RCT	randomized controlled trial

rsfcMRI	resting-state functional connectivity measured with functional magnetic resonance imaging
S1	somatosensory cortex
SM1	sensory and motor cortices
SDF	spike-density function
SMR	sensorimotor rhythm
TE	echo time
TMS	transcranial magnetic stimulation
TR	repetition time
UMIN	university hospital medical information network

Chapter 1 : General introduction

1.1. Recording of sensorimotor function

In this section, the principle of physiology related to the following chapter is described. The basis of this dissertation concept in facilitating neural functional reorganization is the physiological rationale of real-time cortical activity sensing. The author therefore introduces, hereby, several milestones in human brain activity recording, performed in a non-invasive manner.

In the 1930s, a Neurology physician, Hans Berger, recorded cortical-activity derived electrical signals from the scalp, which is the dawn of non-invasive brain activity recording. Since Berger named the observed electrical signal as electroencephalogram (EEG), many studies have revealed the physiological implication of the EEG components. For instance, there are slow shifts in EEG, known as pre-motor potential in the motor cortex and supplementary motor area preceding voluntary movements. The pre-motor potential is a manifestation of cortical contribution to the motor planning of volitional movements (Santucci and Balconi 2009). More recently, the powers of alpha rhythm (8−13 Hz) and beta rhythm (12−30 Hz) recorded over the pericentral region were found to be modulated through motor tasks (Pfurtscheller 2006). EEG signals include mainly two features, namely location and frequency, derived from the activities of neuronal populations (Cohen 2017).

In the 1990s, Ogawa and colleagues (1990) developed an alternative of non-invasive methods to measure brain activity, namely functional magnetic resonance

imaging (fMRI). fMRI measures oxygenation changes in blood flow based on the fact that cerebral blood flow and neuronal activation are coupled. Since fMRI scanners involve strong magnetic fields, magnetic field gradients, and radio waves without exposing radiations, whole-brain activities including those of deep brain regions can be recorded, where EEG is inaccessible to sense of spatial resolution in fMRI is also high up to a millimeter scale. Although the temporal resolution of an fMRI signal is lower than EEG due to the hemodynamic delay (approximately several seconds). fMRI studies have helped us elucidate the brain dynamics associated with a given sensorimotor task. For instance, fMRI has identified activities in the motor and premotor cortices, both of which are associated with the activity in basal ganglia during a motor execution task (Lehéricy et al. 2006). Furthermore, fMRI activity patterns in the motor cortex itself are associated with finger motor execution patterns (Yokoi et al. 2018). Thus, fMRI studies have revealed the functional activities of brain regions including the deeper regions and their associations with cortical and subcortical activities.

In the 2000s, multivariate analysis combined with simultaneous EEG and fMRI recording was developed, which has resulted in some important findings indicating neural origins of a given sensorimotor related EEG component. For instance, the EEG power modulations of alpha rhythm and beta rhythm recorded over the sensorimotor cortex during a motor task were associated with activities in the sensory and motor cortices (Ritter et al. 2009). Furthermore, the changes in the alpha and beta powers during the motor task were negatively correlated with the fMRI signals in sensory and motor cortices (Yuan et al. 2010). Therefore, the development of the non-invasive multimodal

measurement of brain activities has brought us the foundational understanding about sensorimotor nervous system.

1.1.1. Electroencephalography

EEG measures the electrical activity of the neurons in the cortex over the scalp. EEG may represent the electrical activities of pyramidal neurons in layer IV and V of the neocortex and the interneurons, such as those that provide excitatory or inhibitory input to the pyramidal neurons in layer I of the neocortex, and the EEG signal is interpreted as neural ensembles that result from the activities of neuronal populations (10^7 neurons) activities (Kirschstein and Köhling 2009). Because the scalp EEG measures the electrical potentials of the neurons via the skull with low conductivity, the currents flowing from the cortex to the head surface results in a decrease in the power and the spatial resolution of EEG (Malmivuo and Suihko 2004). The power of scalp EEG is approximately 1/10 times, and its spatial resolution is approximately 1/6 times of the intracranial EEG or electrocorticogram (ECoG), in which an electrode sheet is placed directly on the exposed surface of the brain; the amplitude of EEG is 10s μV, and that of ECoG is 100 μV, and the spatial resolution of EEG is 30 mm, and that of ECoG is 5 mm (Buzsáki et al. 2012). Furthermore, EEG signals could often be contaminated with noise from nearby electrical devices, electromyographic signals from facial muscles, and electrooculogram by eye movements. As stated, EEG records activities from large numbers of neurons within the same region. EEG signals therefore often reflect neural rhythmic activities, with transient and synchronized neural activities evoked by impulse-like external stimulations or cyclic

and entrained spontaneous neural oscillations; the major frequency bands observed are historically and empirically determined as delta (0.1−4 Hz), theta (4−7 Hz), alpha (8−12 Hz), beta (12−30 Hz) and gamma (>30 Hz), and are observed in EEG captured during multimodal functions, such as cognitive or sensorimotor processing (Hari and Salmelin 2012). Furthermore, subdivided frequency bands or adjusted frequency bands, other than these frequency bands, are sometimes used for more advanced analyses (Babiloni et al. 2014).

Some known EEG features, such as alpha and beta rhythm, are associated with sensorimotor function, especially when recordings are performed over the sensorimotor cortex. These are called as mu rhythm or sensorimotor rhythm (SMR). Generally, alpha rhythm is generated by the thalamus, because of the intrinsic neural mechanisms of excitation and inhibition between thalamic relay nuclei and thalamic reticular nuclei (Lopes da Silva 1991). Furthermore, the thalamus nuclei forms a network with the cortical nuclei, known as the thalamocortical network, and alpha rhythm is typically recorded over the posterior region with high voltages during wakefulness (Figure 1-1) (Markand 1990; Hindriks and van Putten 2013; Ketz et al. 2015). Alpha rhythm was mostly observed during physical relaxation and relative mental inactivity with the individual's eyes closed, and its amplitude was attenuated in the eyes open state (Ben-Simon et al. 2013). Moreover, the alpha rhythm over the sensorimotor cortex is attenuated by proprioceptive sensory stimulation such as haptic or electrical stimulation (Babiloni et al. 2008). Since the thalamus is known to be part of the sensory pathway (Herrero et al. 2002), the alpha rhythm is correlated with sensory processing. In addition, the power modulation

of the alpha rhythm over the sensorimotor cortex is associated with the excitability of distinct inhibitory and excitatory interneuronal circuits within the motor cortex (Takemi et al. 2013), corticospinal excitability (Hummel et al. 2002), and spinal motoneuronal pool activities (Takemi et al. 2015). Furthermore, in a previous study with magnetoencephalography, the power of the alpha rhythm was attenuated with motor execution, which was located in the sensorimotor area (Pfurtscheller and Lopes da Silva 1999).

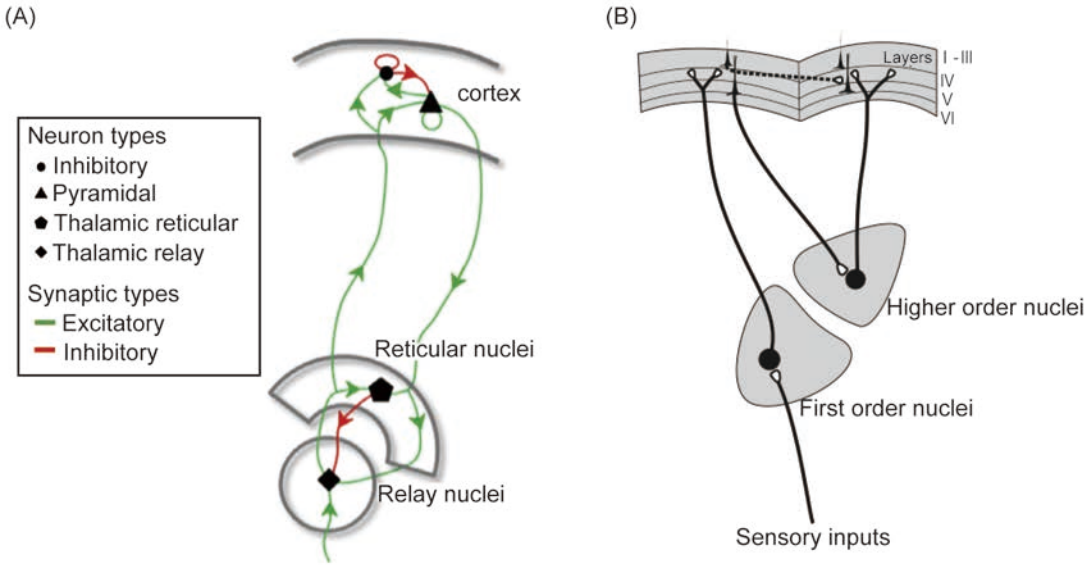

Figure 1-1. Thalamocortical circuits

(A) The excitatory and inhibitory architecture within a single thalamocortical loop that leads to intrinsic oscillations. (B) Thalamic nuclei connectivity with the cortex, where sensory information first influences first order nuclei, which then initiates the cascade of relays through higher order nuclei involving both cortical-cortical connections (represented by dashed lines projecting from superficial layers II and III), and thalamocortical connections (represented as continuous lines projecting from thalamus layer IV, and from the cortex via layers V and VI) (modified from Ketz et al. 2015).

Beta rhythm is more often found in frontal or central areas than in the posterior regions of the cortex. The most commonly known the beta rhythm is the basal ganglia oscillations, which are synchronous with oscillations in the cortical motor areas and are reflected in the scalp-recorded beta rhythm (Kozelka and Pedley 1990). Although the beta rhythm observed over the sensorimotor area quite often has a frequency of approximately 20 Hz, it should not be considered as sub-harmonic of this lower frequency oscillation (Vukelić et al. 2014). Voluntary movements are accompanied by amplitude changes in alpha and beta rhythms as a result of enhancement excitability in the sensorimotor areas (Ritter et al. 2009; Yuan et al. 2010; van Ede et al. 2011). Compared with the alpha rhythm, the beta rhythm fluctuation observed during a sensorimotor task has the much lower power and is localized more around the sensorimotor cortex (Crone et al. 1998). In a motor output task, their powers were attenuated, and the changes in the alpha rhythm were observed slightly posterior than that of the beta rhythm (Figure 1-2) (Pfurtscheller and Lopes da Silva 1999; Ritter et al. 2009). Furthermore, the power of the beta band, shortly following movement termination, increased in bilaterally sensorimotor cortices (Jurkiewicz et al. 2006; Parkes et al. 2006). Therefore, the beta rhythm is mainly interpreted to reflect the motor processing.

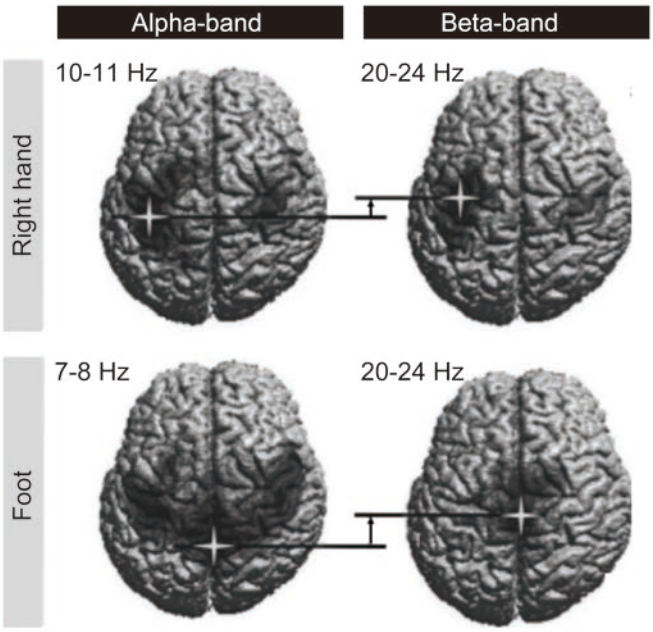

Figure 1-2. The power attenuation of the alpha- and beta-band oscillation maps
Compared to the resting-state, the power attenuation is observed in the sensorimotor region during voluntary right hand (upper panel) and voluntary foot movement (lower panel). The gray color over the cortex indicates the power attenuation and the region at which it reaches its peak is indicated with a white cross point. The peak of the alpha-band is posterior to that of the beta-band in each panel (modified from Pfurtscheller and Lopes da Silva, 1999).

EEG-SMR is mainly used to indicate the alpha and beta rhythm related to the sensorimotor event. EEG-SMR is recorded via an electrode set placed over the sensorimotor cortex or pericentral region. The commonly used electrode position standard is the international 10-20 system (Jurcak et al. 2007). First, the landmark location is set with the two lines across the top of the head between the nasion-inion and the left-right pre-auricular points. The each electrode set the location which is determined by the actual distances between 10% or 20% of the total front-back or right-left distance of the

skull (Figure 1-3). Generally, EEG-SMR during right-hand movement is acquired at C3 (left hemisphere) and that during left-hand movement is acquired at C4 (right hemisphere), since one side of limb movement is dominantly innervated by the other side of the cerebral hemispheres.

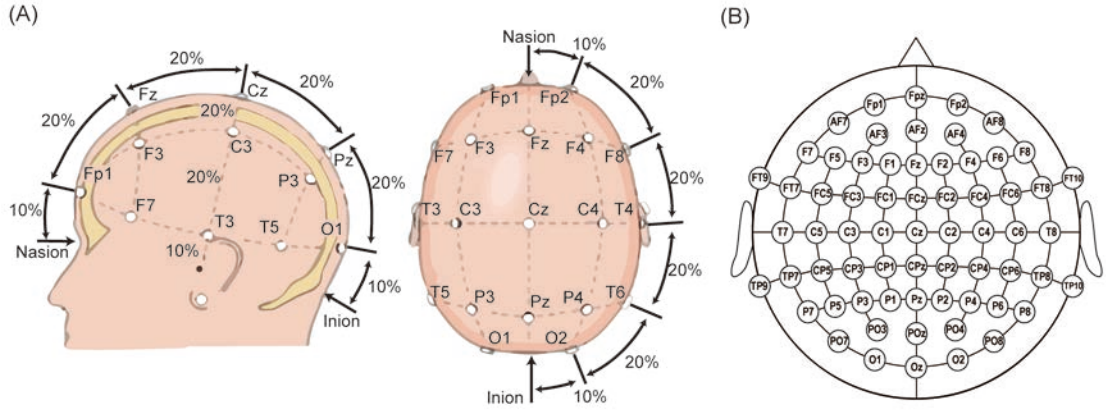

Figure 1-3. Electrode names and positions according to the international 10−20 and 10−10 systems

(A) The standard 19 electrode positions in the conventional 10−20 system and (B) 65 electrode positions in the modified 10−10 system are displayed. Capital letters “Fp”, “F”, “T”, “C”, “P”, and “O” correspond to the prefrontal, frontal, temporal, central, parietal, and occipital cortices, respectively. There are also anterior-frontal (AF), fronto-central/temporal (FC/FT), temporo-/centro-parietal (TP/CP), and posterior-occipital (PO) electrode positions. The small letter “z” refers to an electrode on the midline. Even numbers refer to the electrodes on the right hemisphere, and odd numbers refer to those on the left hemisphere. The electrode located at C3 or C4 indicates the hand region in the sensorimotor area. Generally, 16, 32 and 64 channel whole-brain EEG caps are used, which is the modified 10−20 or 10−10 systems (modified from Simkin et al. 2014).

Since the EEG signals include various components and noises due to its conductive character, some techniques involving spatial filters to detect EEG-SMR signals exist. For

example, the Laplacian montage method with an approximate spatial second derivative, measures the averaged signal between the adjacent four electrodes around a specific electrode to locally record the brain activity under the electrode. This Laplacian montage method is a spatial high-pass filter, which enhances the sensitivity the EEG electrodes as it records a small brain volume immediately below each electrode, thus eliminating the intermixing of brain currents (Hjorth 1991). Conversely, when the potentials of the same level are distributed over a wide space, the signal decreases even if the potential itself is high. Furthermore, in a clinical assessment for mu rhythm or the alpha-band EEG-SMR, the EEG signal is usually obtained using a bipolar filter, by using the electrode located at C3 as a reference to the other electrode that is >20 mm in the forward or backward direction (Kozelka and Pedley 1990). Another existing spatial filtering method involves the use of the average of whole-brain electrodes as a reference (Common Average Reference, or CAR). In a previous study, Mcfarland and colleagues (1997) examined the spatial filter in several candidates in order to obtain EEG-SMR data high sensitivity, and reported that the large-Laplacian montage or CAR spatial filter is effective (Figure 1-4).

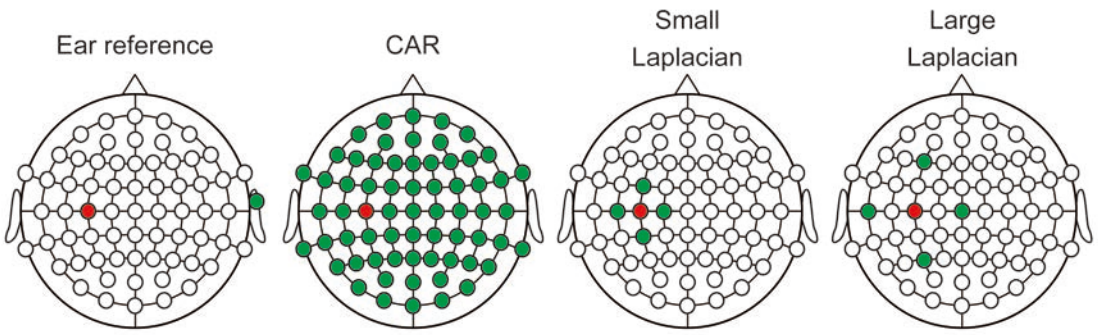

Figure 1-4. The electrode location for each spatial filter method
The EEG signals of the red electrode (which location is correspond to C3 position in 10−20 system) are subtracted from the averaged EEG signals among the green electrodes for extraction of locally EEG-SMR with spatial filters (modified from McFarland et al. 1997).

Recently, an increasing number of studies are focusing on intrinsic brain activities which are defined those recorded in a task-free or resting-state condition. For instance, repetitive transcranial magnetic stimulation (TMS) resulted in increased brain activity in the stimulation area during the sleep (Huber et al. 2007; Massimini et al. 2009). Furthermore, it has been reported that low-frequency components in EEG (< 4 Hz) increased locally in the motor cortex during sleeping, within 1-hour after a motor learning task (Figure 1-5). These studies suggest that intrinsic brain activity reflects the presence of a trace of sensorimotor task experiences. In the resting-state in post-stroke hemiplegic patients, synchrony of the alpha rhythm in the affected motor cortex was positively correlated with clinical motor scores (Dubovik et al. 2013). Therefore, intrinsic brain activity could be a potential peripheral biomarker to assess clinical scores or effectiveness of some interventions.

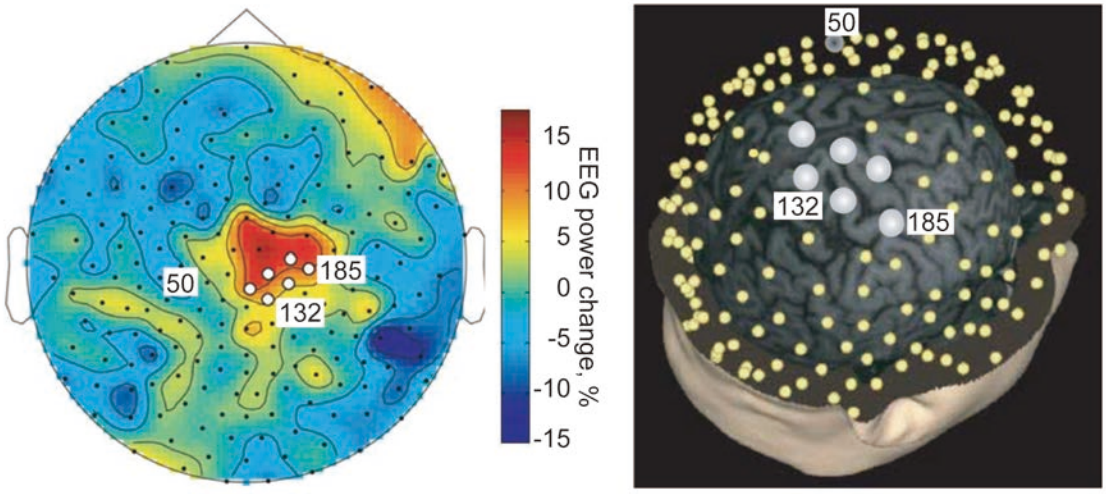

Figure 1-5. Topographic distribution of task-specific percentage change in EEG power spectrum density and the observed region

The color bar in the left panel indicates the task-specific EEG power spectrum density change, and each dot in both panels depicts an EEG electrode. The numbers in both the panels indicate the electrodes' number, and they correspond to each panel. The right panel depicts the anatomical localization of electrodes. The white dots indicate the cluster of six electrodes showing statistically increased brain activity after a novel motor task. These electrodes are located over the sensorimotor region (modified from Huber et al. 2004).

1.1.2. Blood-oxygen-level dependent imaging

Blood-oxygen-level dependent (BOLD) imaging reflects the differential deoxyhemoglobin (deoxy-Hb) content of the blood at different levels of neural activity (Hirsch et al. 2012). Because Hb changes its magnetic susceptibility depending on the bonding state with oxygen, the homogeneity of the magnetic field decreases and the T2* relaxation time shortens in the blood vessel containing deoxy-Hb and the surrounding tissue; the T2* signal around the capillaries is low (Figure 1-6). First, local and regional neural activity in the brain results in increased oxygen consumption, and thus an increase in deoxy-Hb. Local blood flow in the surrounding the capillaries is increased to supply

oxygen to the active neurons. The blood flow increases to between 30 and 50%, which is much higher than the actual increase in oxygen consumption (approximately 5%) (Fox and Raichle 2007). As a result, the blood flow and its velocity in the capillaries increase, and deoxy-Hb is rapidly perfused. Thereafter, the amount of deoxy-Hb per unit volume (namely voxels) of the capillaries surrounding the neuron decreases. As deoxy-Hb levels decrease, the homogeneity of the magnetic field within the voxel increases causing an extended T2* relaxation time and thus resulting in an increased T2* signal. The signal does not simultaneously increase with nerve activity, but appears after 1 to 2 s following neural activity and blood flow increase, and peaks at 5 to 6 s, and returns to baseline levels after approximately 20 s (Glover 1999). The BOLD signal dynamics observed here is known as a hemodynamic response function (HRF) (Figure 1-7). Some studies reported that the HRF varies between or within participants and there are some factors, which induce the differences, such as differences in task strategies or environmental noises (Handwerker et al. 2004; Badillo et al. 2013). Although the exact mechanisms underlying the HRF remain to be debatable yet, however, the averaged HRF empirically explain the relationship between event-related neural activity and brain regional BOLD signal that is reasonable in neurophysiological validity, resulting in a canonical HRF model is commonly employed (Lindquist and Wager 2007; Chang et al. 2009; Wu and Marinazzo 2016).Because of this temporal filter, fast modulation of neural activity unlikely reflects in the vascular response (Boynton et al. 1996).

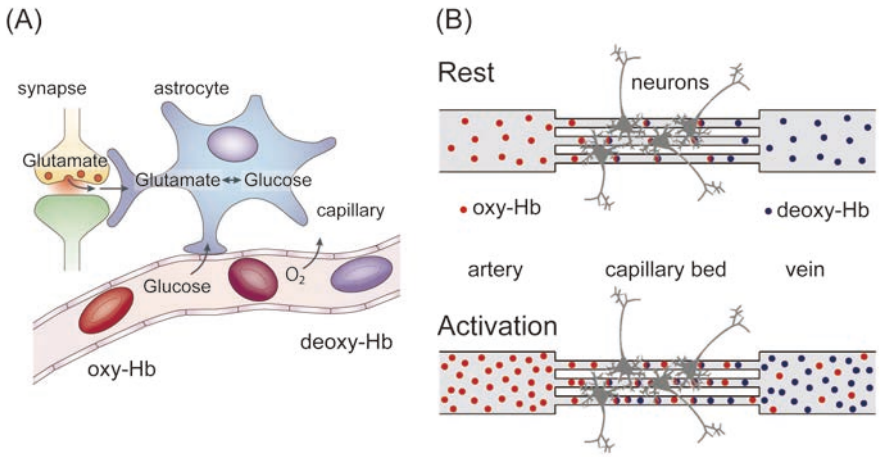

Figure 1-6. Vasculature in the brain and the BOLD effect

(A) The proposed fundamental relationship between synaptic activity, neurotransmitter recycling and metabolic demand is displayed. Neuronal activity increases the oxygen consumption following synaptic metabolic activation. (B) Compared with a resting (or no-stimulation baseline) condition and neuronal activation results in increased oxygen consumption, and thus the conversion of oxyhemoglobin (red dots) to deoxyhemoglobin (blue dots). Although the neuronal activation increased deoxy-Hb, it follows that the cerebral blood flow is increased, resulting in the apparent amount of deoxy-Hb is decreased. The series of processing that neuronal activities give rise to via hemodynamic changes is known as neurovascular coupling, and is a basis of functional neuroimaging of BOLD signal measurement using fMRI. (modified from Dogil et al. 2002; Heeger and Ress 2002).

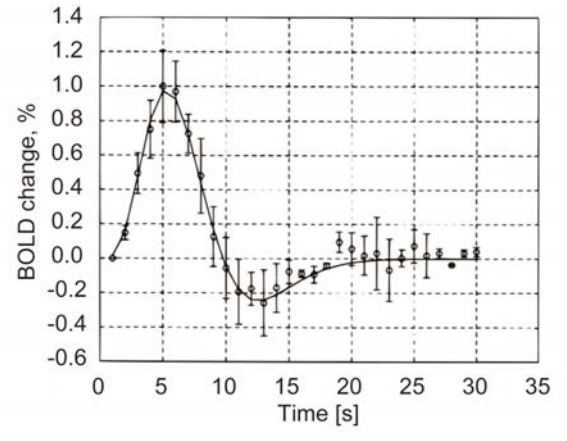

Figure 1-7. Hemodynamic response function

Averaged activation response measured in the motor cortex for five participants during a stimulation task. Open circles represent the mean values, and the error bars indicated the standard deviation among the five participants (modified from Glover, 1999).

Although fMRI measurements have a second-scale resolution in time due to the delayed response of the BOLD signal, its spatial resolution is highest higher in the millimeter-scale, than that of other non-invasive brain activity recordings. Furthermore, fMRI measures BOLD activities in the whole brain including in deep subcortical regions, such as thalamus or basal ganglia. Thus, this advantage of fMRI has increased our understanding of functional activities in the human brain. For instance, a study showed that activity in the basal ganglia is associated with the activities in the motor and premotor cortices during a motor execution task (Lehéricy et al. 2006). In post-stroke patients, neural activities during the movement of the affected hand increase in both hemispheres, especially within the motor cortex of the contralesional hemisphere (Volz et al. 2015) (Figure 1-8). The subsequent return of the activation pattern similar to that recorded in

healthy participants correlated with recovery and gain in hand motor function (Rehme et al. 2011).

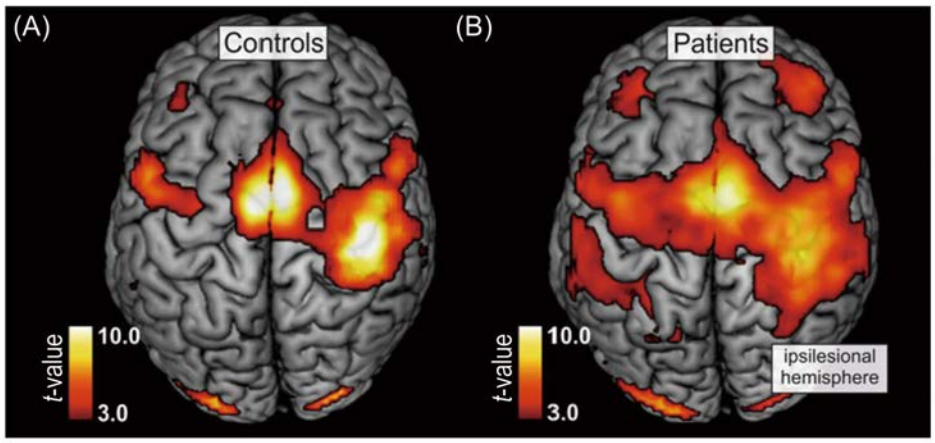

Figure 1-8. Brain activity during movements of the corresponding hand in healthy participants and the affected hand in post-stroke hemiplegic patients

(A) In healthy participants, the motor cortex of the contralateral hemisphere and the supplementary motor area are activated during hand movement. (B) In post-stroke hemiplegic patients, movements of the affected hand are associated with a significant BOLD signal in both hemispheres, especially the motor cortex of the contralesional hemisphere, resulting in fMRI over-activity (right panel). The color bar indicates the *t*-value (modified from Volz et al. 2015).

Functional MRI studies have often examined BOLD responses to external stimulation (i.e. peripheral nerve electrical stimulation), or, to voluntary execution in a given task. In such task-oriented studies, task-uncorrelated spontaneous or intrinsic brain activities were treated as random noise to be eliminated from the average. The brain regions that show statistically significant BOLD dynamics from baseline fluctuation are therefore annotated as 'activated' in an ordinary fMRI analysis.

Inter-regional correlates of activity have proven to be more challenging in the assessment of integration or interaction of neural functions in spatially distinct areas. Because of the increase in computational power in a laboratory-scale equipment, many studies have used multivariate analysis to evaluate interaction in fMRI data, by extracting the functional sub-modules in the brain network. The interaction among brain regions is used to calculate functional connectivity, which is usually inferred from correlations among neuronal activity measurements. Functional connectivity is defined as statistical dependencies among spatially different neural activities, and involve correlation coefficients (Uehara et al. 2013), coherence (Sun et al. 2004), or phase-lock values (Rodriguez et al. 1999; Honey et al. 2007). Although functional connectivity seems to be just statistical correlations, the number of fMRI studies to interpret the neurophysiological meanings of functional connectivity is increasing. Functional connectivity among brain regions is thought to be responsible for the similar functions performed by different brain regions (Fox et al. 2005). For example, bilateral motor cortices are activated during the bimanual finger execution task compared with the resting-state, and these regional activities in the resting-state are strongly correlated with each other (Biswal et al. 1995) (Figure 1-9). In post-stroke patients, functional connectivity between contralesional and ipsilesional sensorimotor cortices in the resting-state is correlated with the motor recovery (Park et al. 2011). Furthermore, longitudinal functional connectivity changes in ipsilesional sensory and motor cortices are associated with motor recovery, and it was observed that the increased functional connectivity occurred in concurrence with a significant improvement in motor function (van Meer et

al. 2010). Thus, functional connectivity in the resting-state can be used to assess the intrinsic brain activity.

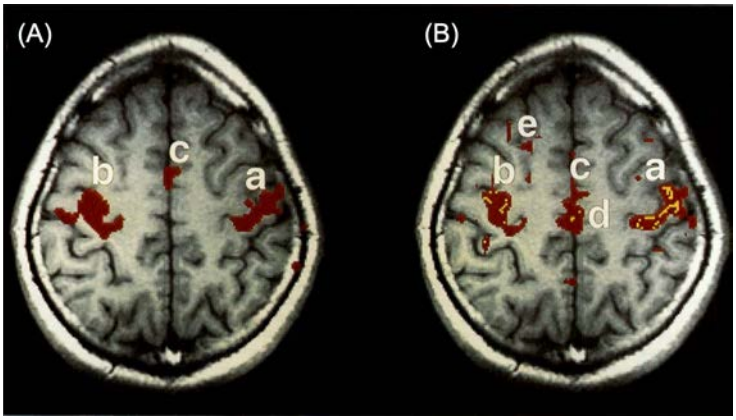

Figure 1-9. Comparison of the task-activated region and correlation of spontaneous activity

(A) The brain regions of "a", "b" and "c" activated during the bilateral left and right finger movement. The region "a" is set as the seed-region for analyzing the resting-state functional connectivity. (B) The fMRI signal is averaged over the seed-region, and the brain region is identified to be correlated with the seed-regional time-course in the resting-state. The red area indicates a positive correlation, and yellow indicates a negative correlation with the seed-regional activity. While coactivation of the regions "e" and "d" and the seed-region is specific to the resting-state, the regions of "b" and "c" are the same regions that are activated during in a motor execution task (modified from Biswal et al. 1995).

1.1.3. Bimodal measurement of brain activity

Simultaneous measurement of a hemodynamic signal and an electrophysiological signal has been performed in mice, cats, and non-human primates to identify the neural correlates of fMRI signals (Logothetis et al. 2001; Viswanathan and Freeman 2007). A previous study showed that the BOLD signal change in fMRI is correlated with local field

potential (LFP) that reflects the synchronous activity of neurons in a larger area (approximately 2 × 2 mm) rather than multi-unit activity reflecting the firing frequency of individual neurons in a narrow area (approximately 0.2 × 0.2 mm) (Figure 1-10). Therefore, it is considered that the BOLD signal reflects not only the action potential of the pyramidal cell itself but also that of its neuronal processes, such as the activities in the functional column or interneurons, as reflected by LFP, ECoG and EEG signals (Logothetis and Wandell 2004).

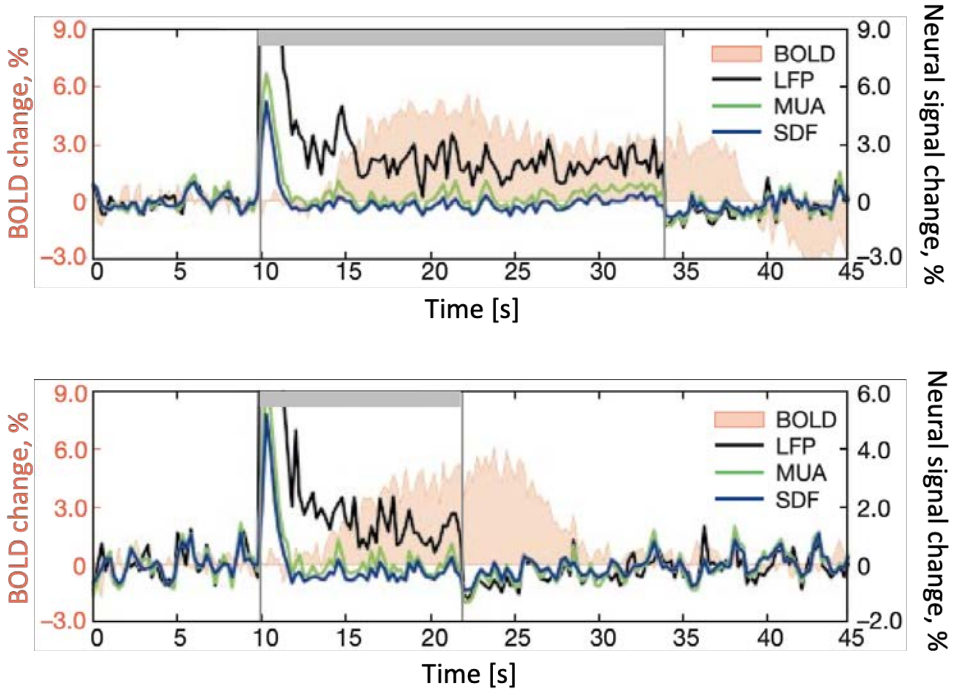

Figure 1-10. Simultaneous measurements of hemodynamic signals and multi-electrical neural signals

The local field potential (LFP, black line) is comparatively associated with a BOLD signal (red area), rather than multi-unit activity (MUA, green line) and spike-density function (SDF, blue line). Both single- and multi-unit responses adapt a few seconds after stimulus onset, with LFP remaining the only signal that is correlated with the BOLD response. The LFP signal reflects the integration of electric current flowing from multiple neurons

within a couple of millimeters, while MUA and SDF signals are associated with the summation of the extracellular spike potentials in a few hundred micrometers. The gray bar indicates the stimulation period and the different durations, 24 s (upper) and 12 s (lower) are shown (modified from Logothetis et al. 2001).

Thereafter, EEG-fMRI simultaneous recording was performed in the 2000s to characterize the EEG components using fMRI (Allen et al. 1998, 2000; Goldman et al. 2000). However, the quality of the EEG data obtained using an fMRI scanner is compromised by artifacts caused by interaction between EEG electrode assemblies and the fMRI scanner's magnetic fields (Allen et al. 1998). The three most significant causes of EEG artifacts in the scanner are (1) gross movements in the magnetic field, for example, the motion artifacts of EEG electrodes' cables due to the participant's movement in the magnetic field; (2) ballistocardiogram and blood flow effects in the statistic magnetic field associated with the participant's pulse; and (3) gradient artifacts and radio frequency pulse artifacts during fMRI image acquisition (Ritter and Villringer 2006). To maintain the image quality along with high signal-to-noise ratio, the EEG electrode cables should be placed out of the radio frequency coil as close as possible, along the side, but as far as possible from both the cap and fMRI coil (Baumann and Noll 1999). Ballistocardiogram pules obscure in EEG activity at alpha-band frequency and lower frequencies, with amplitudes often greater than 150 μV at a 1.5 T field strength, which are much larger than the alpha waves seen in most participants (at most 50 μV) (Bonmassar et al. 2002). Previous studies have reported a suppression in the ballistocardiogram artifacts following major developments in template-subtraction (Allen et al. 2000; Goldman et al. 2000),

principal component analysis based methods (Niazy et al. 2005) and independent component analysis based methods (Srivastava et al. 2005). In these methods, the ballistocardiogram itself using a twisted single-lead electrode placed on the participant's back at the heart region. Based on the peaks detected in the ballistocardiogram, the EEG signal is segmented to epochs and averaged over these epochs per channel. Then, the averaged EEG signals are subtracted from the raw EEG to yield a ballistocardiogram-free EEG. A similar processing method is applied for removing the gradient artifacts and radio frequency pulse artifacts during fMRI acquisition of the EEG signal. Trigger signals from the fMRI scanner to the EEG amplifier are obtained at every fMRI repetition pulse timing as time-locking events. EEG signals are segmented to epochs based on trigger events, and the template of fMRI artifacts on EEG signals is obtained by averaging each epoch. The changes in the magnetic fields across EEG electrode cables due to the participant's movement during fMRI scanning, can usually be avoided by using adaptive temporal templates with a moving average several epochs for both fMRI and ballistocardiogram artifacts (Allen et al. 2000). The averaged EEG signals are subtracted from the raw EEG signals. Generally, the fMRI scanning artifacts in EEG signals are eliminated prior to removal of the ballistocardiogram artifacts.

After overcoming the technical barriers of recording, the combination of EEG and fMRI recording has successfully helped identify brain regions that are significantly associated with a given EEG component. For instance, EEG power modulations of the alpha- and beta-band recorded over the sensorimotor cortex, namely EEG-SMR, are correlated with fMRI signals in the sensorimotor cortex during hand movement (Ritter et

al. 2009). Furthermore, the regions of EEG-SMR power changes are co-localized with the regions of fMRI signal changes, in the tasks performed involving specific body parts (Yuan et al. 2010) (Figure 1-11). These studies show that the EEG-SMR power changes observed during the motor task reflect the activity in the sensorimotor cortex. Moreover, EEG-fMRI simultaneous recording studies in the resting-state show that the intrinsic power modulation of the alpha-band is correlated with thalamic activity (Goldman et al. 2002; Liu et al. 2012; Omata et al. 2013).

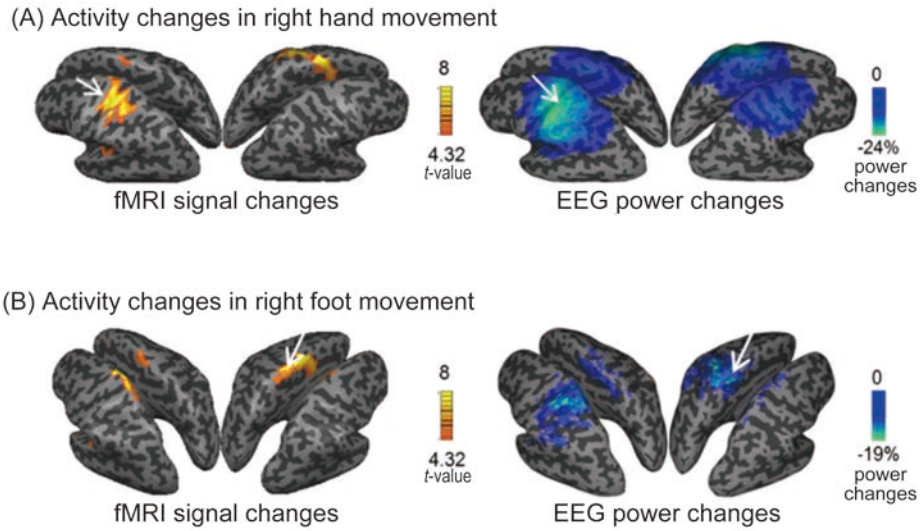

Figure 1-11. Co-localization of fMRI signal changes and EEG power changes in the brain regions during motor execution tasks

(A) Hand movement increases the fMRI signal and EEG power attenuation in the sensorimotor cortex. (B) Foot movement increases fMRI and EEG signal changes in the medial parts of the sensorimotor cortex. The white arrows indicate the peak region of the fMRI signal or EEG power change. fMRI measurements reveal more spatially localized activity than do EEG measurement, although the peak coordination of the EEG result is compatible with that of fMRI result. (modified from Yuan et al. 2010).

1.2. Physical exercises for motor recovery from post-stroke hemiplegic patients

World Health Organization reported that approximately 15 million people experience a stroke every year worldwide. The most frequent type of disability associated with stroke is paralysis of the upper limb, which is found in approximately 80% of stroke survivors with disability (Langhorne et al. 2009). There is a long history of learned compensatory movement with remaining unaffected body parts being the major choice for rehabilitation of persons with physically disabilities in daily life, since the inconveniences associated with the affected limb increases effort and possible frustration during attempted movement (Taub et al. 2006).

However, in the 1980s and 1990s, some clinical studies reported that the forced use of the affected upper limb after immobilization of the unaffected limb resulted in clinically notable improvement in the motor control of the affected upper limb (Ostendorf and Wolf 1981; Taub et al. 1999). Focusing on the possibility of motor recovery in the affected upper limb for post-stroke hemiplegic patients, these studies led to the establishment of constraint-induced movement (CI) therapy (Kwakkel et al. 2015). It has also been reported that, under the non-constraint condition, functional activity of the paralyzed limb that is rarely used regularly is decreased owing to conditioning due to frequent physical exercise (Fritz et al. 2012).

In order to increase the rate of physical exercise and reduce the burden of therapist-assisted training, a growing number of studies have investigated robot-aided motor exercises (Chang and Kim 2013). These studies have revealed that physical exercises for

motor recovery induce neural reorganization in post-stroke hemiplegic patients (Chen et al. 2002).

Currently, artificially activation of human muscles or muscle nerves by neuromuscular electrical stimulation (NMES) is widely used in clinical rehabilitation for post-stroke hemiplegic patients (Langhorne et al. 2009). NMES is a therapeutic interventions that has been developed to attempt to induce the motor recovery because sensory input enhances corticomotoneuronal excitability, which often affects upper motor neurons and/or their neuronal pathways to lower motor neurons (Kaelin-Lang et al. 2002; Takeda et al. 2017).

In addition to modulating the neural excitability of the affected upper limb by passive stimulation, a mental practice training called motor imagery therapy is widely used as a clinical therapeutic intervention (Braun et al. 2006). Motor imagery therapy for motor recovery consists of rehearsed or simulated volitional movement of the affected limb. The kinesthetic imagery of movement activates the same brain areas that are activated during actual movement (Munzert et al. 2009).

Consequently, neurofeedback interventions, such as the brain-computer interface (BCI) that has the potential to induce directly the modulation of neural excitability with biomarkers reflecting cortical sensorimotor activity, have been developed for motor recovery in case of post-stroke hemiplegic patients (Wolpaw et al. 2002). Most BCI studies for post-stroke hemiplegic patients have combined motor imagery and robot-aided motor exercises by using NMES and/or some visual feedback in a closed loop manner (Cervera et al. 2018). In other words, BCI is consistent with a closed-loop strategy as

cortical sensorimotor activity triggers sensorimotor feedbacks and the BCI helps persons with post-stroke hemiplegic patients recognize how to modulate their own brain activity via feedback (Sitaram et al. 2017). Recent research has focused on the clinical efficacy of BCI as a neurorehabilitation tool for post-stroke hemiplegic patients. Further research is required to understand the neural mechanisms underlying neurofeedback intervention (Clausen et al. 2017).

The following section provides a detailed description of each rehabilitative intervention, aiding the understanding of the neurological rationales for BCI aided motor exercise, as BCI systematically includes all these elements.

1.2.1. Constraint-induced movement therapy

The inconvenience faced by post-stroke hemiplegic patients in using the affected limb increases effort and possible frustration; furthermore, the patients gradually hesitate to use the affected limb, resulting in the suppression of behavior (Uswatte and Taub 2005). In other words, unsuccessful motor attempts of the affected limb are recognized as a type of punishment such as failure or incoordination, leading to less movement or learned non-use of the affected limb (Taub et al. 2006). CI therapy or the forced use of the affected upper limb, which prevents or overcomes such learned non-use of the affected limb, is a therapeutic approach to reshape physical movement by restraining the unaffected upper limb and employing intensive practice with the affected upper limb (Taub et al. 1999). Generally, CI therapy is designed with the gradually increasing difficulty, which progressively includes complex action patterns for the affected upper limb to avoid the

unsuccessful motor attempts and to enhance positive experiences in using the affected limb (Figure 1-12). The neurophysiological evidence for CI therapy has been reported in mapping studies with TMS, suggesting that CI therapy increases the size of the cortical motor output area of the affected hand muscle, which indicates cortical reorganization (Liepert et al. 1998, 2000). Thereafter, many clinical studies have confirmed its efficacy and safety in practice (Kwakkel et al. 2015). More recently, Phase III clinical trials with randomized controlled designs were conducted, and these trials reported that CI therapy showed significant improvement in functionality of the affected upper limb, an increase in the frequency of use in daily life, and therapeutic effects lasting 1 year after treatment, compared to control intervention (Page et al. 2005; Brogårdh and Sjölund 2006; Wu et al. 2007). According to the 2015 Japanese guidelines for the management of stroke, CI therapy is now rated as a Class A grade therapy for patients with mild paralysis.

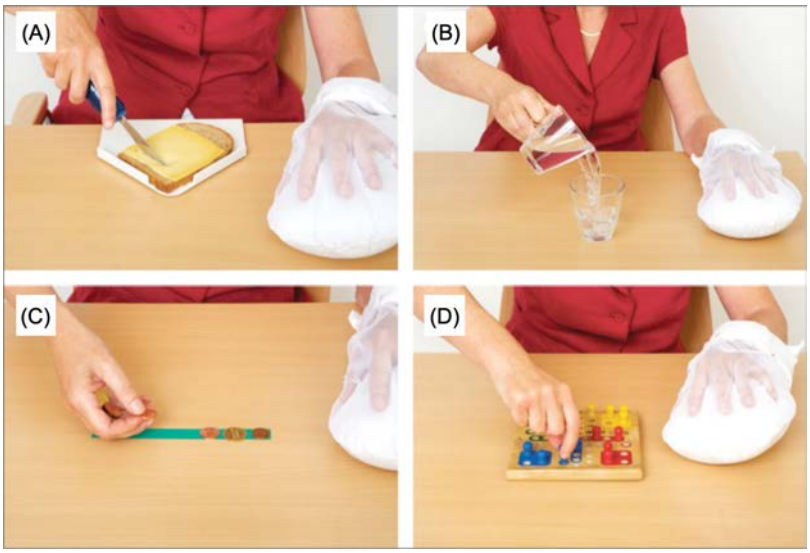

Figure 1-12. CI therapy designed with gradually increasing difficulty tasks for the affected upper limb

CI therapy comprises typical tasks used in daily life including (A) cutting bread, (B) pouring water, (C) picking up and replacing money, and (D) playing a game. The difficulties in these movements are associated with coordinated movement between different elements such as the shoulder and hand and with precision in movement such as that in pinching of a finger. CI therapy restricts the use of the unaffected limb by using a padded mitt (modified from Kwakkel et al. 2015).

1.2.2. Robot-aided intervention

Post-stroke hemiplegic patients require continuous medical care and intensive physical exercise along with frequent one-on-one in-person interaction with a physical therapist. To reduce the burden of the intensive physical exercise currently restricted to the therapist, a technological approach has helped in the rehabilitation field. Robot therapy enables precise repetition training of the same operation and patients perform the much motor exercise provided robot-aided intervention (Kwakkel et al. 2008). It is then possible for a therapist to deal with instances that require more significant intervention,

while providing a sufficient amount of training to the patient. For example, BiManuTrack (Hesse 2004) or Rutgers Master II (Bouzit et al. 2002) interacts with the user only at the hand or finger level (Figure 1-13(A, B)). These robots could offer flexible solutions as alternative assistance for post-stroke patients in repetitive simple physical exercises. Furthermore, rehabilitation robotics were initially developed for motor training, and the use of this method in diagnostics has also been drawing attention. Inmotion 2 and KINARM are devices with visual feedback that move a robot arm with the paralyzed hand fixed at the point indicated on the screen (Figure 1-13(C, D)) (Krebs et al. 2004; Chang and Kim 2013; Little et al. 2015). These robotic devices can be used as assessment devices for upper limb sensorimotor function because these devices can record various types of kinetic and kinematic variables, such as the trajectory of upper limb, time required for movement, and peak torques around the limb joints (Scott 1999). Furthermore, these robotic devices, which set the load force as assistive or resistant for upper limb movements, provide a more advanced solution for physical exercise. For instance, robotic devices assist the affected limb movement by reducing effort and frustration, and the assistive force gradually decreases as affected limb movement improves (Casadio et al. 2009). On the other hand, robotic devices can proved resistance against the affected limb movement owing to accumulating evidence that higher effort by the impaired limb can help improve motor function (Morris et al. 2004). Robot-aided therapy has shown the potential to effect motor recovery for post-stroke hemiplegic patients, and it plays a crucial role in clinical rehabilitation. However, robot-aided intervention mainly applies to patients with mild-to-moderate hemiplegia on the premise

of voluntary motor execution of the affected upper limb, and such intervention is underutilized for patients with severe hemiplegia, as the robots cannot provide assistance or resistance to the affected upper limb unless there is voluntary motor output. On application to patients with severe hemiplegia, the robot-aided intervention only results in passive movement and thus fewer benefits of robot-aided motor exercise.

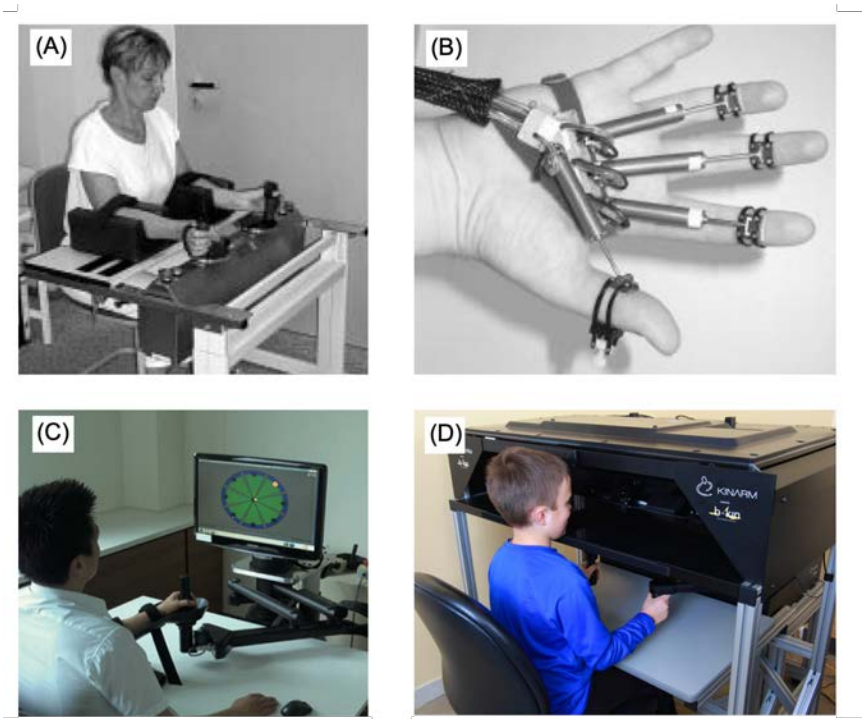

Figure 1-13. Robotic devices in upper-limb motor rehabilitation

(A) BiManuTrack is a proven assistive device for highly paretic patients for repetitive training of the wrist and forearm, i.e., flexion/extension of wrist (modified from Hesse, 2004); (B) Rutgers Master II is designed for dextrous interactions in virtual environments, and this glove provides force feedback (modified from Bouzit et al. 2002); (C) Inmotion 2 has two translational degrees of freedom in the upper limb, and it provides continuous stall torque. The position of the forearm is calculated continuously, providing visual feedback (modified from Chang and Kim, 2013); (D) KINARM also provides visual and torque feedback to the participant with a bimanual motor learning environment for coordinated movement of the upper limbs (modified from Little et al. 2015).

1.2.3. Neuromuscular electrical stimulation

NMES is a technique that is widely used for the treatment of central nervous disorders, such as stroke and spinal cord injury to restore sensorimotor function because NMES elicits sensory and motor nerve activity, resulting in enhanced excitability of the sensorimotor cortex (Sheffler and Chae 2007; IJzerman et al. 2009; Maffiuletti et al. 2013). Alteration of the afferent input by NMES has been shown to lead to reorganization of the sensory cortex (Sanes et al. 1992; Ridding and Taylor 2001; Page et al. 2010). Paired-associative stimulations, such as an electrical pulse stimulation of NMES to the affected upper limb and a single pulse stimulation with TMS to the motor, have also been reported to induce neural plasticity in the sensorimotor cortex (Stefan et al. 2000). In addition, NMES stimulates afferent sensory nerve fibers as well as efferent motor nerve fibers and the pulse intensity of NMES is set high enough to activate efferent nerve fibers, consequently eliciting muscle contractions (Maffiuletti 2010). The sensorimotor coupling between sensory nerve activation by NMES and the increased proprioceptive signals from the evoked movements increases sensorimotor excitability, thus leading to improved function (Kottink et al. 2007; Chae et al. 2009; Malhotra et al. 2013). NMES administered during voluntary motor execution or electromyographic (EMG)-triggered NMES lead to a synchronized presynaptic and postsynaptic coupling activities, facilitating synaptic remodeling (Cauraugh et al. 2000; Rushton 2003). Notably, this could also be applied to mild motor impairment because some voluntary movement is needed to initiate and continue the exercise.

1.2.4. Motor imagery therapy

A mental practice in the form of movement imagination, called motor imagery, has been hypothesized to activate the sensorimotor circuit similar to actual motor execution (Sharma et al. 2006). Previous studies with positron emission tomography or fMRI have revealed that motor imagery consistently enhanced the disclosed activity in cortical and subcortical motor areas, which substantially overlap the neural substrates for motor execution (Malouin et al. 2003; Hanakawa et al. 2008). Because it improves motor function without a physical load for patients with severe hemiplegia, motor imagery therapy is considered an effective therapeutic tool for post-stroke hemiplegic patients. Furthermore, motor imagery therapy can be deployed in combination with other treatments. A meta-analysis study on motor imagery therapy aimed at the recovery of affected upper limb motor function in post-stroke patients reported that motor imagery therapy is provided in addition to other therapies, such as conventional therapy comprising occupational and physical therapy, CI therapy, robot-aided therapy, or NMES, and that motor imagery therapy is an effective complementary therapy (Park et al. 2018). However, motor imagery is an internal mental process with a consequent lack of visual or proprioceptive feedback; thus, task compliance with sufficient activation of the sensorimotor neural pathways may vary among trials and even for a single participant (Braun et al. 2013). Such limitations may reduce the clinical efficacy and reliability of this therapy.

1.2.5. Sensorimotor exercise aided by brain-computer interface

Since motor imagery therapy induces somatotopic reorganization of cortical activation patterns in the sensorimotor area, an effective strategy for ensuring the quality of motor imagery has been proposed; this advanced strategy requires that patients learn how to control motor imagery enough to enhance sensorimotor cortical activity via visual and/or somatosensory feedback, which is reflected by monitored brain activity (Figure 1-14) (Daly and Wolpaw 2008; Chaudhary et al. 2016). Such biofeedback intervention, especially using neural activity, is called neurofeedback intervention, involving BCI. This BCI allows participants to reach motor imagery compliance through feedback reflecting computed brain activity, thus forming a closed-loop strategy (Hochberg et al. 2012; Sitaram et al. 2017; Cervera et al. 2018). Motor imagery therapy combined with BCI intervention can support motor rehabilitation; consequently, the use of BCI rehabilitation has been increasing (Wolpaw et al. 2002; Ono et al. 2014a; Ang et al. 2015; Soekadar et al. 2015). Most studies employing BCI to aid motor imagery for post-stroke patients have used EEG-SMR as a biomarker reflecting activity in the sensorimotor cortex (Zhang et al. 2015). Although EEG recording is limited in terms of the discriminable motor output pattern and accuracy, it is easier to use EEG to record brain activity than to use fMRI or ECoG, which enables continuous day-by-day training (Teo and Chew 2014; Young et al. 2015, 2017; Bundy et al. 2017). Buch and colleagues (2008) reported that long-term BCI aided motor exercise, which is EEG-SMR activity contingent robot-aided motor output for the affected hand, for stroke patients induced a reorganization of brain activity pattern. Furthermore, some studies have described BCI-triggered NMES of the affected finger

muscle (Daly et al. 2009; Mukaino et al. 2014). The combination of BCI and other physiotherapies (such as robot-aided therapy and NMES) have been reported to induce improvement of affected upper limb function (Shindo et al. 2011; Ono et al. 2014a). Furthermore, recent randomized controlled trials (RCTs) have also reported that long-term EEG-SMR based BCI intervention contingent on sensorimotor feedbacks for post-stroke patients induced sensorimotor functional recovery in the affected hand (Ramos-Murguialday et al. 2013; Ang et al. 2015; Pichiorri et al. 2015). In addition, a meta-analyses systematic review of clinical studies with BCI aided motor exercises reported that an effectiveness of BCI neurorehabilitation training is significantly high in the finger or upper-limb motor functional recovery after stroke (Cervera et al. 2018). Compared to traditional motor rehabilitation training, there are many indications for treatment of BCI aided motor exercise for post-stroke hemiplegic patients, admitting motor functional recovery for chronic and heavy post-stroke hemiplegic patients (Shindo et al 2011). Therefore, there is increasing interest in the use of BCI aided motor excises for motor rehabilitation of upper limb motor function in post-stroke hemiplegic patients.

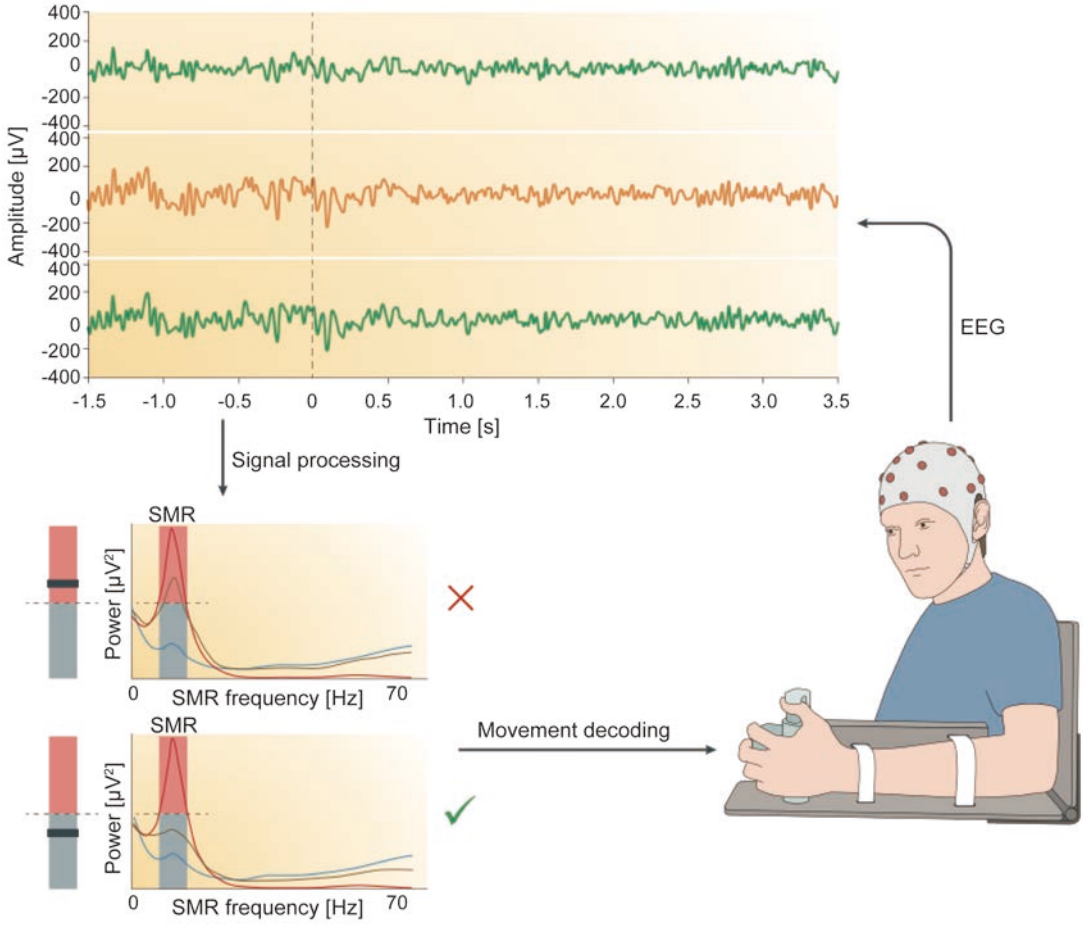

Figure 1-14. Use of BCI in a case of severe chronic stroke

Some features in the EEG signal recorded for the sensorimotor cortex are used to drive a robotic exoskeleton attached to a patient's paretic arm or hand (bottom right). The patients are instructed to attempt to imagine moving the affected limb, and if the power attenuation of EEG-SMR is noted, the robotic-orthosis actuated and/or electrical stimulation administered to the affected limb. The bottom left panels show representative EEG-SMR power spectrograms in successful and unsuccessful trials. In these panels, the red and blues traces depict typical spectrograms for EEG-SMR power when at rest (higher power) and task (lower power), respectively. The red and gray areas of the bar represent high or low EEG-SMR power, respectively. If the EEG-SMR power traces resemble the brown trace in the lower spectrogram, successful motor imagery is detected and sensorimotor feedback is provided to the affected arm. On the other hand, the sensorimotor feedback device does not work if the EEG-SMR power is high. This contingent association between motor imagery and the sensorimotor feedback facilitates sensorimotor excitability (modified from Chaudhary et al. 2016).

1.3. Neural mechanisms of sensorimotor functional recovery

Previous animal studies have reported that neural plasticity contributes to learning and reorganization of functional recovery from paralysis. For instance, cortical regions compensate for lost neural function from the damaged part of the brain, resulting in changes in a somatotopic map of the ipsilesional motor cortex (Nudo et al. 1996). In long-term functional recovery with a representational motor map, synaptogenesis and dendrite remodeling are associated with increases in neurological activity (Biernaskie and Corbett 2001). In humans, studies using non-invasive brain imaging methods, such as fMRI or TMS, have reported that the long-term effect of CI therapy increases fMRI activity and representational size of the affected upper limb (Liepert et al. 1998; Rijntjes et al. 2011). This functional reorganization is modified by use-dependent plasticity, which plays a significant role in functional recovery post-stroke, caused by synaptic efficacy in an activity-dependent manner (Hess and Donoghue 1994). In this section, the author introduces neural plasticity related to BCI intervention. In this thesis, the concepts of neural plasticity for sensorimotor functional recovery have been proposed separately in different fields of study, such as cell biology, neurophysiology, and neuropsychology . It should be noted that there is the possibility that one field of study may encompass a concept in another field of study, and they are not strictly separated.

1.3.1. Hebbian-like plasticity

Hebbian synaptic plasticity is hypothesized to play an important role in storing information by the co-occurrence of the pre- and postsynaptic activities (Caporale and

Dan. 2008). It consists of the broader framework of the two synaptic phenomena: long-term potentiation (LTP), an activity-dependent, persistent, and an increased synaptic strength phenomenon; and long-term depression (LTD), a corresponding decreased synaptic strength phenomenon (Turrigiano and Nelson 2004). LTP and LTD are two of the principal neural mechanisms behind learning or memory function.

In this thesis, the author uses the term of Hebbian-like plasticity or timing-dependent plasticity to refer to the phenomenon, where the synchronous activity of two different neuronal populations enhances the synaptic transmission efficiency between their active neurons. This is because to deal with Hebbian plasticity, which occurs at a neuronal level and with a 10 ms (at most <100 ms) activation pattern, there are some gaps and leaps in neurophysiological evidence to discuss beyond layers from single neuron activities to neural population activities, which are recorded by EEG or fMRI. For example, the paired-associated stimulations composed of a single pulse stimulation with TMS to the motor cortex, and an electrical pulse stimulation to the peripheral sensory nerve, induces the neural plasticity within a given stimulation interval (Stefan et al. 2000). When the neural activity induced by the magnetic stimulus, and the neural activity transmitted by the peripheral sensory fiber co-occur in the motor cortex, it induces the excitability-enhancing effect in the motor cortex (Carson and Kennedy 2013). Similarly, in the BCI rehabilitation, it is inferred that excitability enhancement in the sensorimotor cortex is induced through this type of Hebbian-like condition, because the electrical stimulation and robot-aided motor execution are administered only when the sensorimotor cortex is considered being activated during the motor imagery.

1.3.2. Use-dependent plasticity

There are some instances candidates of neural plasticity in post-stroke hemiplegic patients undergoing sensorimotor rehabilitation. For example, one of the most critically hypothesized mechanisms behind CI therapy, is the use-dependent plasticity. As mentioned above, the CI therapy allows restrained usage of the unaffected limb, and an increased usage of the affected limb, to increase the rate of using the affected limb in daily life tasks (Taub et al. 2006). Nudo and colleagues (1996) have revealed using animal models that motor map in the motor cortex, a topographic representation of motor threshold for a targeted muscle, enlarges its territory in a use-dependent manner. In the non-human primate stroke models, intensive finger-pinching training under the CI-like condition induced expansion of the somatotopic region of the proximal part in the affected upper limb, which was forced to use (Figure 1-15). A clinical study, with voxel-based morphometry of MRI, also reported that CI therapy for post-stroke hemiplegic patients increased gray matter density in the bilateral sensorimotor and the hippocampus regions compared to the controlled intervention (Gauthier et al. 2008). Also, a previous study on health participants reported that after a motor task, where the thumb was repeatedly moved in a specific directional, the characteristics of the motor cortex reshaped to allow the motion in the intended direction (Classen et al. 1998).

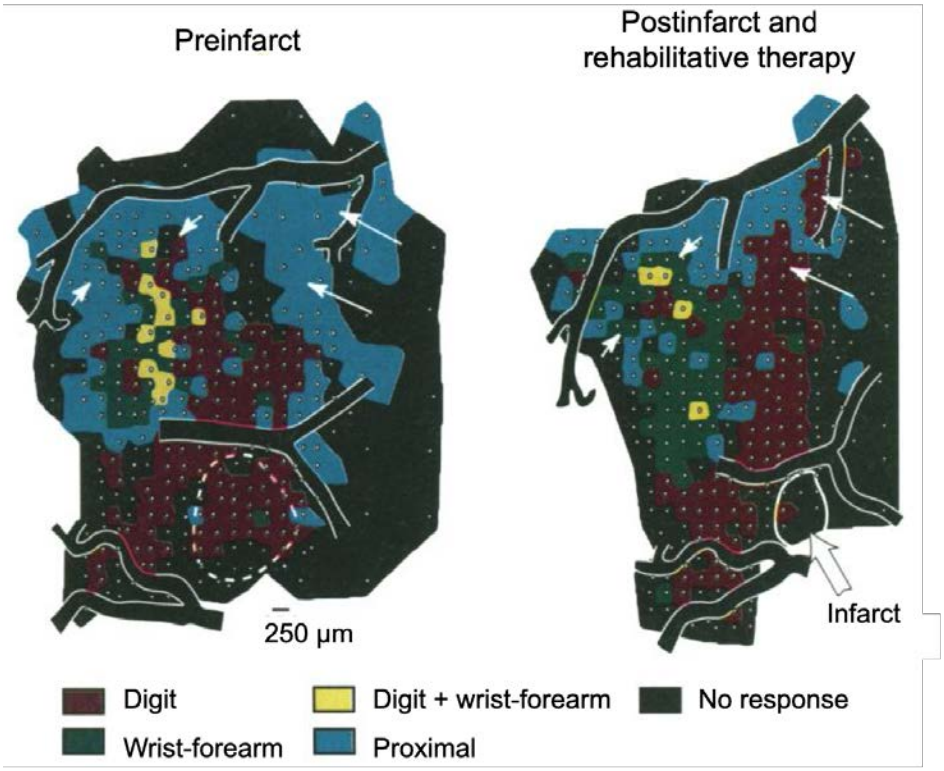

Figure 1-15. Reorganization of hand representations in the motor cortex
Before an infarct (left), and after a focal ischemic infarct and rehabilitative training (right), each motor map was recorded with the intracortical microstimulation techniques, which is widely used for mapping the functional topography of the motor cortex. After the rehabilitative exercise, the digit and the wrist-forearm representational areas were increased. The dashed white circle in the preinfarct map, and the solid white circle in the postinfarct map indicates the infarcted regions. The thin white arrows in each map, depict the digit or wrist-forearm representations from the formerly proximal (elbow or shoulder) representations (modified from Nudo et al. 1996).

Such evidence about the use-dependent plasticity suggests that EEG-SMR based BCI has the potential to induce the functional reorganization of the sensorimotor network through repeated use of the ipsilesional sensorimotor cortex. Since, the EEG-SMR modulation recorded over the sensorimotor cortex, is known to be related to the excitability of the sensorimotor cortex (Ritter et al. 2009; Yuan et al. 2010), the

corticospinal tract, and the spinal motoneuron (Hummel et al. 2002; Takemi et al. 2015); even if the paralysis-hand movement is not actually executed, the repeated motor imagery contingent EEG-SMR based BCI, guarantees a significant amount of activity in the sensorimotor cortex in the ipsilesional hemisphere. A previous clinical study has reported that the BCI intervention for the post-stroke hemiplegic patients improved the BOLD signals of the ipsilesional sensorimotor cortex in the lesion hemisphere, during the affected-hand motor imagery (Young et al. 2015).

1.3.3. Reinforcement learning

Reinforcement learning is described as one of the processes of decision making so that ensures optimum response in a given situation (Daw et al. 2006). It takes place by comparing the actual results that occurred during an action with the predicted results. If the result generated by an action yields a better result than the expected result, then the probability of that action will increase (Peters and Schaal 2008). Similarly, if the actual result of the selected action is worse than the expected result, the probability of the action decreases. In this way, reinforcement learning is the process by which the selected action type is narrowed down by the result of good or bad. The amount of error between the predicted value and the actual outcome is calculated in the dopaminergic neurons of the basal ganglia and the striatum, and this calculation is said to be an essential factor for realizing the reinforcement learning (Schultz 1998). A previous study applied the reinforcement learning to the post-stroke sensorimotor rehabilitation and reported that the hemiplegic patients with reward significantly improved their walking speeds compared

to the control, suggesting that the reward encouraged exercise-based motor recovery (Dobkin et al. 2010).

Since the post-stroke patients with chronic severe hemiplegia lack clues for proper motor execution, even an attempt or imagery with appropriate brain activity is challenging to elicit motor imagery of the affected limb. Also, even if the motor imagery is formed by learned non-use, the patient repeatedly performs the motor imagery tasks in his/her own way without recognizing if the trial is true or false (Braun et al. 2013). Motor imagery therapy aided by the BCI provides the compliant and quality of motor imagery to the patient, through visual/somatosensory feedback, because the BCI monitors the brain activity which is enough to enhance the sensorimotor-cortical excitability (Ushiba and Soekadar 2016). The patient recognizes the feedbacks as rewards of attempting motor imagery, and thus the probability of appearance of motor imagery increases. Although, it is not identified whether the brain activity fluctuates among the trials, or the patient changes the planning strategy of motor imagery; the patient gradually improves motor imagery with BCI-aided clues, resulting in a modulated earning of sensorimotor excitability and sensorimotor functional recovery (Ono et al. 2014b).

1.4. Objective of the dissertation

For patients who become disable owing to various reasons, such as stroke, spinal cord injury, limb deficiency, and miotic intractable diseases, the study provides hope that patients can move their body again of their own will. BCI, or alternatively, brain-machine interface technology allows for the direct translation of brain activity into control signals

for a machine, robot, or computer to enable voluntary movement. BCI was originally applied as a prosthetic tool to practice compensatory movement using the remaining functional activity of intact body parts; lately, several studies on post-stroke hemiplegic patients have reported that combined intervention using BCI and physical exercises for the affected limb improves the patient's biological motor function. This is of importance in our understanding of assistive devices since these studies first showed the potential of BCI in helping the brain to fault tolerance in an engineering sense; however, later studies have revealed a different potential use of this technology, in actuating the biological process of neural re-functioning to overcome irreversible structural damage. BCI has been therefore attracted much attention owing to its potential applications in rehabilitation medicine.

For practical translations of BCI technology into clinics, non-invasive methods of recording brain activity is indispensable. Scalp EEG is the most common method among existing modalities of non-invasive brain activity recording; thus, the present study used EEG-based BCI aiding motor recovery for post-stroke hemiplegic patients. In such a BCI system, decryption of the patient's volitionally motor attempts is achieved through online detection of self-induced motor-related electrical activities, one of which is EEG-SMR. EEG-SMR is recorded over the sensorimotor cortex in the resting-state and is interpreted as an indication of the idling state of the sensorimotor cortex (Pfurtscheller et al. 1996a). The EEG-SMR based BCI system with contingent endogenous neural stimulation, such as actions of the motor-driven orthosis (Hochberg et al. 2012), NMES (Bouton et al. 2016), or virtual reality (Leeb et al. 2007), forms a closed-loop process, which occurs in

behaviorally relevant functional networks and can be used to provide self-administered therapy.

Some clinical studies including case studies or case series have reported that physical exercises combined with BCI over several weeks induces motor functional recovery of the affected limb in post-stroke patients (Shindo et al. 2011; Ono et al. 2014b). Furthermore, a few RCTs reported that BCI interventions could be potentially beneficial in improving motor outcome measures (Ramos-Murguialday et al. 2013; Pichiorri et al. 2015). Because of the novelty of BCI interventions, however, there remains a need to define the mechanisms of underlying impact of BCI in order to guarantee the neurophysiological assessments; therefore, results should be interpreted with caution before making recommendations for clinical practice, and further studies with larger and clearly stratified patient cohorts should be conducted.

Most BCI studies aimed at neurological rehabilitation have focused on its efficacy related to behavioral motor recovery and the subsequent/consequent neurophysiological changes for several weeks (Shindo et al. 2011; Ramos-Murguialday et al. 2013; Ono et al. 2014b; Pichiorri et al. 2015); no researchers have investigated the acute, direct effects on intrinsic neural activities. This may be because intrinsic neural activities are so subtle that the brain regions that may be affected by BCI or that may be correlated with the EEG signal used as the BCI biomarker in the resting-state are still unknown. Therefore, the author first studied the simultaneous EEG and fMRI recordings in order to identify the brain regions correlated with spontaneous EEG-SMR fluctuation. This study revealed that the spontaneous EEG-SMR is strongly involved in the activity of the sensorimotor cortex

located under the EEG electrode. Furthermore, the EEG-SMR components contain the activities of the corresponding sensory and motor cortices respectively activities.

The author further evaluated the neurophysiological effectiveness of the EEG-SMR based BCI in inducing acute changes in stroke patients and further conducted a double-blind, sham-controlled, randomized crossover confirmatory study in developmental phase II or III following consolidated standards of reporting trials (CONSORT) guidelines. This study revealed that motor exercise combined with BCI increases activity in the ipsilesional sensorimotor cortex in the resting-state for post-stroke hemiplegic patients. The discussion will provide insight regarding the hypothesis that BCI intervention is a promising strategy in neurorehabilitation to improve the intrinsic neural pattern.

In Chapter 1 of this dissertation, the principles of neurophysiology are reviewed and an outline of BCI technology is provided. In Chapter 2, the investigation of the brain region reflecting the spontaneous EEG-SMR in the resting-state in the simultaneous EEG-fMRI recording study is described. In Chapter 3, the investigation of the neurophysiological effectiveness of EEG-SMR based BCI evaluated using the intrinsic fMRI signal in post-stroke hemiplegic patients is described. Finally, in Chapter 4, the author expresses a perspective on the contribution of this dissertation to the scientific and technological breakthroughs in the field of neurofeedback by summarizing the findings of the two aforementioned studies.

Chapter 2 : Resting-state fluctuations of EEG sensorimotor rhythm reflect BOLD activities in the pericentral areas: A simultaneous EEG-fMRI study

* This chapter was based on the author original article, “Tsuchimoto et al. Resting-State Fluctuations of EEG Sensorimotor Rhythm Reflect BOLD Activities in the Pericentral Areas: A Simultaneous EEG-fMRI Study. *Front Hum Neurosci* 11, ~~Article ID~~ 356(10 pages), 2017.” The author has a right to use this dissertation.

2.1. Introduction

As introduced in the Chapter 1, since Berger’s first electroencephalogram (EEG) recordings from the human scalp in the late 1920s, a number of studies have led to new insights into the function and mechanisms of intrinsic oscillations underlying brain activities (Cohen 2017). One of the characteristic EEG rhythms is the sensorimotor rhythm (SMR), a spontaneous EEG (i.e., in the absence of somatosensory input or motor output) with an arch-shaped waveform in alpha (e.g., 7−11 Hz) and beta (e.g., 12−30 Hz) frequency bands (Kuhlman and Allison 1977; Kuhlman 1978; Kozelka and Pedley 1990; Arroyo et al. 1993; Laufs et al. 2003; Hasan et al. 2016). The EEG-SMR signals are recorded from the C3 channel that is located closest to the hand area in sensorimotor area and its amplitude is known to be reduced by desynchronized neural activities in association with motor-related events, such as kinesthetic motor imagery or actual muscle contraction, suggesting a possible electrophysiological sign of sensorimotor excitability (Pfurtscheller et al. 2006). Actually, such EEG-SMR power change, namely event-related desynchronizations are often localized over the pericentral gyri, and the degree of EEG-

SMR power attenuation is associated with cortico-spinal tract excitability (Takemi et al. 2013) as well as with intracortical disinhibition of the motor cortex.

Modulations of the EEG-SMR can be segregated into two physiologically different components. The alpha frequency band is located slightly posterior to the beta (Pfurtscheller and Lopes da Silva 1999; Ritter et al. 2009) and shows prominent reaction to somatosensory events (Babiloni et al. 2008; van Ede et al. 2014). On the other hand, the amplitude of the beta frequency band EEG is attenuated, but the phase synchronization is maintained between the beta frequency band EEG and the spinal motoneuronal pool activities during tonic motor contraction tasks (Conway et al. 1995; Leocani et al. 1997; Bayraktaroglu et al. 2013). Furthermore, in the post-movement period, the amplitude of the beta band consistently returns to and exceeds pre-movement levels via synchronization (Pfurtscheller et al. 1996b; Bauer et al. 2006; Jurkiewicz et al. 2006; Parkes et al. 2006). These studies suggest that the beta component of the EEG-SMR is more motor-related.

Does EEG-SMR also show some spontaneous fluctuations during the resting-state, and, if so, is the resting-state EEG-SMR fluctuation correlated with blood-oxygen-level dependent (BOLD) signal changes in the sensorimotor areas? Spatial localization of alpha and beta components of the resting-state EEG-SMR has yet to be directly confirmed, but several lines of collateral evidence have supported such correlations. For instance, studies on sensory stimulation have shown that the prestimulus amplitude of the alpha-band SMR has a significant impact on sensory stimulus detection (Linkenkaer-Hansen et al. 2004; Zhang and Ding 2009). A few studies using single-pulse transcranial magnetic

stimulation (TMS) over the motor cortex have shown an association between motor cortex activity or corticospinal tract excitability and the amplitude of the spontaneous beta-band SMR during the resting-state (Mäki and Ilmoniemi 2010; Berger et al. 2014). Spontaneous fluctuations of the resting-state EEG may be much subtler than the motor task-related variations. However, similar to the fact that the level of the SMR synchronization reflects sensorimotor cortex activity during the course of a movement task (Pfurtscheller et al. 2000), the characteristics of the SMR may also be indicative of sensorimotor cortex activity during the resting-state.

Here, based upon previous knowledge suggesting an association between spontaneous EEG-SMR fluctuation during the resting-state and activity of the pericentral brain regions, the author addressed the following hypotheses: (1) the spontaneous EEG-SMR power modulations were correlated with a surrogate marker of brain activity that covaries with resting-state sensorimotor cortical activity as measured by functional magnetic resonance imaging (fMRI) in the pericentral area, and (2) the area correlated with alpha-band EEG-SMR was located posterior to the area correlated with beta-band EEG-SMR. To test such hypotheses, the author employed EEG-fMRI simultaneous recording to identify the relationship between EEG-SMR modulations and whole-brain activity during the resting-state.

2.2. Methods

2.2.1. Participants

Nineteen healthy participants (13 men and 6 women; aged 21−25 years) were recruited in this study. This study is a validation study to determine the brain region of which is correlated with the intrinsic SMR using EEG and fMRI simultaneous recording. The authors determined to conduct this research in health participants to avoid an experimental load to post-stroke patients. None had any sleep, medical, or psychiatric disorders. The purpose and experimental procedure were explained to the participants, and all participants gave informed written consent. The study was conducted in accordance with the Declaration of Helsinki and was approved by Keio University Faculty of Science and Technology Bioethics Committee and Saiseikai Kanagawa-ken Hospital Ethics Committee.

2.2.2. Data acquisition

The participants were asked to lie still on a scanner bed in the dark for 10 min with their eyes opened and fixed on a small black cross. EEG signals were recorded with an MR-compatible amplifier (BrainAmp MR plus, Brain Products GmbH, Germany) and an EEG electrode cap (BrainCap MR, Brain Products GmbH, Germany) providing 63 EEG channels and 1 electrocardiogram (ECG) channel. Their electrodes were placed according to the modified International 10−10 system (Jurcak et al. 2007). The ground electrode was placed at the AFz, the reference electrode at the FCz, and the impedance of all electrodes was kept lower than 5 kOhm throughout the experiment. The ECG electrode

was placed on the back of participants to obtain the electrocardiographic data and to subsequently correct ballistocardiographic artifacts. Raw record was sampled at 5 kHz with a bandpass filter between 0.1 and 2500 Hz using the Brain Vision Recorder, (Brain Products GmbH, Germany). The amplifier system was set beside the participant's head within the scanner during fMRI scanning.

Functional images were acquired on a 1.5-T MR scanner (Signa Exite, GE Medical Systems, UK) and whole-brain, T2-weighted BOLD data were acquired using an with a single-shot gradient echo planar image sequence (repetition time TR = 3000 ms; echo time TE = 40 ms; flip angle = 70 degrees; slice order = ascending; voxel size = 3.75 × 3.75 × 4.0 mm^3; 30 axial slices with no gap, 200 scans). To achieve phase synchronization clocks for digital sampling between the MRI data and the EEG system, the EEG system clock was synchronized with a SyncBox device (Brain Products GmbH, Germany) and the MRI scanner's 10 MHz master synthesizer. The scanner also delivered each TR trigger signal that marked the onset time of every fMRI volume acquisition. These markers were used for fMRI scanning artifact correction of the EEG data.

2.2.3. Data analyses

An outline of the analyses is shown in Figure 2-1. The several-seconds scale of modulation in the SMR resting-state amplitude was first extracted from EEGs of healthy volunteers, and the EEG-SMR power time-series was convolved with the canonical hemodynamic response function (HRF) to model the BOLD signals co-varying with the EEG-SMR modulation. A voxel-wise correlation analysis was then conducted in the

whole-brain to identify the cortical and subcortical activities with which the modulation of EEG-SMR amplitude was associated.

EEG data were processed by Brain Vision Analyzer 2.0 (Brain Products GmbH, Germany) and the MR gradient-artifacts and ballistocardiogram in the EEG signals were corrected using the average template subtraction method (Allen et al. 2000). First, to create the gradient-artifact template, EEG data were averaged over 3 volumes (9 s) with the reference to each TR trigger signal. The template was computed for each TR interval using the sliding window. The gradient-artifact template was subsequently subtracted from the original EEG data. Second, the ballistocardiographic artifacts were removed in a similar way. The template in this case was constructed by averaging of the EEG data with the reference to the peaks of the R-waves in the ECG signal. After the gradient-artifacts and ballistocardiographic corrections, the EEG data was bandpass filtered (3-70 Hz with 48 dB/octave phase shift-free Butterworth) with a notch (50 Hz for avoiding power line contamination), and the sampling rate of the data was decreased to 250 Hz.

It is known that the EEG signal obtained around the pericentral area contains cognitive components, such as activity related to the "mirror neuron systems," in addition to the sensorimotor idling activity component (Yin et al. 2016). Because the author focused on the sensorimotor processing component, the author obtained EEG-SMR signals from the C3 channel that is located closest to the pericentral area. Furthermore, the re-reference to the common average reference should remove global-signal to emphasize the relevant localized activities around the pericentral area (McFarland et al. 1997). The power time courses of EEG data in the C3 channel were calculated by a fast

Fourier transform (FFT) with a 1-s moving time window and no overlap. The author first selected four different frequency bands [7−11 Hz (alpha), 12−16 Hz (beta1), 17−21 Hz (beta2), 22−30 Hz (beta3)] as candidates for the sensorimotor-related features (Arroyo et al. 1993; Rangaswamy et al. 2002, 2004; Ritter et al. 2009), and the power time courses of EEG-SMR were obtained by calculating the power in every time window to be demodulated the EEG-SMR amplitude-fluctuation signals. To confirm that these frequency components were localized over the sensorimotor cortex, simple linear regression coefficients at a 0-lag were calculated between the C3 and the other channels. The coefficients were assigned to each channel position where the correlation with C3 was calculated, and a topographic map was obtained using the nearest neighbor interpolation with the biharmonic spline interpolation methods at implemented toolbox on MATLAB (MathWorks, Natick, MA, USA). After calculating the regression coefficients for each individual participant, a one-sample *t*-test was performed for group analysis.

The fMRI data were pre-processed with Statistical Parametric Mapping (SPM12, Wellcome Department of Imaging Neuroscience, http://www.fil.ion.ucl.ac.uk/spm) on MATLAB. First, the slice-timing correction was applied with the reference slice based on the middle of each TR, and each volume was spatially realigned with the first volume. After the timing and spatial corrections, each volume was normalized according to the Montreal Neurological Institute (MNI) template, and was resampled to 2-mm cubic voxels. The normalized volumes were then smoothed with an isotropic Gaussian kernel

(Full width at half maximum (FWHM) = 8 mm), and were 0.0078 Hz high-pass filtered. These parameters were set in SPM function initialises as the default parameters.

For the correlation analysis of BOLD signals with EEG-SMR power modulation in each frequency band, the author followed a previous approach in the simultaneous EEG-fMRI study (Huster et al. 2012). First of all, the EEG-SMR power time series for bandwidth was convolved with HRF provided by SPM12 to take into account the hemodynamic delay of the BOLD signal. After the convolution, to conform the temporal resolution of the fMRI data, the EEG-SMR power time courses were down-sampled with the data point sampled at the reference of the fMRI slice timing correction; namely, one data point was sampled in the middle of every TR. To identify the brain regions with correlations between BOLD signals and EEG-SMR fluctuations, each alpha and beta frequency band of EEG-SMR power was used as a predictor for the BOLD signal in the general linear model (GLM). Because the alpha- and beta-band EEG-SMR power modulations were significantly correlated, a GLM model was created for each frequency of EEG-SMR power to avoid multicollinearity. The six realignment parameters (three translation and three rotations) were used as nuisance variables to remove head motion artifacts, and the cerebrospinal fluid (CSF) signal was also used as a nuisance variable to exclude non-neural noise originating from cardiac effects and respiration. The CSF time series were obtained by averaging the signal over all voxels within the Lateral Ventricles Mask, which were anatomically defined by the SPM12 atlas.

In the first-level analysis, the author generated regression coefficient contrast images of alpha- and beta-band EEG-SMR modulations for each participant. Then, for

the second-level, group data analysis, the contrast images were fed into a one-sample *t*-test. For all data, the fMRI results were subjected to peak- and cluster-extent-based thresholding, the most popular thresholding method for dealing with the issue of multiple comparisons over many voxels (Woo et al. 2014; Worsley et al. 1992). The initial voxel threshold was set to $p < 0.001$ uncorrected for multiple comparisons (this level was considered reasonably conservative against a false positive finding). Thus, clusters were considered significant if they survived an extent threshold of $p = 0.05$ family-wise error (FWE) corrected for multiple comparisons for statistical inference. In each region of the sensorimotor cortex correlated with alpha- or beta-power fluctuations of the EEG-SMR, the author performed statistical evaluation tests to validate that these correlated regions were spatially different using a two-sample Kolmogorov-Smirnov test.

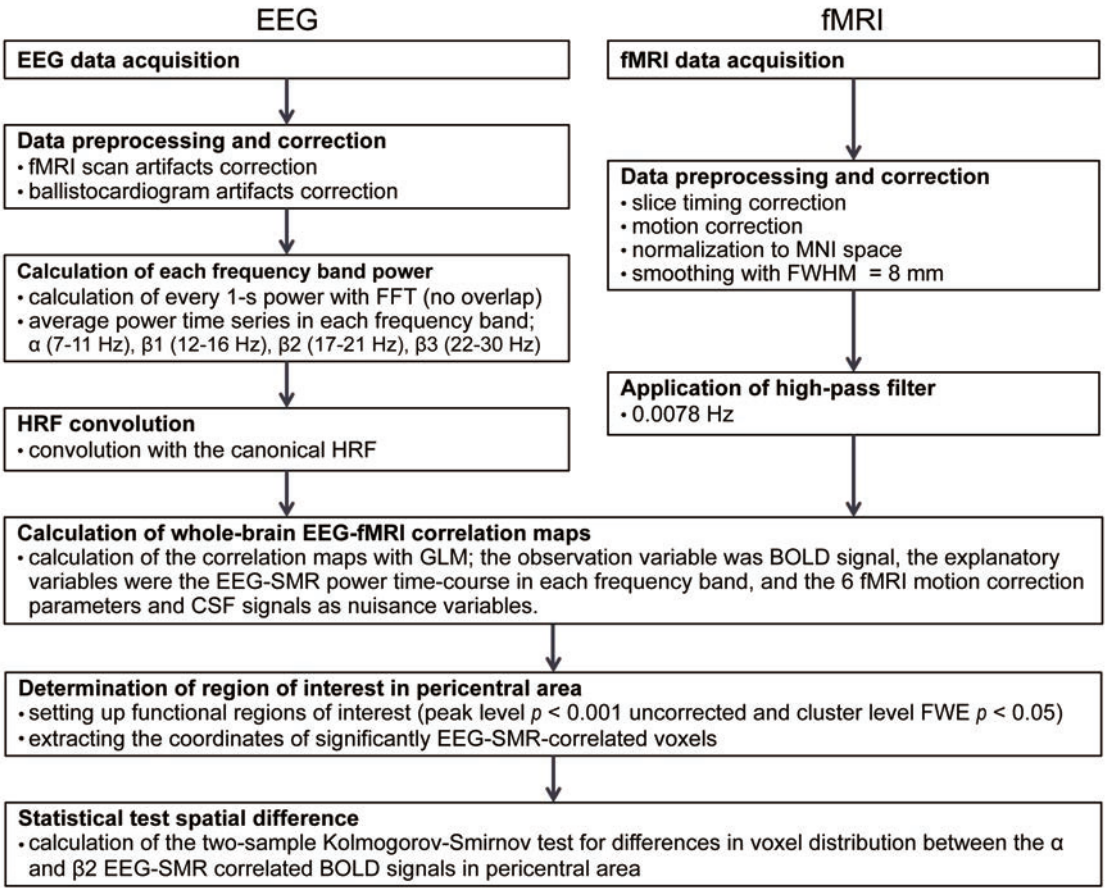

Figure 2-1. Outline of EEG-fMRI simultaneous recording study

2.3. Results

2.3.1. EEG results

A typical EEG-SMR time series of a single participant is shown in Figure 2-2(A), and the power spectrum densities of the EEG-SMR in all participants are depicted in Figure 2-2(B). Although EEG signal power varied among the participants, the averaged power spectrum density showed that the overall frequency structures were shared across the participants, with the peak-frequencies at 10−12 Hz and 22−26 Hz. The averaged power spectrum densities in the alpha- and beta1-band were 6.8×10^{-10} V^2/Hz and 2.9 ×

10^{-10} V^2/Hz, respectively. The powers of beta2- and beta3-band were 6.0×10^{-11} V^2/Hz and 7.5×10^{-11} V^2/Hz, respectively, and were relatively small in comparison with the former two frequency bands. These power-modulation-depth ratios were calculated the mean and standard variance among all participants for time-fluctuation as coefficients of variation for alpha: 85 ± 16%; beta1: 112 ± 20%; beta2: 88 ± 39%; and beta3: 68 ± 19% in the resting-state. Figure 2-3(A) shows the spatial distribution of the selected frequency modulation components from C3 using statistical values of group analysis. All of the distribution maps showed positive correlations locally around C3 and its contralateral (C4) electrode, with notable localization in the alpha and beta2 components.

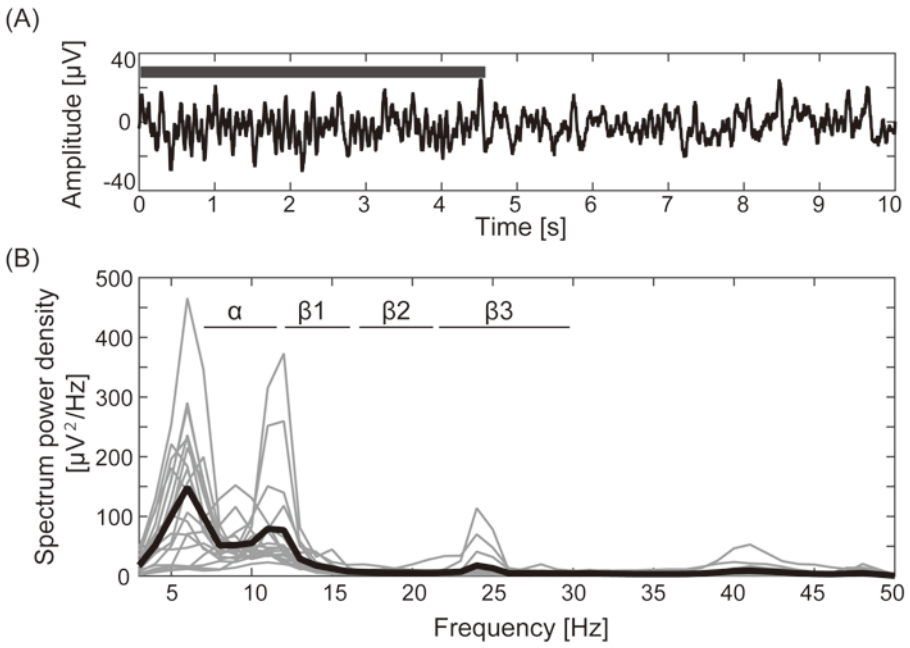

Figure 2-2. Time course and power spectrum density results of EEG

(A) Filtered EEG data (3-70 Hz with 48 dB/octave phase shift-free Butterworth bandpass filter and 50 Hz notch filter) elicited from the C3 channel of one participant. The black bar indicates the time period during which the typical EEG-SMR occurred. (B) The spectral density was calculated with Welch's power spectral density estimation for each participant (thin lines) and the averaged spectram from all participants (thick line).

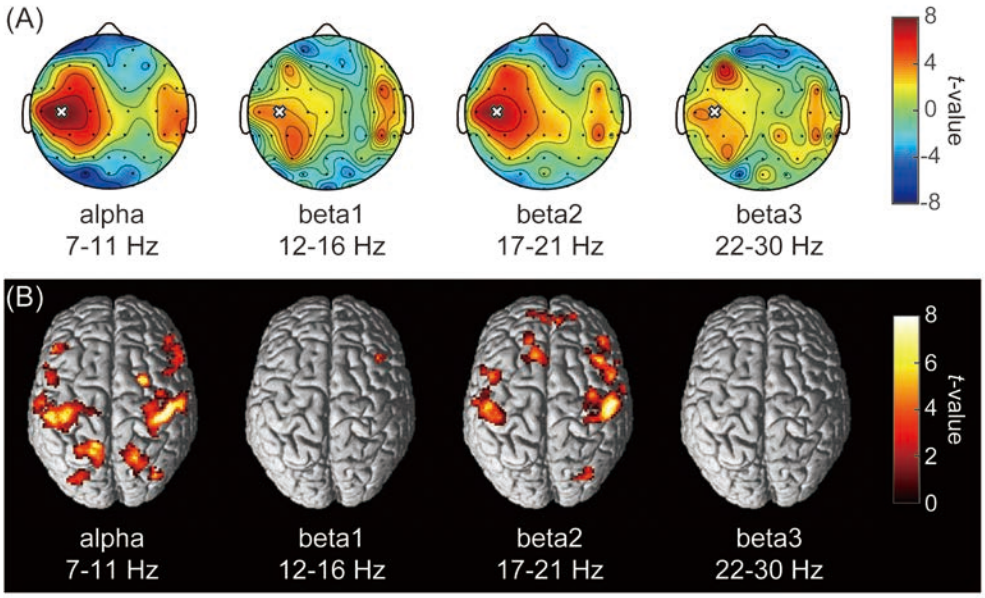

Figure 2-3. Correlation maps of the EEG-SMR modulation wave elicited from C3 in each frequency band

(A) Each topography map shows the spatial distribution of the correlation coefficient between the EEG-SMR modulation elicited from C3 and that at other electrodes. The white crosses represent the C3 channel and the black dots represent other EEG channels. The color bar shows the strength of correlation. (B) The statistical *t*-maps of fMRI negative correlations of each component of EEG-SMR modulation with the BOLD signals (peak-level $p < 0.001$ uncorrected, cluster-level FWE $p < 0.05$).

2.3.2. fMRI results

Figure 2-3(B) depicts the statistically significant *t*-maps of fMRI correlates (BOLD signals) of EEG-SMR modulation, which were assessed separately for the alpha and each beta component. The alpha-band EEG-SMR modulation was negatively correlated with the activities of the bilateral pericentral cortices ($p < 0.001$ peak level uncorrected; $p < 0.05$ voxel level FWE corrected). The *t*-values and MNI coordinates are shown in Table 2-1. Similar to the correlation of BOLD signals with the alpha-band EEG-SMR modulation, the beta2-band EEG-SMR modulation was negatively correlated with the

activities of the bilateral pericentral cortices (Table 2-2). The beta3-band EEG-SMR modulation was not correlated with any region. The beta1-band EEG-SMR modulation was negatively correlated with the BOLD signal in the right middle frontal gyrus; this correlation was also seen in the analysis of the alpha- and beta2-band EEG-SMR modulations.

The author further examined a spatial topography of fMRI signal correlated with both the alpha- and beta2-band EEG-SMR modulations in the left pericentral area, where the C3 electrode was located. Figure 2-4 shows the pericentral activity correlated with alpha-band EEG-SMR, beta2-band EEG-SMR, and overlap of both. The peak coordinate of the alpha-band EEG-SMR-correlated activity was MNI (x, y, z) = (-52, -32, 52) and that of the beta2-band EEG-SMR was MNI (x, y, z) = (-44, -28, 50). Furthermore, Figure 5 displays the distribution of these correlated areas along the anterior-posterior (y) axis. The spatial distributions of alpha-band EEG-SMR and beta2-band EEG-SMR correlated activities were different in both the postcentral (Figure 2-5(A)) and precentral (Figure 2-5(B)) areas (two-sample Kolmogorov-Smirnov test, $p < 0.001$). More precisely, the alpha-band EEG-SMR-correlated BOLD signals were distributed posterior to those correlated with the beta2-band EEG-SMR.

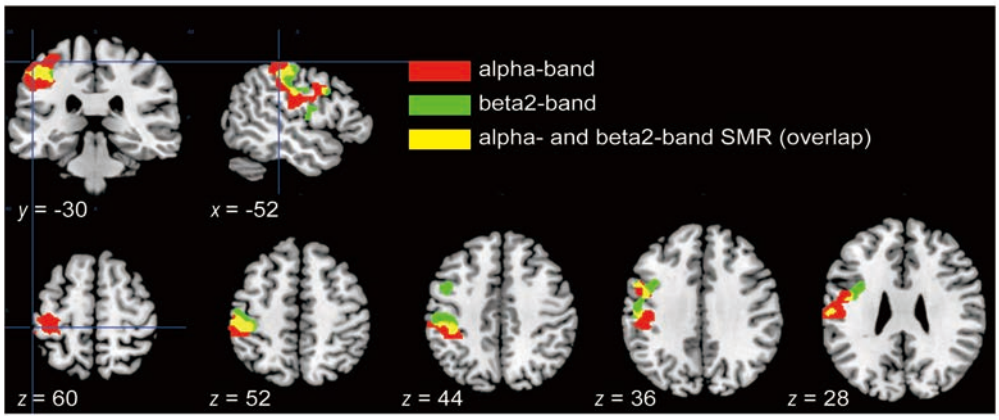

Figure 2-4. Spatial distributions of the correlations between BOLD signal and each EEG-SMR modulation in the pericentral area

Red areas correlated with alpha-band EEG-SMR modulation, green areas correlated with beta2-band EEG-SMR modulation, and yellow areas are overlapped regions correlated with modulations of both alpha- and beta2-band EEG-SMR. These regions were adjusted from statistical maps to those based on the atlas of the pericentral area in SPM12.

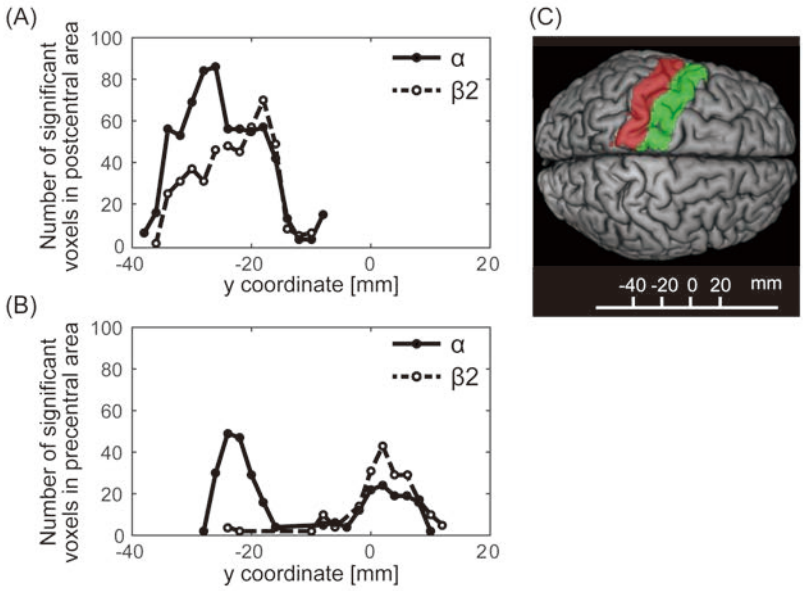

Figure 2-5. The distributions of statistically significant voxels along the anterior-posterior axis

The black lines show the number of significant voxels correlated with alpha-band EEG-SMR modulation and the dashed lines show those correlated with beta2-band EEG-SMR modulation. (A) the distribution of significant voxels in the postcentral area; (B) their distribution in the precentral area; (C) the y-axis MNI coordinates superimposed on the SPM12 atlas showing the postcentral (red) and precentral (green) areas.

Table 2-1. Brain regions whose activity correlated with the power of the alpha-band EEG-SMR modulation

Model	Correlation type	Brain region	Side	MNI coordinates			*t*-value	*p*-value	Cluster size
				x	*y*	*z*			
alpha	negative	Triangular part of the inferior frontal gyrus	Right	50	38	-6	5.95	6.30×10^{-5}	316
		Postcentral gyrus	Left	-52	-32	52	5.88	7.23×10^{-6}	2002
			Right	46	-28	62	5.85	7.61×10^{-6}	1250
		Middle frontal gyrus	Left	-44	28	28	5.57	1.36×10^{-5}	430
		Superior parietal lobule	Right	22	-68	50	5.53	1.50×10^{-5}	791
			Left	-16	-58	64	5.25	2.72×10^{-5}	642
		Superior frontal gyrus	Right	26	2	62	5.25	2.73×10^{-5}	241
		Opercular part of the inferior frontal gyrus	Right	56	22	16	5.03	4.34×10^{-5}	838
		Middle occipital gyrus	Left	-34	-84	30	4.54	1.27×10^{-4}	202

Brain regions are named based on the SPM12 atlas, *p*-value, cluster-level FWE rate of 0.05.

Table 2-2. Brain regions whose activity correlated with the power of the beta1- and beta2-band EEG-SMR

Model	Correlation type	Brain region	Side	MNI coordinates			*t*-value	*p*-value	Cluster size
				x	*y*	*z*			
beta1	negative	Middle frontal gyrus	Right	38	20	30	6.38	2.61×10^{-5}	314
beta2	positive	Thalamus	Right	2	-12	4	4.42	1.65×10^{-4}	270
			Left	-6	-8	6	3.71	8.06×10^{-4}	270
	negative	Superior frontal gyrus	Left	-10	24	58	6.51	2.00×10^{-6}	326
			Right	22	54	30	4.72	8.47×10^{-5}	202
		Postcentral gyrus	Left	-44	-28	50	6.33	2.86×10^{-6}	1262
			Right	52	-18	52	5.94	6.41×10^{-6}	1024
		Opercular part of the inferior frontal gyrus	Right	42	14	24	6.09	4.64×10^{-6}	1758
		Posterior orbital gyrus	Right	32	24	-18	5.88	7.22×10^{-6}	313
		Superior temporal gyrus	Left	-60	-20	2	5.40	1.98×10^{-5}	293
		Lingual gyrus	Left	-20	-68	-10	5.01	4.50×10^{-5}	219
			Right	20	-66	-4	4.68	9.34×10^{-5}	376
		Middle occipital gyrus	Right	32	-82	32	4.72	8.52×10^{-5}	224
		Superior frontal gyrus medial part	Right	6	50	18	4.58	1.17×10^{-4}	340
		Middle temporal gyrus	Right	60	-30	0	4.40	1.73×10^{-4}	228

Brain regions are named based on the SPM12 atlas, *p*-value, cluster-level FWE rate of 0.05.

2.4. Discussion

In the present study, the author employed simultaneous EEG-fMRI recordings in healthy human participants to investigate the whole-brain hemodynamic responses associated with spontaneous EEG-SMR fluctuations. The author found significant correlations between BOLD signals of activities in the sensorimotor regions and modulation of EEG-SMR in the resting-state. In addition, the regions with negative correlations between BOLD signals and the alpha-band EEG-SMR were distributed posterior to those correlated with the beta-band EEG-SMR.

2.4.1. SMR frequency components in alpha- and beta-band

Two of the four frequency components, alpha- and beta2-band, showed distributions of significant correlations locally around C3 and its periphery. According to Ritter and her colleagues' study using a blind source separation algorithm (Ritter et al. 2009), the EEG-SMR power modulations of the alpha (around 10 Hz) and beta (around 20 Hz) frequency bands were associated with the motor task. Thus, the amplitude modulation of the alpha- and beta2-band EEG-SMR may reflect fluctuations in activity in the sensorimotor regions. Moreover, both the alpha- and beta2-band EEG-SMR components were correlated with BOLD signals around the bilateral pericentral areas, that periphery area of around C3 as well as the contralateral C4 area. The homologue C4 of bilateral pericentral areas, which is consistent with the fact that the two cerebral hemispheres have anatomical connections via the corpus callosum and each hemisphere

communicates with the contralateral hemisphere by inhibitory and excitatory inputs (Bloom and Hynd 2005; Palmer et al. 2012).

2.4.2. Correlation between intrinsic EEG-SMR fluctuations and BOLD signals

Both the alpha- and beta2-band EEG-SMR components were correlated with BOLD signals around the bilateral pericentral areas. Previous fMRI studies also found that in the resting-state, BOLD signals in the bilateral sensorimotor cortices were correlated with one another, a phenomenon referred to as the sensorimotor network (Biswal et al. 1995; Beckmann et al. 2005). Furthermore, the alpha or beta synchronizations are interpreted as correlates of "idling" motor cortex neurons (Pfurtscheller et al. 1996a; Ritter et al. 2009). Therefore, the intrinsic alpha- and beta-band EEG-SMR modulations might reflect the sensorimotor network in the resting-state. In addition, another simultaneous EEG-fMRI study showed that alpha- and beta-band EEG-SMR modulations were negatively correlated with the sensorimotor network (Yin et al. 2016). The present results are compatible with these previous findings, suggesting that it is valid to draw correlations between the intrinsic EEG-SMR modulations and activity in the sensorimotor cortex.

2.4.3. Functional properties of alpha- and beta-band EEG-SMR

Although the topographic map of the alpha-band EEG-SMR correlation was similar to that of the beta2-band EEG-SMR correlation, it may reflect somatosensory-dominant activities of the cortex. The present fMRI results may indicate functional differences

between the alpha- and beta-band EEG-SMR. Although both EEG-SMR components were correlated with BOLD signals around the pericentral area, the area correlated with the alpha-band EEG-SMR was in the parietal region and that correlated with the beta-band EEG-SMR was the frontal region. Recent findings suggest that the functional role of alpha oscillations is closely related to the activity of intrinsic cortical networks, indicating that the alpha-band signal occurs in different cortical layers (Klimesch et al. 2007; Palva and Palva 2007; Ben-Simon et al. 2008; Bazanova and Vernon 2014; Sigala et al. 2014). Activities in the beta-band, however, are known to be connected with motor functions (Brovelli et al. 2004; Jurkiewicz et al. 2006; Tzagarakis et al. 2015). In addition, in a TMS evoked EMG study with concurrent EEG recording, the Farzan group (2013) reported that EEG components correlated with the TMS-induced silent period in EMG, and that the cortical inhibitory processes in humans were related to the power of beta oscillations more locally than to that of the alpha oscillations.

2.4.4. Spatial distributions of alpha- and beta-band EEG-SMR

Previous studies reported the SMR to be most prominent in central scalp regions in the area of the sensorimotor cortex (Pfurtscheller and Neuper 1997; Birbaumer et al. 2000; Blankertz et al. 2010), while the present results depict the spatial differences of correlation areas in intrinsic alpha- and beta-band SMR. In studies of SMR power modulation associated with motor execution or motor imaginary tasks, the attenuated alpha- and beta-band SMR amplitudes were localized around the contralateral sensorimotor area (Crone et al. 1998; Sauseng et al. 2013). Furthermore, the center of

event-related desynchronization of the alpha-band SMR was located more posterior than that of the beta-band SMR in EEG/MEG studies (Pfurtscheller and Lopes da Silva 1999; Jurkiewicz et al. 2006). The task-related reactive sources of the alpha-band SMR were localized in the postcentral area and those of the beta-band SMR were in the precentral area during sensory input (Cheyne et al. 2003) or motor output (Salmelin et al. 1995). Although it is not obvious that the neural processing of the intrinsic EEG-SMR modulation during the resting-state is equivalent to that of event-related task modulation, the present results indicate that the spontaneous modulations of the EEG-SMR may be based upon a similar mechanism with that of the EEG-SMR modulated by sensory inputs or movements which were already shown by event-related studies to represent pericentral activities; thus the EEG-SMR modulation in the resting-state is also likely to reflect pericentral activities. Therefore, insight into the relationship between EEG-SMR modulation and the pericentral area, which has been examined in event-related studies, has now been extended to the activities of the intrinsic EEG-SMR modulation during the resting-state. In the present study, neural activity correlated with EEG-SMR modulation at rest showed similar spatial localization with the neural activity correlated with movement-related EEG-SMR modulation in the literature. Although it remains a testable hypothesis that a similar mechanism may underlie EEG-SMR modulation during a motor task and during a resting-state, the author has provided the evidence that intrinsic EEG-SMR modulation during the resting-state associated the sensorimotor activities. This evidence will be referred to that EEG-SMR based brain-computer interface (BCI) intervention affects the sensorimotor activities in the resting-state, and changes of the

intrinsic sensorimotor activities after EEG-SMR based BCI intervention is potentially promoted.

Chapter 3 : Motor exercise with EEG-SMR based BCI increases sensorimotor connectivity in the resting-state for post-stroke hemiplegic patients

* This chapter was based on the author original article, “Tsuchimoto et al. Sensorimotor connectivity after motor exercise with neurofeedback in post-stroke patients with hemiplegia. Neuroscience, submitted.” The author has a right to use this dissertation.

3.1. Introduction

In post-stroke hemiplegic patients, synchronous electric oscillations and functional connectivity between brain regions are disrupted (Dubovik et al. 2012). These disruptions within the ipsilesional primary sensorimotor cortex accompany the additional, significant deficits in sensorimotor function after stroke (van Meer et al. 2010). As the brain initiates a dynamic process of functional remodeling in neural circuitry following post-stroke (Gauthier et al. 2008; Wang et al. 2010; Park et al. 2011), recovery of sensorimotor function is associated with the subsequent retrieval of intra- and inter-hemispheric functional connectivity and their oscillations within the sensorimotor system (Carter et al. 2010; van Meer et al. 2010). However, this process typically halts when it reaches a chronic stage, approximately six months post-stroke (Hermann and Chopp 2012).

Motor imagery has long been envisioned as a cognitive strategy to enhance post-stroke motor recovery (Langhorne et al. 2009). The neurophysiological rationale behind motor imagery treatment for post-stroke rehabilitation is that mental practice with motor content engages areas of the brain that associate movement execution (Cicinelli et al. 2006). Some studies reported that such motor imagery facilitates motor restoration in

post-stroke hemiplegic patients (Munzert et al. 2009; Ietswaart et al. 2011). Because such reiterated engagement of motor areas is intended to influence brain plasticity phenomena, the context of motor imagery is a critical factor in improving functional outcomes (Guillot et al. 2009). On the other hand, a randomized controlled trial study reported that there was no significant clinical improvement (Ietswaart et al. 2011), likely because, although motor imagery supports the cerebral and corticospinal excitability to promote the sensorimotor functional recovery, the extent and magnitude of sensorimotor activation during motor imagery is known to vary among participants (Munzert et al. 2009). Motor imagery task was subtle for maintaining task-compliance; thus, a direct quantitative measurement of cerebral functions modulated by motor imagery might preserve the reproducibility of the motor-related neural rehabilitation.

Electroencephalographic (EEG) or magnetoencephalographic (MEG) oscillatory signals are known electromagnetic analogues of sensorimotor oscillatory activity and are space- and frequency-specific (Pfurtscheller and Lopes da Silva 1999). The research presented in Chapter 2 extended previous work by showing that the alpha- and beta-band of the sensorimotor rhythm (SMR) are inversely correlated with excitatory levels in the sensorimotor cortices beneath the electrodes; thus, the up-conditioning of the desynchronization of these oscillations while imagining movement of a paralyzed finger helps recovery of the sensorimotor-related oscillation and functional connectivity in the ipsilesional hemisphere (Young et al. 2014). Clinical studies have reported up-conditioning of the desynchronization of alpha- and beta-band EEG/MEG oscillations

associated with partial improvement of finger motor function, and more recently, randomized control trials have documented its clinical effectiveness over other standardized interventions (Pichiorri et al. 2015), such as robotic exercises alone or combined with repeated motor imagery (Ramos-Murguialday et al. 2013). Although these clinical studies reported favorable outcomes in the relationships between oscillatory signals and behaviors, neurophysiological alterations in the targeted sensorimotor cortex have not yet been directly reported. Such direct evidence of brain changes has long been requested, as it would provide indispensable information of the mechanism underlying EEG oscillation-based neurofeedback as a therapeutic intervention for post-stroke finger paresis (Sitaram et al. 2017; Cervera et al. 2018).

The purpose of this research was to investigate neural modifications in the ipsilesional sensorimotor cortex induced by motor imagery paired with contingent, EEG-SMR based brain-computer interface (BCI), which accompanied by robotic exercise and neuromuscular electrical stimulation (NMES). To evaluate the possible neurophysiological rationale behind the BCI intervention, the present study employed resting-state functional connectivity measured with functional magnetic resonance imaging (rsfcMRI) as the primary outcome. rsfcMRI represents a reliable and promising means of assessing the intrinsic transfer of neural information within a network while avoiding many task-based confounds (Damoiseaux et al. 2006). Examining its relation to plasticity may illuminate the possible functional roles of spontaneous neural activity in both preserving and changing sensory and motor experience (Sporns 2013). Moreover, the intrinsic synchronized fluctuations in blood-oxygen-level dependent (BOLD) signal

intensity among regions, namely, the patterns of rsfcMRI, reflects network of connectivity resulting from a history of task-dependent activity or co-activation of functionally connected regions (Power et al. 2011). Furthermore, as spontaneous hemodynamic signals or local neural activities have previously been used for novel evaluation of motor learning or neurophysiological disease as neurophysiological biomarkers (Vahdat et al. 2011; Carter et al. 2012; Drysdale et al. 2017), rsfcMRI can be regarded as a robust neural trace reflecting experiential modifications.

To test the superiority of the proposed EEG-SMR based BCI intervention over other treatments, this study adopted a combination of standard medical treatments in rehabilitation with non-contingent intervention as a control experiment and a crossover design with double-blinded outcome evaluation of the neural activity in pre/post interventions.

3.2. Methods

3.2.1. Study design and oversight and patients recruitment

This was a confirmatory study with developmental phase II or III of repeated motor imagery exercise under EEG-SMR based BCI intervention with robotic and NMES. Note that a clinical trial is conducted following in each developmental phases; the new treatment has been tested to work in phase II study and compared in the viewpoint of the safety and effectiveness against the current standard treatment in phase III study. The neurophysiological effectiveness, which was defined as an enhancement of the intrinsic rsfcMRI in this exercise was evaluated to potentially increase the hypothesized beneficial

effects in neurophysiology to post-stroke hemiplegic patients in a double-blind, sham-controlled design and in a randomized crossover-designed study following consolidated standards of reporting trials (CONSORT) guidelines. To evaluate the neurophysiological effectiveness of BCI intervention in the point of view of clinical rehabilitation, the sham-controlled intervention is a simple combination of standard medical treatments in rehabilitation.

Intervention assignment was blinded for all participants and for the scientific-clinical personnel. The author analyzed the data while blinded to the interventions. This research was registered at the University hospital Medical Information Network (UMIN) Clinical Trials Registry - identifier UMIN000017233; the research had conducted from April 2015 to September 2017. The present study was conducted in accordance with the tenets of the Declaration of Helsinki and the study protocol was approved by a central medical ethics committee and the research board of each participating institute in Keio University Faculty of Science and Technology Bioethics Committee and Tokyo Metropolitan Rehabilitation Hospital Ethics Committee.

Because a previous study with EEG-SMR based BCI intervention for post-stroke hemiparesis reported a significant size effect (Cohen's $d = 0.91$) on the improvement of the affected upper limb motor score over the controll condition (Ramos-Murguialday et al. 2013), we adopted a large effect size ($\omega^2 = 0.25$) and calculated that 16 patients were needed to achieve a power of 95% (at a two-sided significance level of 5%). Anticipating a 10% loss due to withdrawal and a crossover effect, we planned to recruit 18 patients. Compared to the previous study evaluating acute changes in rsfcMRI with motor exercise

(Rajab et al. 2014), this sample size was also estimated to be sufficient to detect a mean improvement in neural modification by motor exercise with EEG-SMR based BCI intervention.

3.2.2. Patients

Patients were recruited from the Tokyo Metropolitan Rehabilitation Hospital, and eighteen patients were recruited, and characteristics of all patients' demographics, functional data, and lesion side are presented in Table 3-1. The purpose and experimental procedure were explained to the patients before the experiment, and all patients gave informed written consent. The criteria for inclusion in the study were more than two months from the first stroke onset (except for subarachnoid hemorrhage), an age from 20 to 80, no or moderate cognitive function deficits (Mini Mental State Examination; MMSE >23), no metal preventing MRI scanning, no medication such as anticonvulsants or antidepressant, no severe comorbidity and no psychiatric disorders. All patients participating in this study met these inclusion criteria. Although neglect was not set as an exclusion criterion, the patients in our study did not exhibit signs of neglect. We did not keep a log of patients who were screened for eligibility. Patients were randomly assigned the order in which the interventions would occur (either BCI - control or vice versa). None of the patients or therapists were able to identify the intervention assignment as reflected in the results of the placebo and motor function scales given below.

Table 3-1. Characteristics of all patients

ID	Gender	Age	Time since stroke (months)	Lesion side	Lesion location	Type of stroke	FMA upper limb		SIAS		MMSE
							Motor	Sensory	Finger-function	Upper extremities tone	
1	Male	53	100	Right	Thalamus	Hemorrhage	19	6	1A	1A	26
2	Male	67	7	Right	Cerebral peduncle	Infarction	57	10	4	2	30
3	Male	72	234	Left	Putamen	Hemorrhage	11	6	1A	1A	27
4	Male	52	3	Left	Corona radiata	Infarction	65	11	3	3	30
5	Male	71	180	Left	Putamen	Hemorrhage	21	10	1B	1A	25
6	Male	63	90	Right	Putamen	Hemorrhage	19	10	1B	1A	30
7	Female	67	5.5	Left	Basal ganglia Corona radiata	Infarction	16	10	1B	1A	29
8	Female	70	4	Right	Basal ganglia Corona radiata	Infarction	62	12	4	3	30
9	Male	47	4	Left	Putamen	Hemorrhage	30	10	1B	1A	27
10	Male	72	104	Right	Thalamus	Infarction	60	12	3	1A	30
11	Female	56	6	Left	Putamen	Hemorrhage	8	6	1A	2	30
12*	-	-	-	-	-	-	-	-	-		-
13	Female	53	7	Left	Putamen Corona radiata	Infarction	8	10	1A	2	28
14	Male	46	7	Left	Nucleus lentiformis Corona radiata	Infarction	12	10	1A	1A	29
15	Male	40	5	Right	Putamen	Hemorrhage	20	12	1B	1A	30

ID	Gender	Age	Time since stroke (months)	Lesion side	Lesion location	Type of stroke	FMA upper limb		SIAS		MMSE
							Motor	Sensory	Finger-function	Upper extremities tone	
16	Male	50	6.5	Left	Putamen	Hemorrhage	50	10	4	2	29
17	Male	48	5	Left	Corona radiata	Infarction	12	12	1A	1A	30
18	Male	54	4.5	Left	Putamen	Hemorrhage	12	6	1A	1A	30

3.2.3. Intervention protocols

This study was designed to assess the effectiveness of the EEG-SMR based BCI intervention for the post-stroke hemiplegic patients, including severe hemiplegic patients who cannot perform voluntary finger movements, and we employed the motor imagery task, which is a substitute for performing the actual movement. Paretic hand motor imagery with EEG-SMR based BCI intervention consisted of standard medical treatments with motor imagery (Zimmermann-Schlatter et al. 2008), robot-aided sensorimotor stimulation (Dobkin 2004), and NMES to paretic muscles (Bolton et al. 2004). A meta-analytical, systematic review of clinical studies has shown that these treatments are effective neurorehabilitation training regimens assists the finger or upper-limb motor functional recovery after stroke (Langhorne et al. 2009). All the components were functionally linked as follows (Figure 3-1). Throughout the experiment, the EEG was monitored over the ipsilesional and contralesional sensorimotor cortices in a bipolar manner: C3 (left) or C4 (right) position for one electrode, and its horizontal for the other electrode. First, to construct an EEG-SMR based BCI system that correctly detected increased excitability of the ipsilesional sensorimotor cortex during paretic hand motor imagery, the authors conducted a calibration session to extract the sensorimotor component of the EEG modulated by motor imagery. Before each intervention training, a classifier for each patient was calibrated following the protocol established previously (Ono et al. 2014; Ramos-Murguialday et al. 2013; Shindo et al. 2011). The patients were asked to imagine extension of the affected finger without actual execution during 5 s after voluntary relaxation for 5 s; thus, each trial lasted 10 s, the decoding session was

conducted without feedback for 15 trials. There was a 5 s interval between trials and the patients determined the start of the trials. In this calibration session, the patients performed the same task of imagining affected finger movement but received no feedback. The EEG montage and frequency band for deriving event-related EEG-SMR power attenuation in the subsequent BCI training sessions were determined from the EEG-SMR power attenuation results obtained in these sessions. The threshold of EEG-SMR activity necessary for sensorimotor feedbacks was determined in order to divide the EEG-SMR activities between rest and motor imagery using linear discrimination analysis. This calibration session was conducted for each intervention because the EEG results depended on the exact electrode positions, which may vary even if they were set as precisely as possible according to the international system (Neuper et al. 2006). In the training session, every 5 s per trial, the patients were repeatedly asked to kinesthetically imagine (not visual imagery) extending the paretic finger on the affected side. A total of 30 trials were successively conducted within 40−60 min. In cases where the EEG-SMR powers in the alpha (8−13 Hz) and beta (15−23 Hz) frequency bands were attenuated during motor imagery and a successful EEG-SMR power attenuation was discriminated by the decoder constructed in the calibration session, a motor-driven orthosis attached to the paretic hand was actuated to aid the finger-extending action, and NMES was simultaneously applied to the paretic finger extensor muscle (extensor digitorum communis). Successful discrimination was determined to have occurred when the alpha- and beta-band EEG-SMR activity during motor imagery was significantly attenuated from baseline resting activity continuously for 1 s, while in the control intervention,

sensorimotor feedbacks were given in all trials during the motor imagery period. In other words, sensorimotor stimulations were not provided in the trials in which the EEG-SMR power attenuation was not detected. On the other hand, in the controlled intervention, sensorimotor stimulations were given in all trials during motor imagery, irrespective of the actual EEG-SMR activity. Note here that in motor imagery, all patients avoided volitionally extending their paretic finger, and just performed the mental rehearsal of motor execution, since post-stroke hemiplegic patients often have accompanying pathophysiological co-contraction of finger flexors and associated reactions in proximal muscles. Patients performed one intervention on a given day and the other intervention 1 or 2 weeks later to minimize any carryover effect of the preceding intervention.

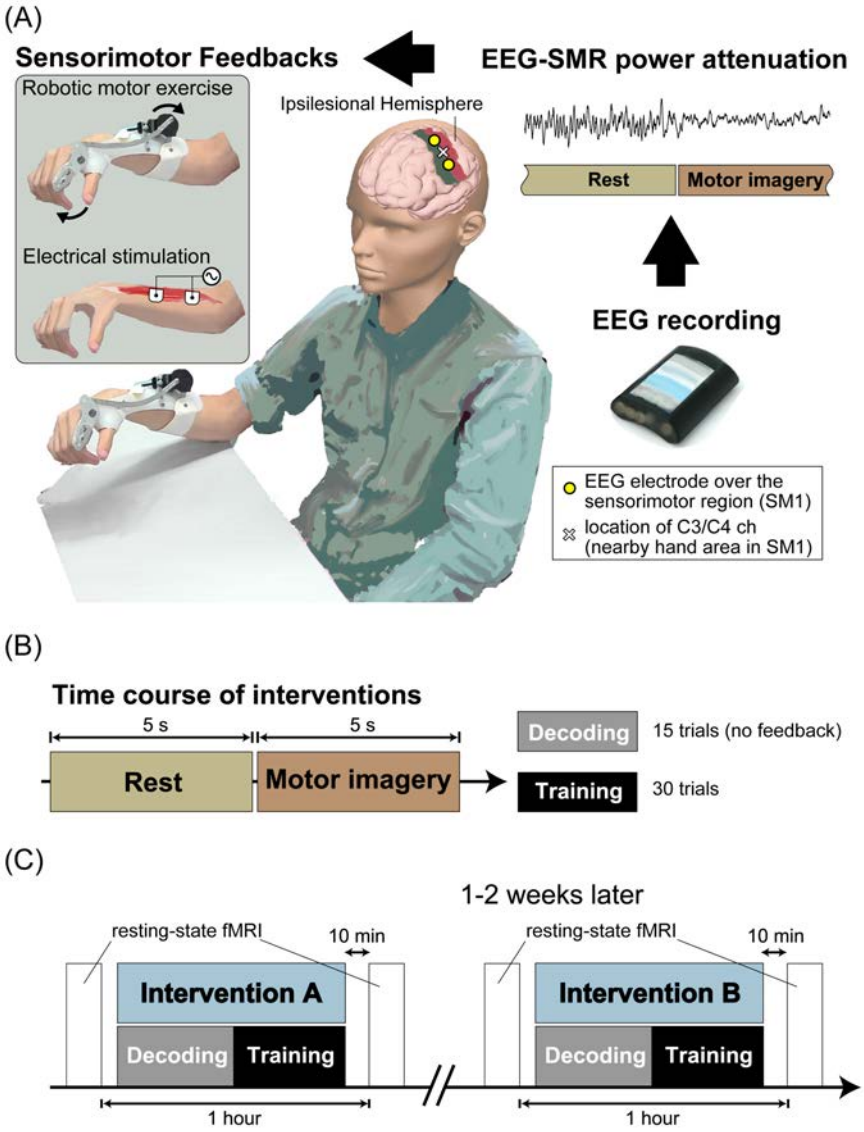

Figure 3-1. Experimental paradigms of EEG-SMR based BCI interventions

(A) Schematic of EEG-SMR based BCI intervention. The red and green regions in the ipsilesional hemisphere indicate the sensory and motor cortices (SM1), respectively. The EEG electrodes were placed 2 cm lateral and medial of the C3 (or C4) location that is located closest to the hand region in the sensorimotor cortex according to the international 10−20 systems. EEG data was transferred to a personal computer and processed online. The computer sent trigger signals to the motor-driven orthosis and electrical stimulator to provide sensorimotor feedbacks. (B) Time course in each session. After a rest period, patients were asked to kinesthetically imagine extension of the affected finger without actual execution. The decoding sessions consisted of 15 trials without sensorimotor feedbacks and the training session consisted of 30 trials. (C) Procedure and time course

of interventions. The resting-state fMRI was recorded in the timing of pre- and post-interventions and its interval was approximately one-hour. This study design was a crossover design and the other intervention was done 1−2 week after one treatment was conducted.

When EEG-SMR activities were successfully discriminated during motor imagery, robotic exercise treatment was used to drive the orthosis attached to the paralyzed finger and to facilitate enhancement of sensorimotor excitability. Rehabilitation robotics has some advantages over conventional treatment approaches (Norouzi-Gheidari et al. 2012). Advanced and intelligent robotic devices are able to provide consistent training and to measure performance with high reliability and accuracy (Dobkin, 2004). Most importantly, robots enable patients to train more correctly with brain activity in such neurofeedback treatments. In this study, the motor-driven robotic orthosis was attached to a servomotor and enabled the paralyzed finger to open using the metacarpophalangeal joint as a fulcrum. During every intervention before the sequence, the range of the orthosis was adjusted for aiding the paralyzed fingers to move from a pinching grip to an open position, and resulted in a change in metacarpophalangeal joint angle from approximately 45 degrees of flexion to 10 degrees of extension within 500 ms.

To enhance the excitability of the sensorimotor cortex, NMES was also applied during the training intervention. Previous studies showed that in moderately impaired post-stroke patients, assisted voluntary movement with NMES through surface electrodes is effective in improving finger and wrist motor functions (Kimberley et al., 2004). Electrical stimulation to the peripheral nerves induces changes to the sensorimotor

network and cortical reorganization (Cecatto and Chadi, 2007). Furthermore, electrical stimulation administered during the motor execution enhances neural plasticity, induced by the neural co-activation between peripheral stimulation input and motor output (Krucoff et al., 2016). Electrical stimulation coupled with task-related motor execution is more beneficial in enhancing neural plasticity rather than electrical stimulation alone (Knutson et al., 2015). Since post-stroke patients with severe hemiplegia might fail to perform sufficient motor execution, electrical stimulation was combined with the increased excitability of the sensorimotor cortex to promote functional motor recovery of the hemiplegic upper limb (Mukaino et al., 2014). Some research groups have also applied electrical stimulation only if the sensorimotor cortex is activated during motor imagery (Young et al., 2014; Biasiucci et al., 2018). In this research, a pair of self-adhesive electrodes was placed over the muscle belly of extensor digitorum communis muscle on the paralyzed side and the ground electrode was placed over the ulnar styloid process. The NMES pattern was 20 Hz with a single pulse width of 100 μs through a prototype electrical stimulator with maximum intensity of 100 V. The intensity of NMES was adjusted and fixed at just over motor threshold for evoking visible contraction of extensor digitorum communis muscle before each sequence (15−20 mA). Based on the present knowledge, the author cannot conclude either robotic assistance or neuromuscular electrical stimulation (or, combination of both) is best effective for the up-conditioning of the sensorimotor excitability. Thus, in this study, we employed combined robotic and electrical stimulation as an infallible neurofeedback (Shindo et al., 2011; Ono et al., 2014; Kawakami et al., 2016; Nishimoto et al., 2018).

3.2.4. Data acquisition in the interventions

EEG signals were recorded using 5 silver-silver chloride disc electrodes (φ = 10 mm) placed over the sensorimotor regions of both hemispheres. Electrodes were placed 20 mm lateral and medial to the C3 and C4 locations closest to the hand region in the sensorimotor regions according to the international 10－20 system. A bipolar derivation of the EEG was used to detect the EEG-SMR amplitude modulation focally around the sensorimotor cortices. The ground electrode was placed on the forehead. The signals were amplified (g.MOBIlab; Guger Technologies, Graz, Austria), bandpass filtered (0.5−100 Hz) and digitized (sampling frequency 256 Hz). EEG signals were recorded from both the ipsilesional and contralesional hemispheres for assessment, but only the ipsilesional signals were used as the source for EEG-SMR based BCI intervention.

Because patients were instructed to imagine movement without motor execution, surface electromyograms (EMG) of the affected limbs were monitored to avoid increases in EMG. The EMG of the extensor digitorum communis and flexor digitorum superficialis muscles on the affected upper limb were also recoded with the same amplifier (g.MOBIlab). The EMG signals monitored during the experiment were bandpass filtered (0.5－100 Hz) and digitized (sampling frequency 256 Hz). When increased EMG activity was observed between trials, patients were instructed to relax and after relaxation, the next trial was started.

The functional MRI (fMRI) data were collected on a 3-T MR scanner (Discover MR750w, GE Medical Systems, United Kingdom) with a single-shot gradient echo echo-

planar imaging (EPI) sequence: repetition time TR = 2500 ms; echo time TE = 30 ms; flip angle = 80 degrees; FOV = 212 × 212 mm^2, matrix = 64 × 64, slice thickness = 3.2 mm with 0.8 mm gap; slice order = ascending; voxel size = 3.31 × 3.31 × 3.2 mm^3; 36 axial slices parallel to the anterior commissure - posterior commissure line covering the whole brain, 240 scans. The patients were asked to lie still on a scanner bed in the dark for 10-min with their eyes opened and fixed on a small black cross.

3.2.5. Outcomes

EEG-SMR power attenuation during motor execution and/or motor imagery is correlated with sensorimotor cortex excitability (Ritter et al. 2009; Yuan et al. 2010), and it is hypothesized that the sensorimotor cortices become potentiated following the intervention. Thus, the primary outcome was measured with rsfcMRI between the sensory and motor cortices in the ipsilesional hemisphere during resting-state. Furthermore, rsfcMRI in the sensorimotor cortex provides a robust indication of the trace of the motor exercise because increased co-activation effects were reported in the sensory and motor cortices during the resting-state after motor exercise (Rajab et al. 2014), and increases in rsfcMRI associated with subsequent retrieval underlie behavioral recovery after brain injury (van Meer et al. 2010). Secondary outcomes included the clinical assessments of Fugl-Meyer Assessment (FMA) in the upper limb and Stroke Impairment Assessment Set (SIAS) for motor performance, and the total duration of EEG-SMR based BCI training when the contingent of the reduction in spectral power of the EEG-SMR had been met.

The latter has been established as a method of EEG evaluation reflecting the excitability of the sensorimotor cortex (Yuan et al. 2010; Takemi et al. 2013).

3.2.5. EEG data analyses

EEG signals were processed using MATLAB (MathWorks, Natick, MA, USA) and the power time courses of the EEG data were then calculated by a fast Fourier transform (FFT) with a 1-s moving time window, 84% overlap, and a time resolution of the power series of 16 Hz. Because the alpha-band EEG-SMR is known to reflect the prominent component of sensory cortex activity and the beta-band of the EEG-SMR reflects motor cortex activity, these frequencies were considered valid to reflect somatosensory activity and were used to construct a classifier to discriminate between baseline relaxed and kinesthetic motor imagery activity with linear discrimination analysis.

Since sensorimotor feedbacks were administered depending on successful alpha- and beta-band EEG-SMR power attenuation during the EEG-SMR based BCI training, the covariance of these frequency-bands EEG-SMR power modulations recorded over the rest-motor imagery period for each trial was calculated with a 0-lag Pearson correlation coefficient, subjected to Fisher's *z*-transformation and averaged over all trials. Moreover, the dose of sensorimotor excitability during motor imagery was calculated as the total duration of successful alpha- and beta-band EEG-SMR power attenuation, which was determined by the decoder.

3.2.6. fMRI data analyses

An outline of the analyses is shown in Figure 3-2. The fMRI data were pre-processed with Statistical Parametric Mapping (SPM12, Wellcome Department of Imaging Neuroscience, http://www.fil.ion.ucl.ac.uk/spm) on MATLAB. First, EPI volumes were applied to estimations of the spatial alignment with the first volume to obtain the motion parameters. The slice-timing correction was applied with the reference slice based on the middle of each TR. Each volume was subjected to re-slice processing after co-registration to the EPI template, and an averaged EPI volume was obtained. The lesion-side was then set to the left side by flipping the map from right to left based on the mid-sagittal line for patients with lesions on the right side. After the timing and spatial corrections, each volume was normalized according to the deformation field that was obtained by normalizing the mean volume to the EPI template and was resampled to 2-mm cubic voxels. The normalized volumes were then smoothed with an isotropic Gaussian kernel (Full width at half maximum; FWHM = 8 mm). These parameters were set in SPM function initialises as the default parameters.

After preprocessing, the BOLD signals were extracted in pre/post central regions, which defined by automated anatomical labeling (Tzourio-Mazoyer et al. 2002). The whole-brain, white matter, and cerebrospinal fluid signals also were extracted based on the anatomical region predefined by the SPM12 template, and each signal was then averaged. These signals and the six realignment parameters (three translations and three rotations) were used as nuisance variables to remove non-neural noise originating from head motion artifacts, cardiac effects, respiration, and scanner noise. The time series in

each voxel in the sensory and motor cortices were then band-pass (bidirectional 12th-order Butterworth) filtered to retain signals only within the range of 0.009 and 0.1 Hz, the same frequency filter that is traditionally used for preprocessing resting-state fMRI data (Meszlényi et al. 2017; Sasai et al. 2011). To calculate rsfcMRI between the sensory and motor cortices in the ipsilesional hemisphere, the BOLD signals were extracted according to the pre/post-central regions anatomically defined by automated anatomical labeling (AAL) (Figure 3-3(A)). After preprocessing for noise reduction, the fMRI time series was averaged in each region and the functional connectivity was calculated with a lag-0 Spearman's rank correlation, and Fisher's *z*-transformation was applied (Figure 3-3(B)(C)).

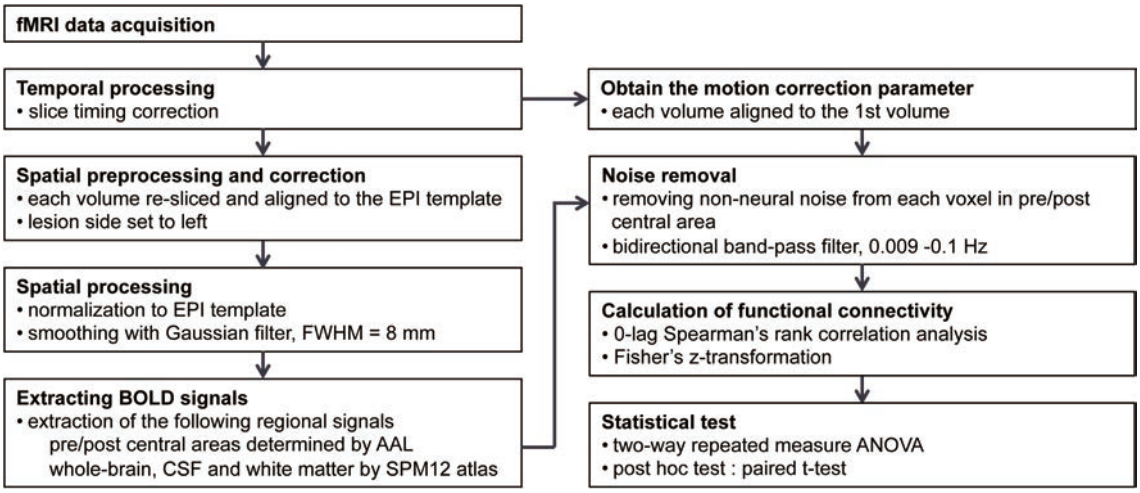

Figure 3-2. Outline of fMRI data preprocessing and analyses conducted in the current study

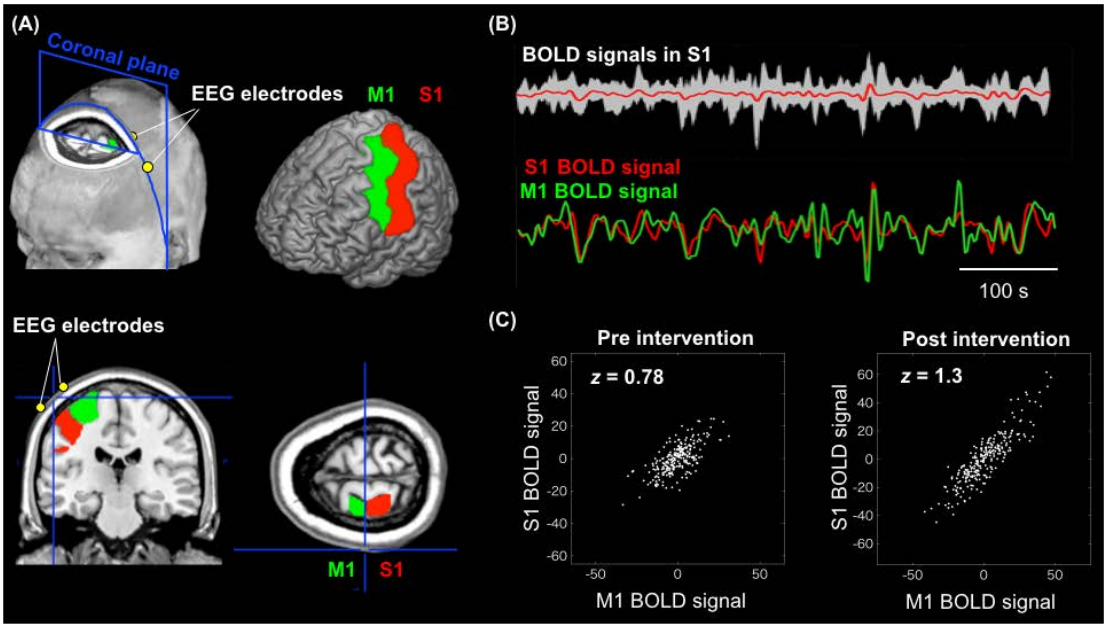

Figure 3-3. Analysis scheme for rsfcMRI calculation

(A) Montage of EEG electrode location and the sensorimotor region. EEG electrodes were placed across the C3 location on the central coronal plane. The red and green regions indicate the sensory cortex (red: S1) and motor cortex (green: M1), based on pre/post-central gyrus anatomically defined by automated anatomical labeling. The coronal and axial images depict sliced in the location of C3, where the intersection of the blue line is the C3 point. (B) Time course of BOLD signals. BOLD signal of each voxel in S1 and

M1 was extracted, and these time courses were averaged in each region (red line: S1 BOLD time course; green line: M1 BOLD time course). (C) Intrinsic correlation between S1 and M1 BOLD signals. Time series scatter plot depicts rsfcMRI between S1 and M1, which was obtained by 0-lag Spearman's rank correlation coefficient with an application of the Fisher's *z*-translation.

3.2.7. Statistical analyses

After performed the Levene's test for equality of variance in the dataset, a two-way repeated-measures analysis of variance (ANOVA) was used, and $p < 0.05$ was set as the significance level to determine whether motor exercise with EEG-SMR based BCI intervention was superior to the control intervention in the recovery of rsfcMRI after stroke. Post-hoc comparisons were used, and two-tailed paired-samples *t*-tests were used for the pre- and post-interventions. Similarly, after performed the Levene' test, the two-tailed paired-samples *t*-tests were performed to detect differences in the alpha- and beta-band EEG-SMR power covariance and to detect differences in the levels of sensorimotor stimulation between both interventions. Statistical tests were performed using the SPSS version 24 (IBM Corporation, United States).

3.3. Results

3.3.1. Parameters and results of the interventions

The interventions were conducted in 17 of the recruited patients, as one patient dropped out during the first fMRI recording due to feeling uncomfortable with the scanning noise. The interventions were completed as planned in the protocol. Among the 30 trials per patient during which paired EEG-SMR based BCI intervention was possible,

successful EEG-SMR attenuation during imagined finger extension was found in 68 ± 32% of the trials across patients (Table 3-2). Robotic and NMES feedback was subsequently given in each of these instances. In the control intervention, robotic and NMES were given during motor imagery for all 30 trials per patient. The scores of the upper limb FMA and the SIAS were unchanged through these 40-min interventions in both experimental and control sequences.

Table 3-2. Classifier parameters and the EEG-SMR based BCI success rate

ID	EEG-SMR based BCI		Control		BCI success rate, %	Intervention
	Alpha [Hz]	Beta [Hz]	Alpha [Hz]	Beta [Hz]		
1	9 – 11	22 – 26	9 – 13	28 – 32	37	BCI - Control
2	9 – 15	18 – 26	8 – 12	18 – 22	33	BCI - Control
3	9 – 13	21 – 25	10 – 14	18 – 23	11	Control - BCI
4	11 – 16	17 – 23	9 – 13	15 – 19	100	Control - BCI
5	14 – 18	23 – 30	8 – 13	18 – 22	93	BCI - Control
6	8 – 13	17 – 23	8 – 12	14 – 18	90	BCI - Control
7	9 – 13	16 – 25	9 – 13	16 – 21	73	BCI - Control
8	7 – 12	16 – 24	9 – 13	17 – 27	67	BCI - Control
9	7 – 11	17 – 21	9 – 13	17 – 21	94	BCI - Control
10	9 – 13	18 – 22	7 – 11	18 – 22	90	BCI - Control
11	9 – 13	16 – 20	8 – 11	17 – 21	87	Control - BCI
12	-	-	-	-	-	-
13	8 – 12	18 – 22	12 – 14	18 – 20	17	Control - BCI
14	8 – 12	18 – 21	13 – 17	21 – 25	43	Control - BCI
15	8 – 12	18 – 22	8 – 12	27 – 29	77	Control - BCI
16	12 – 14	20 – 22	11 – 13	21 – 24	90	BCI - Control
17	11- 15	18 – 22	12 – 16	24 – 28	100	Control - BCI
18	8 – 12	13 – 17	10 – 14	16 – 18	43	BCI - Control

3.3.2. Functional connectivity between ipsilesional sensory and motor cortices

Levene's test showed the equality of variance on rsfcMRI between the ipsilesional primary somatosensory and motor cortices in the pre- and post-interventions (Levene statistic = 0.783, $p = 0.508$). A two-way repeated measures ANOVA showed a significant time (pre and post) × intervention interaction ($F(1,16) = 5.346$, $p = 0.034$). There was no main effect of time ($F(1,16) = 1.640$, $p = 0.219$) or intervention ($F(1,16) = 0.007$, $p = 0.935$) alone. Post-hoc comparisons using a two-tailed paired-samples *t*-test revealed a significant increase in rsfcMRI for the EEG-SMR based BCI when comparing pre- and post-intervention ($t(16) = 2.693$, $*p = 0.016$) and no significant increase in rsfcMRI for the control intervention (Figure 3-4). The order and carryover effects of each intervention were not statistically significant (data not shown). Although one may claim that there might be different effects depending on the type of stroke, such as hemorrhage or infarction, or convalescent stage (2−6 months) or chronic stage (after the 7 months), there were no significant effects between pre- and post-intervention by motor imagery with EEG-SMR based BCI intervention (Figure 3-5).

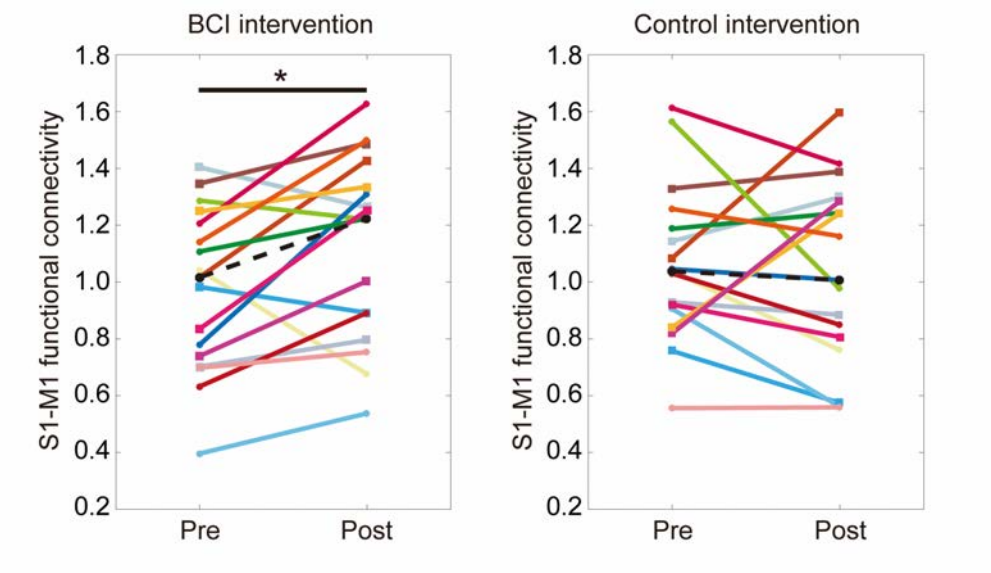

Figure 3-4. Functional connectivity between sensory and motor cortices pre- and post- intervention

Each solid-colored line indicates a patient and the dashed black line indicates the median value among patients ((A) EEG-SMR based BCI intervention and (B) sham-controlled intervention). Two-way repeated measure ANOVA showed a significant time (pre and post) × intervention ($p < 0.05$) interaction. Post-hoc comparisons using a two-tailed paired-samples *t*-test revealed a significant increase in rsfcMRI for the experimental intervention comparing pre- and post-neurofeedback intervention (*$p < 0.05$).

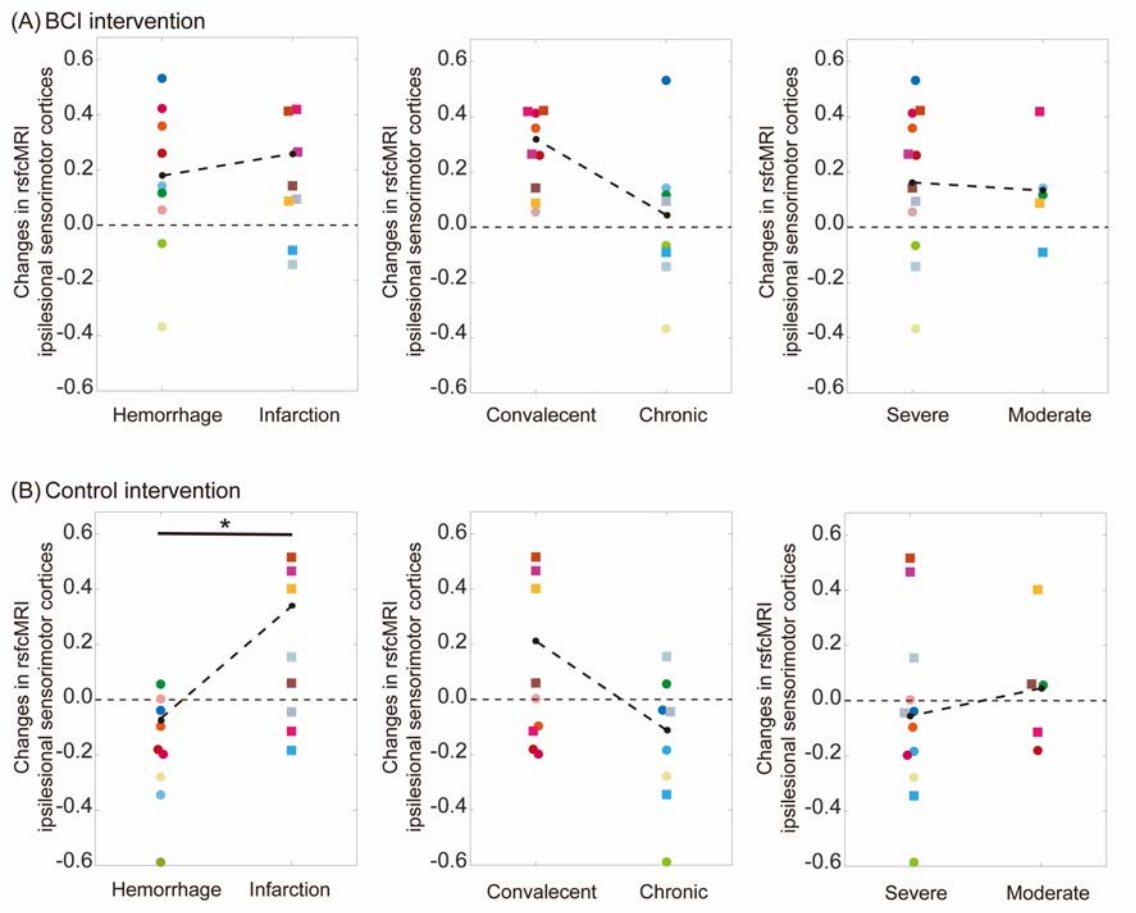

Figure 3-5. rsfcMRI changes of each intervention for different types of post-stroke hemiplegic patients

(A) Before performing the two-sample *t*-tests, Levene's tests were administered to assess the equality of variances, and there were no statistically significant to reject the null hypothesis that there is no difference in the variances. In the EEG-SMR based BCI intervention, a Bonferroni-corrected *t*-test showed that the neurofeedback has no significant effects on the rsfcMRI changes between the hemorrhage and infarction (Levene statistic = 0.382, $p = 0.546$; $t(15) = -0.109$, $p = 0.915$), between the convalescent stage (2-6 months) or chronic stage (after the 7 months) (Levene statistic = 1.603, $p = 0.225$; $t(15) = -2.300$, $p = 0.036$), or between impairment levels (moderate and severe) (Levene statistic = 1.590, $p = 0.227$; $t(15) = -0.222$, $p = 0.828$). (B) The sham-control intervention for infarction affects to rsfcMRI significantly higher than hemorrhage (Levene statistic = 1.789, $p = 0.201$; $t(15) = 2.978$, $p = 0.009$, Bonferroni-corrected *t*-test, $*p < 0.05$) and there is no significant deference of the rsfcMRI changes between the

convalescent and chronic stages (Levene statistic = 0.768, $p = 0.395$; $t(15) = -1.943$, $p = 0.071$), or impairment levels (Levene statistic = 0.512, $p = 0.485$; $t(15) = 0.616$, $p = 0.547$).

3.3.3. Relationship between changes rsfcMRI and EEG-SMR power modulation

Time-frequency maps of the EEG data during each intervention indicated that there was a specific frequency of EEG-SMR oscillatory modulation related to imagining paretic finger extending (Figure 3-6(A)). The covariance of the alpha- and beta-band EEG-SMR powers with the time course of the rest-and-motor imaging was significantly stronger in the EEG-SMR based BCI intervention than in the sham-controlled intervention (i.e., stronger desynchronization in the alpha- and beta-band while imagining extending the paretic finger; Levene statistic = 0.082, $p = 0.777$; Levene's test; $t(16) = 2.65$, $*p = 0.018$; two-tailed paired-samples *t*-test; Figure 3-6(B)). Although the number of trials with EEG-SMR attenuation rewarded by sensorimotor feedbacks in the EEG-SMR based BCI intervention was smaller than in the sham-controlled intervention, the total contingent duration of successful power attenuation of the ipsilesional EEG-SMR during motor imaging among all trials was significantly longer than during the control intervention (Levene statistic = 1.034, $p = 0.317$; Levene's test; $t(16) = 2.57$, $*p = 0.020$; two-tailed paired-samples *t*-test; Figure 3-6(C)).

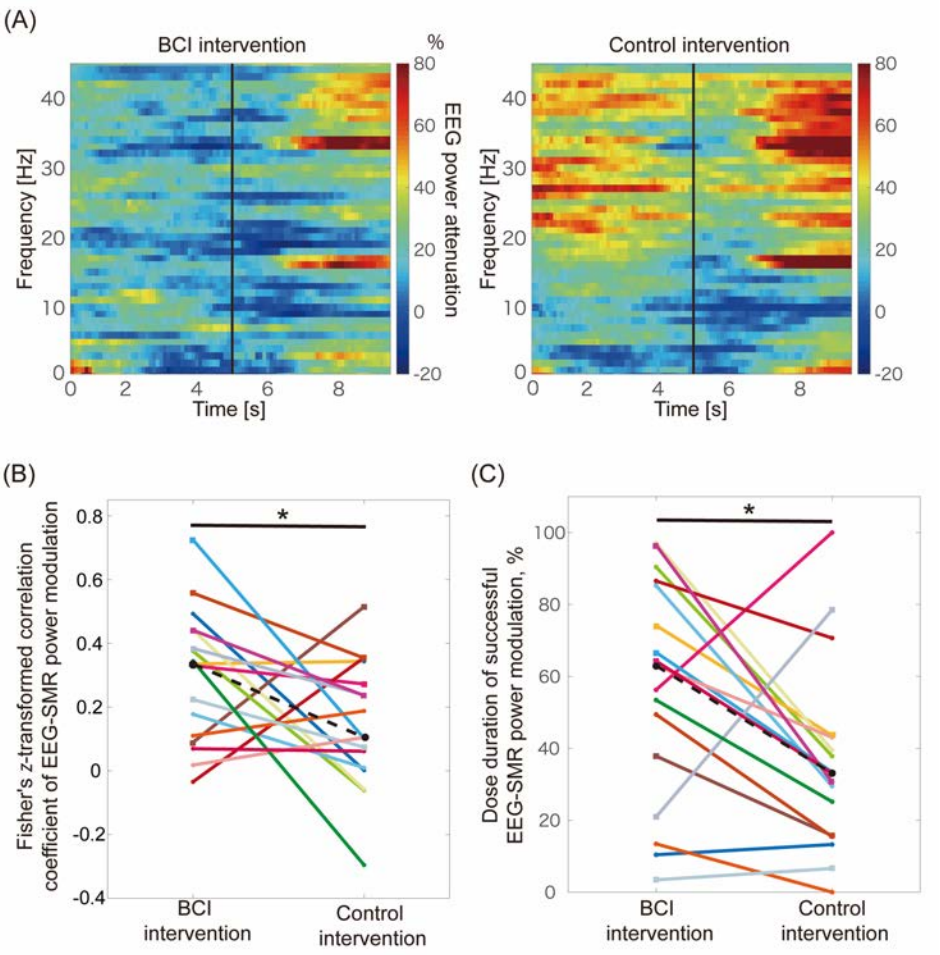

Figure 3-6. The results of EEG-SMR power modulation in each intervention

(A) Time-frequency map of EEG data in each intervention. The spectral power time course during EEG-SMR based BCI intervention (left panel) and during sham-controlled intervention (right panel). After the patients were instructed to relax during the period 0−5 s, they kinesthetically imagined opening the paralyzed finger during the period 5−10 s. Color bar indicates the relative power attenuation of EEG in each frequency. The power attenuation was normalized based on the power recorded during each decoding session. Negative values (blue colors) indicate attenuation from the reference power, and positive values (red colors) indicate increases from the reference power. (B) Comparison of the Fisher's *z*-transformed correlation coefficient of the alpha- and beta-band EEG-SMR modulations. The covariance of the alpha- and beta-band EEG-SMR power modulations along with the time course of the rest-to-motor-imagery in the EEG-SMR based BCI intervention was significantly higher than in the control intervention (two-tailed paired-samples *t*-test, $*p < 0.05$). The alpha- and beta-band covariance was calculated with the

0-lag Spearman's rank correlation coefficient, subjected to the Fisher's *z*-transformation and averaged over all trials. Each solid-colored line indicates a patient and dashed black line indicates the median value among patients. (C) The total contingent duration of the successful EEG-SMR power attenuation was discriminated. The success ratio of the EEG-SMR based BCI intervention was statistically stronger than that of the control intervention (two-tailed paired-samples *t*-test, $*p < 0.05$). Each solid-colored line indicates a patient and dashed black line indicates the median value among patients.

During the interventions, the alpha-band EEG-SMR power attenuation was associated with the beta-band EEG-SMR power attenuation, which resulted from the desynchronization of sensorimotor neural oscillation with motor imagery (Figure 3-7(A)). There was a statistically positive correlation between the alpha- and beta-band EEG-SMR power modulations (EEG-SMR based BCI intervention: Spearman's rank correlation $r = 0.62$, $p = 0.009$; sham-controlled intervention: Spearman's rank correlation $r = 0.78$, $p < 0.001$). Furthermore, when the sensorimotor feedbacks were administered in each intervention, a correlation was observed between the covariance of the alpha- and beta-band EEG-SMR power modulation and rsfcMRI changes in the ipsilesional sensory and motor cortices (EEG-SMR based BCI intervention: Spearman's rank correlation $r = 0.57$, $p = 0.018$; sham-controlled intervention: Spearman's rank correlation $r = 0.49$, $p = 0.049$; Figure 3-7(B)). In addition, the rsfcMRI changes were also considered with respect to the dose of EEG-SMR parameters reflecting sensorimotor excitability during intervention; plots showing the changes in rsfcMRI versus the covariance of the alpha- and beta-band EEG-SMR power modulations with the time course of the rest-to-motor-imagery, the dose duration of the desynchronized EEG-SMR, and the ratio of sensorimotor stimulated

trial were shown in Figure 3-8. Note that the covariance of the alpha- and beta-band EEG-SMR power modulations was obtained from the median value of all trials, which included not only the trials where sensorimotor feedbacks was administered but also unsuccessful trials in EEG-SMR based BCI intervention. There was no significant correlation between changes in the rsfcMRI in the ipsilesional sensorimotor cortices and the covariance of the alpha- and beta-band EEG-SMR modulations (EEG-SMR based BCI intervention: Spearman's rank correlation $r = 0.16$, $p = 0.55$; sham-controlled intervention: Spearman's rank correlation $r = 0.35$, $p = 0.17$) or the total duration that the EEG-SMR power was successfully attenuated (EEG-SMR based BCI intervention: Spearman's rank correlation $r = -0.15$, $p = 0.57$; sham-controlled intervention: Spearman's rank correlation $r = -0.41$, $p = 0.11$).

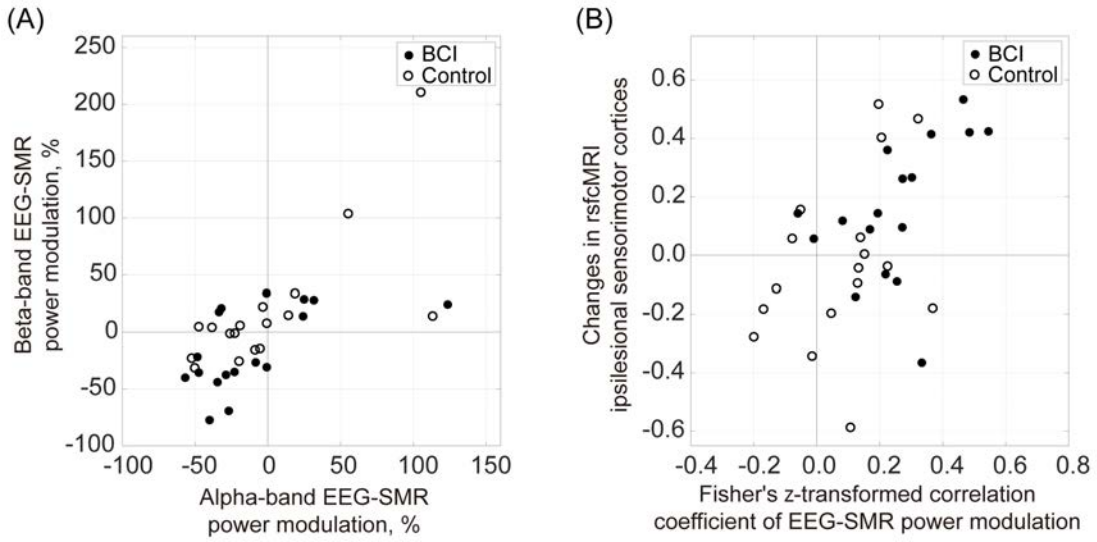

Figure 3-7. Relationship between the alpha- and beta-band EEG-SMR correlation coefficients during intervention and the relationship between the coefficients and rsfcMRI changes in the ipsilesional sensorimotor cortices

(A) The relationship between of the alpha- and beta-band EEG-SMR power modulation. Scatter plots of the relationship between the alpha- and beta-band EEG-SMR power modulation during each intervention (black: EEG-SMR based BCI intervention; white: sham-control intervention). These power modulations depict the median values through all trials in each intervention. There was the statistically positive correlation between the alpha- and beta-band EEG-SMR power modulations in each intervention (Spearman's rank correlation, $p < 0.05$). The alpha- and beta-band EEG-SMR powers were prone of more attenuated in the EEG-SMR based BCI intervention than in the sham-controlled intervention. (B) The relationship between the Fisher's *z*-transformed correlation coefficient of the alpha- and beta-band EEG-SMR power modulation and rsfcMRI changes. Scatter plots of the relationship between the Fisher's *z*-transformed correlation coefficient of the alpha- and beta-band EEG-SMR power modulation when the sensorimotor feedbacks were given and rsfcMRI changes in ipsilesional sensorimotor cortices (black: EEG-SMR-based BCI intervention; white: sham-controlled intervention). The correlation coefficient between the alpha- and beta-band EEG-SMR was calculated using the 2-s period before the sensorimotor administered to the paralyzed finger during the intervention. The changes in ipsilesional sensorimotor cortices rsfcMRI were the

statistically significant positive correlation with the EEG-SMR parameter in each intervention (Spearman's rank correlation, $p < 0.05$).

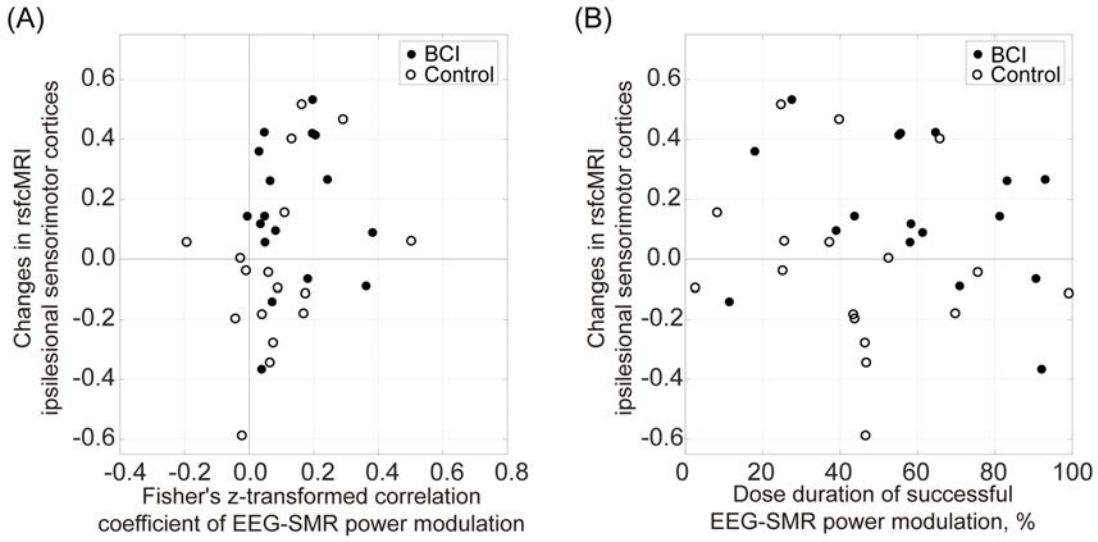

Figure 3-8. Relationship between the dose duration of successful EEG-SMR during intervention and rsfcMRI changes in the ipsilesional sensorimotor cortices

Scatter plots of the relationship between rsfcMRI changes and (A) the covariance of the alpha- and beta-band EEG-SMR modulations in all trials, or (B) the dose duration of the EEG-SMR power successfully attenuation. There was no statistically significant correlation in either of the parameters. Note that the covariance of the alpha- and beta-band EEG-SMR power modulations was obtained from all trials, which include not only the trial administered to sensorimotor feedbacks but also not-successful trials in BCI intervention.

3.3.4. Neurophysiological effects on contralesional sensory and motor cortices

Similar to the analysis of the ipsilesional rsfcMRI, Levene's test showed the equality of variance in the pre- and post-interventions (Levene statistic = 0.039, $p = 0.990$). A two-way repeated measures ANOVA on rsfcMRI between the contralesional sensory

and motor cortices in the pre- and post-interventions showed that there were no main effects of time ($F(1,16) = 2.51$, $p = 0.13$) and intervention ($F(1,16) = 0.11$, $p = 0.74$) or their interaction effect ($F(1,16) = 2.30$, $p = 0.15$, Figure 3-9(A)). In addition, there was no significant difference between neurofeedback and sham-controlled intervention in the synchrony of alpha- and beta-band EEG-SMR power modulation during motor imagery (Levene statistic = 0.104, $p = 0.750$; Levene's test; $t(16) = 2.00$, $p = 0.062$; two-tailed paired-samples *t*-test; Figure 3-9(B)).

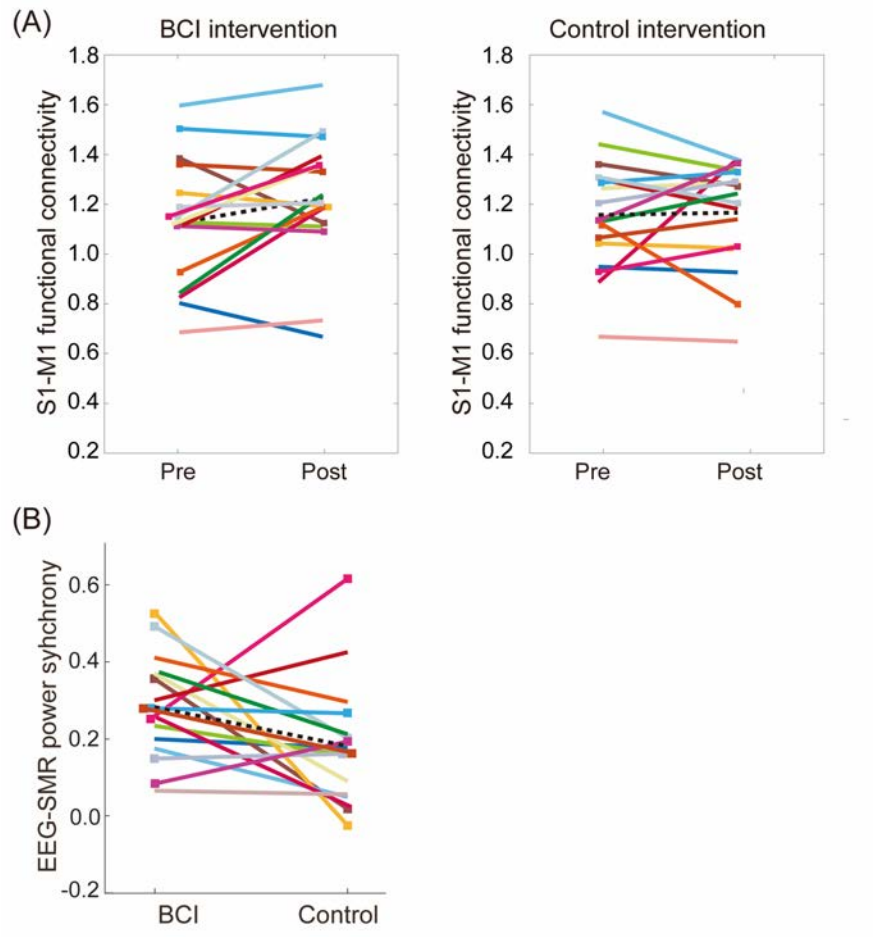

Figure 3-9. Neurophysiological effects on the contralesional sensory and motor cortices

(A) Functional connectivity between sensory and motor cortices pre- and post-intervention in neurofeedback and in sham-controlled intervention. Each solid-colored line indicates a patient, and the dashed black line indicates the mean value among patients. A two-way repeated measures ANOVA analysis shows that there were no main effects of time, intervention, or their interaction effect. **(B) Comparison of the Fisher's z-transformed correlation coefficient of the alpha- and beta-band EEG-SMR modulations in contralesional sensorimotor cortex during interventions.** Each solid-colored line indicates a patient, and the dashed black line indicates the mean value among patients. There was no significant difference between EEG-SMR neurofeedback and sham-controlled intervention.

3.4. Discussion

In this study, the authors examined whether motor imagery paired with contingent neurofeedback, which directly manipulates brain oscillations with EEG-SMR based BCI intervention, promotes the remediation of targeted neural activity within a 40-min intervention in a double-blind, sham-controlled design and a randomized controlled study. The present results indicate that contingent EEG-SMR based BCI intervention adjuvant to standard medical motor imagery of the affected hand results in significant increases in rsfcMRI in post-stroke hemiplegic patients not found in the sham-controlled intervention.

Since the motor imagery therapy induces somatotopic reorganization of cortical activation patterns in the sensorimotor area, an effective strategy for ensuring the quality of motor imagery has been proposed; this advanced strategy requires that patients learn how to control motor imagery enough to enhance sensorimotor cortical activity via visual and/or somatosensory feedback, which is reflected by monitored brain activity (Daly and Wolpaw, 2008; Chaudhary et al., 2016). In this study, EEG-SMR based BCI intervention was employed to facilitate the engagement of the sensorimotor cortices during motor imagery. Furthermore, the authors showed that EEG-SMR-based neurofeedback induced greater ipsilesional sensorimotor activity specifically compared to that of contralesional sensorimotor activity. The EEG-SMR recorded over the sensorimotor cortices reflects sensorimotor activity. The author have presented in Chapter 2 that the EEG-SMR recorded over the sensorimotor cortices reflects cortical activity. The EEG-SMR amplitude is diminished as the cortex is excited from the resting to the motor

execution/imagery period (Ritter et al. 2009). The power decrease in the EEG-SMR is thought to be coupled with disinhibition of intracortical GABAergic inhibition (Takemi et al. 2013), increased corticospinal tract excitability (Hummel et al. 2002), and increased excitability of spinal motor neuron pools (Takemi et al. 2015). EEG-SMR based BCI intervention helps to monitor and regulate these neurophysiological conditions, thus exogenously provoking the functional unmasking of the remaining motor fibers originating from the ipsilesional motor cortex. In EEG-SMR based BCI intervention, successful EEG-SMR power modulation during motor imagery was also rewarded by robotic movement support and NEMS. Providing reward following the success of the intended movement control facilitates motor learning and retention of the learned movement in post-stroke hemiplegic patients (Quattrocchi et al. 2017). Several recent RCT studies have revealed the effectiveness of motor restoration in post-stroke hemiplegic patients with EEG-SMR based BCI rehabilitation (Ramos-Murguialday et al. 2013; Pichiorri et al. 2015).

The significant differences in the duration of successful power attenuation of the ipsilesional EEG-SMR during motor imaging between the experimental BCI intervention and the sham-controlled intervention indicates that it is not the simple combination of motor imagery and sensorimotor feedbacks, but rather the contingency of imagery-induced EEG-SMR attenuation and robotic and NMES that is critical to up-conditioning the sensorimotor cortex co-activity. Since the alpha-band EEG-SMR is known to reflect the prominent component of the activity in sensory cortex and the beta-band EEG-SMR

maintains the activity in the motor cortex, the EEG-SMR based BCI intervention, which used the alpha- and beta-band EEG-SMR desynchronization as biomarkers, could be associated with rsfcMRI changes in the sensorimotor cortices. This result also supports the resting-state studies that illustrate the functional roles of spontaneous neural activity in preserving and continually rehearsing traces of sensory and motor experiences. Furthermore, rsfcMRI changes were associated with the Fisher's *z*-transformed correlation coefficient of the alpha- and beta-band EEG-SMR when the sensorimotor stimulations were administered rather than the dose duration of successful power attenuation of EEG-SMR in all trials during interventions. These results show that reinforcement learning and/or spike-timing-dependent plasticity may be possible neurophysiological mechanisms behind the BCI intervention (Ushiba and Soekadar 2016). Immediate and correct sensorimotor feedbacks as rewards within the framework of reinforcement learning constitute the critical ingredient for neural modification in the present case (Abe et al. 2011). Therefore, the present study provides important evidence that the integrating EEG-SMR and sensorimotor feedbacks at a neurophysiological level leads to rsfcMRI changes through the principle of closed-loop brain training.

The presence of rsfcMRI changes despite the absence of changes in the FMA or SIAS scores cannot be explained simply by different qualities of behavior, but may be explained by neural up-conditioning with BCI intervention. Biasiucci et al. (2018) reported that neuromuscular stimulation contingent on brain activity induced the functional motor recovery concomitant with an increase in EEG-based functional connectivity in sensorimotor areas in the affected hemisphere. The spatial resolution of

the EEG, however, is limited to identifying the cortical activity in sensory and motor cortices, and it is still unclear which EEG-based neurofeedback affects sensory and motor cortices. Hence, our results are compatible with the results reported by Biasiucci's group and directly addressed the neurophysiological evidence with rsfcMRI between the sensory and motor cortices. A previous study on post-stroke rsfcMRI analysis in rats reported that improvement of rsfcMRI between the sensory and motor cortices in the ipsilesional hemisphere coincided with the recovery of sensorimotor performance in the acute stage of post-stroke (van Meer et al. 2010). Although it is known that rsfcMRI in the sensorimotor cortices represents an important factor concerning the level of motor function of the paralyzed hand and its recovery, it has not been directly determined what strength of measured rsfcMRI is necessary for inducing clinically meaningful motor functional recovery (Wang et al. 2010; Park et al. 2011). As an estimation of an effective rsfcMRI change, for example, a motor learning study in healthy participants reported that an approximately 0.1 points rsfcMRI change was necessary for significant motor performance improvement (McGregor and Gribble 2017). Furthermore, in a stroke study, rsfcMRI changes of approximately 0.1 points accompanied paralyzed hand motor performance recovery (Westlake and Nagarajan 2011). In the present study, the increase in rsfcMRI following a single, 40-min training with EEG-SMR based BCI intervention was confirmed to be at least as equivalent to the changes observed in these previous studies. The results of the present research were interpreted as indicating greater involvement of the ipsilesional sensorimotor cortical co-activation during contingent intervention than during control intervention. The brain's intrinsic sensorimotor

oscillation in patients with hemiplegia collapses, and its motor-related response is unstable (Grefkes and Fink 2014); thus, it is feasible that rewarding the desynchronization of ipsilesional EEG oscillations with contingent movements of a finger orthosis accompanied by NMES to the paretic finger extensor muscle potentiates the cortical motor response during motor imagery.

Chapter 4 : Conclusion

The purpose of this dissertation was to determine the relationship between intrinsic sensorimotor rhythm (SMR) of electroencephalographic (EEG) power modulation and the sensorimotor cortical activity in the resting-state, and to reveal the neurophysiological effectiveness of EEG-SMR based brain-computer interface (BCI) intervention on the sensorimotor cortex in post-stroke hemiplegic patients. The author approached these questions using EEG and functional magnetic resonance imaging (fMRI) for measurements of the intrinsic cortical activities.

In Chapter 2, the author demonstrated EEG-fMRI simultaneous recording to identify the brain regions of which activities are correlated with the intrinsic EEG-SMR power modulations in the resting-state. As a result, the author demonstrated two main findings; (1) the intrinsic EEG-SMR power modulation was associated with the activity in the sensorimotor cortex, and (2) the brain region in the sensorimotor cortex which was associated with alpha-band EEG-SMR power modulation was located posterior to the brain region which was associated with the beta-band EEG-SMR power modulation. These results suggested that the alpha-band EEG-SMR modulation in the resting-state was referred to the sensory cortical activity whereas the beta-band EEG-SMR modulation in the resting-state was attributed to the motor cortical activity.

Chapter 3 revealed the neurophysiological effectiveness of EEG-SMR based BCI intervention on the sensorimotor cortex in post-stroke hemiplegic patients. Since covariance of the signals in the ipsilesional somatosensory and motor cortices in the

resting-state fMRI, or resting-state functional connectivity MRI (rsfcMRI), is a known predictive biomarker of motor recovery in post-stroke, the author evaluated the rsfcMRI changes via the confirmatory study with developmental phase II or III in a double-blind, sham-controlled, randomized crossover design following the consolidated standards of reporting trials guidelines. The author demonstrated that rsfcMRI in the ipsilesional sensory and motor cortices was increased after motor imagery aided by EEG-SMR based BCI compared with the sham-control intervention. In addition, the changes in rsfcMRI correlated with the mean covariance between alpha- and beta-band EEG-SMR power modulations when the sensorimotor feedbacks were administered rather than the mean covariance in all trials (involving trials not given the feedbacks) or the total duration of the EEG-SMR attenuations. These results suggested that peripheral sensory stimulation coupled with central voluntary motor signals is a key to have a neuromodulation effect on the targeted cortical regions in post-stroke hemiplegic patients rather than simple combination of motor volition and peripheral sensory stimulation.

It has been known for the decades that EEG-SMR amplitude is decreased during motor attempt or imagery, and such event-related power decrease has been interpreted as the enhancement of sensorimotor cortical activities. However, the cortical origins of EEG-SMR itself observed in the resting-state have not precisely described so far due to a limitation of accessible analytics. To overcome this issue, the author first employed a multimodal and simultaneous recording with EEG and fMRI to perform a statistically valid search of cortical regions in which intrinsic resting-state activity is correlated with EEG-SMR. Successful identification of the sensory and motor cortices as a signal origin

of EEG-SMR guarantees physiological relevance of the use of EEG-SMR in BCI-based rehabilitation.

Another MRI based assessment on the cortical activity in this dissertation also provide physiological relevance of the BCI-based rehabilitation. The study clearly identified increased coupled activity of sensory and motor cortices following single-day intervention of EEG-SMR based BCI, rather than the sham-control intervention, which is a simple combination of standard medical treatments in rehabilitation. This result was notable since it was the first report to provide neurophysiological effectiveness of BCI interventions that had been too often explored with regard to behavioral effects only. Moreover, the double-blind, sham-controlled study design is highly valuable in this context to disentangle unspecific intervention effects.

The most of existing each of these motor exercise therapies for post-stroke hemiplegic patients is limited their efficacy (Langhorn et al. 2009); for example, the sever hemiplegic patients with difficulties in voluntary movement profits less the efficacy from robot-aided motor exercise. In addition, motor imagery therapy is not guaranteed its imagery quality enough to enhance the ipsilesional sensorimotor activity. Motor imagery aided by EEG-SMR based BCI intervention, on the contrary, promotes neuromodulatory effects in the neurologically relevant cortical regions for these sever hemiplegic patients, suggesting BCI is a one-and-only assessible treatment.

However, some limitations still exist in terms of the differences between resting-state and sensorimotor task or healthy participants and stroke patients. It remains a testable hypothesis that a similar mechanism in post-stroke patients may underlie the

intrinsic EEG-SMR modulation during a motor task and during a resting-state. The remaining issues will be assessed to the design of the EEG-SMR based BCI intervention affected the individual sensorimotor activities in the resting-state, referring to the findings of this dissertation. The author could not provide any information as to what extent improvements in rsfcMRI in ipsilesional sensory and motor cortices form a single-day intervention would contribute to motor recovery if the intervention continued. Also, the author did not verify its retention of the neurophysiological effect due to minimization of patients burden as a hospitalization policy. Since it is known that daily intervention improves motor function (Ramos-Murguialday et al. 2013; Pichiorri et al. 2015; Ushiba and Soekadar 2016), it is expected that retention or convolutional of the neurophysiological effect would last beyond a single day and a future study will be warranted to the test this hypothesis. The author also did not show if the stratified analyses for neurophysiological effects differed in the post-stroke patients. Although the present results illustrated a tendency for rsfcMRI changes in subgroup analyses, the author did not have a sufficient sample size to detect the differences between some biases. In this study, the patients' sample suffered from a gender bias (14 male and 3 female), a mixture of subacute and chronic patients, as well as various levels of impairment and a mix of right and left hemisphere lesions. Further studies will be warranted to identify differences in neurophysiological effects with neurofeedback intervention. Although there was some different neurophysiological effectiveness of EEG-SMR based BCI intervention depending on the type of strokes, such as hemorrhage or infarction, and convalescent or chronic stage, this study is not designed for identification of differences between post-

stroke subtypes. It also remains unclear that EEG-SMR components are associated with activities in the sensory and motor cortices in the resting-state, in common with post-stroke patients admitting to stroke subtypes. In other words, further studies should be conducted to identify the frequency components of EEG-SMR which reflected the sensorimotor activities, and the identification of changes of the intrinsic functional activities after EEG-SMR based BCI is warranted in the future. Having knowledge of recovery patterns of different stroke subtypes can help allocate beneficial EEG-SMR based BCI rehabilitation resources effectively to patients. Lastly, the authors also have no information on the identification of additional regions throughout the brain that underwent rsfcMRI changes. Because the sensorimotor system receives a cascade of signals from the premotor cortex or the supplementary motor area and functional information, such as internal motivation, exercise planning, and motor learning, from upstream areas such as the basal ganglia, cerebellum, or prefrontal cortex (Yin and Knowlton 2006; Vahdat et al. 2011), in the future, the author intends to extend this approach with a more comprehensive analysis of activities in a wide range of brain areas as well as by an examination of the long-term retention of the effect.

The present finding suggests that the EEG-SMR based BCI that provides the sensorimotor feedbacks contingent upon the ipsilesional alpha- and beta-band SMR modulation induces the co-activation of the sensorimotor cortex in the resting-state. The neurophysiological effectiveness behind EEG-SMR based BCI may be derived from Hebbian-like plasticity in the sensorimotor cortex, suggesting the importance of the sensorimotor closed-loop neurofeedback system for post-stroke patients with hemiplegia.

Since the author provided the evidence that the intrinsic EEG-SMR modulation reflects sensorimotor cortical activities in the resting-state, it encourages further development of EEG-SMR based BCI as a customized neurorehabilitation system for various stroke subtypes, advancing ideal neuroscience based rehabilitation.

Acknowledgements

This dissertation has been written under the direction and guidance on Associate Professor Junichi Ushiba in Department of Biosciences and Informatics, Faculty of Science and Technology, Keio University, Japan.

Firstly, I would like to express my deepest gratitude to my advisor, Associate Professor Junichi Ushiba, for the continuous support of my Ph.D. study and related research. His guidance helped me in all the time of research and daily life during my Ph.D. course. Thanks to his unique and sophisticated philosophy in science, I could have carefully finished my Ph.D. studies. Honestly, I respect him so much that I would like to be like him someday. I could not have expressed my gratitude to him enough, and I will through my research. I will never forget what he has done for me.

I am grateful to all the professors on my dissertation committee, Professor Kotaro Oka, Professor Yasubumi Sakakibara in Department of Biosciences and Informatics, Faculty of Science and Technology, and Professor Eiji Okada in Department of Electronics and Electrical Engineering, Faculty of Science and Technology, thankfully agreed to sit on my committee and made valuable comments on my Ph.D. study.

I would also like to thank Professor Emeritus Yutaka Tomita and Professor Emeritus Satoshi Honda in Keio University. Their scientific philosophy has brought me variable insights into the science and engineering fields.

I appreciate Dr. Takashi Hanakawa who is Director in Department of Advanced Neuroimaging, Integrative Brain Imaging Center, National Center of Neurology and Psychiatry, for introducing me to advanced neuroimaging and bring me to sophisticated insights into the neurophysiological field. Furthermore, I am also grateful for the much supports from Drs. Shindo Keiichiro, Fujiko Hotta, Hiroki Ebata, and Professor Meigen Liu in the Department of Rehabilitation Medicine, Keio University School of Medicine, and all staffs in Saiseikai Kanagawa-ken Hospital and Tokyo Metropolitan Rehabilitation Hospital. Their support helped me to conduct the EEG-fMRI study and BCI intervention for post-stroke hemiplegic patients.

I would like to express my gratitude to Associate Professor Junichi Ushiyama in Faculty of Environment and Information Studies, Keio University and Associate Professor Kotaro Takeda in Faculty of Medical Technology, Fujita Health University, and Drs. Shoko Kasuga, Kenji Kato and Nobuaki Mizuguchi for giving me helpful advice

to improve my research, and to Drs. Takashi Ono, Mitsuaki Takemi, and Ryosuke Matsuya for having variable knowledge of EEG and fMRI measurement in BCI studies. It is obvious that the experience of intensive discussion with them are indispensable for my life.

I would also like to thank all members in Ushiba laboratory, and especially Mr. Takaharu Suzuki, Mr. Akito Kosugi, Ms. Midori Kodama, Mr. Kenichi Takasaki, and Mr. Kohei Okuyama for their warm encouragement as Ph.D. candidates each other. Further expression of my gratitude goes to Ms. Shuka Shibusawa and Ms. Kihiro Yuasa for their help to conduct EEG-fMRI simultaneous recording and BCI training for post-stroke hemiplegic patients. I also thank Ms. Sayoko Ishii, Ms. Kumi Nanjo, and Ms. Sawako Ohtaki for their technical support and taking care of a variety of paperwork.

Furthermore, I would like to appreciate Dr. Ariel Graff, who is Head of Multimodal Imaging Group and all members of his group in the Centre for Addiction and Mental Health, Toronto, Canada. I also thank Drs. Yusuke Iwata, Fernando Caravaggio, Eric Plitman and all members in Graff's laboratory for an intensive discussion about multimodal MRI analyses in Canada.

I am deeply grateful to Drs. Kazuhiko Higashi and Hikaru Kawauchi to mutually enhance each other with talking about dreams and philosophy to the science.

Lastly and most importantly, special thanks also go to Ms. Natsumi Momose, for continuous supporting me and intensive discussion anytime and anywhere. Also, I wish to thank my family; my parents, brothers and sisters for supporting me throughout my life.

To them I dedicate this dissertation.

Funding source

The studies in Chapter 2 and Chapter 3 were partially supported by Strategic Research Program for Brain Sciences from the Japan Agency for Medical Research and Development (16dm0107033h005) and (17he0402255h0004), Grants-in-Aid for the Japan Society for the Promotion of Science (JSPS) Fellows (17J04792), Grant-in-Aid for Scientific Research (C), MEXT (16K01469), and Keio Institute of Pure and Applied Sciences (KiPAS) research program.

References

Abe M, Schambra H, Wassermann EM, Luckenbaugh D, Schweighofer N, Cohen LG. Reward improves long-term retention of a motor memory through induction of offline memory gains. *Curr Biol* 21(7), 557−562, 2011.

Allen PJ, Josephs O, Turner R. A method for removing imaging artifact from continuous EEG recorded during functional MRI. *NeuroImage* 12(2), 230−239, 2000.

Allen PJ, Polizzi G, Krakow K, Fish DR, Lemieux L. Identification of EEG events in the MR scanner: The problem of pulse artifact and a method for its subtraction. *NeuroImage* 8(3), 229−239, 1998.

Ang KK, Chua KSG, Phua KS, Wang C, Chin ZY, Kuah CWK, Low W, Guan C. A randomized controlled trial of EEG-based motor imagery brain-computer interface robotic rehabilitation for stroke. *Clin EEG Neurosci* 46(4) 310−320, 2015.

Arroyo S, Lesser RP, Gordon B, Uematsu S, Jackson D, Webber R. Functional significance of the mu rhythm of human cortex: An electrophysiologic study with subdural electrodes. *Electroencephalogr Clin Neurophysiol* 87(3), 76−87, 1993.

Babiloni C, Capotosto P, Brancucci A, Del Percio C, Petrini L, Buttiglione M, Cibelli G, Romani GL, Rossini PM, Arendt-Nielsen L. Cortical alpha rhythms are related to the anticipation of sensorimotor interaction between painful stimuli and movements: A high-resolution EEG study. *J Pain* 9(10), 902−911, 2008.

Babiloni C, Del Percio C, Arendt-Nielsen L, Soricelli A, Romani GL, Rossini PM, Capotosto P. Cortical EEG alpha rhythms reflect task-specific somatosensory and motor interactions in humans. *Clin Neurophysiol* 125(10), 1936−1945, 2014.

Badillo S, Vincent T, Ciuciu P. Group-level impacts of within- and between-subject hemodynamic variability in fMRI. *NeuroImage* 82, 433−448, 2013.

Bauer M, Oostenveld R, Peeters M, Fries P. Tactile spatial attention enhances gamma-band activity in somatosensory cortex and reduces low-frequency activity in parieto-occipital areas. *J Neurosci* 26(2), 490−501, 2006.

Baumann SB, Noll DC. A modified electrode cap for EEG recordings in MRI scanners. *Clin Neurophysiol* 110(12), 2189−2193, 1999.

Bayraktaroglu Z, von Carlowitz-Ghori K, Curio G, Nikulin VV. It is not all about phase: Amplitude dynamics in corticomuscular interactions. *NeuroImage* 64(1), 496−504, 2013.

Bazanova OM, Vernon D. Interpreting EEG alpha activity. *Neurosci Biobehav Rev* 44, 94−110, 2014.

Beckmann CF, DeLuca M, Devlin JT, Smith SM. Investigations into resting-state connectivity using independent component analysis. *Philos Trans R Soc Lond B Biol Sci* 360(1457) 1001−1013, 2005.

Ben-Simon E, Podlipsky I, Arieli A, Zhdanov A, Hendler T. Never resting brain: Simultaneous representation of two alpha related processes in humans. *PLoS ONE* 3(12), e3984(9 pages), 2008.

Ben-Simon E, Podlipsky I, Okon-Singer H, Gruberger M, Cvetkovic D, Intrator N, Hendler T. The dark side of the alpha rhythm: fMRI evidence for induced alpha modulation during complete darkness. *Eur J Neurosci* 37(5), 795−803, 2013.

Berger B, Minarik T, Liuzzi G, Hummel FC, Sauseng P. EEG oscillatory phase-dependent markers of corticospinal excitability in the resting brain. *BioMed Res Int* 2014, 936096(8 pages), 2014.

Biasiucci A, Leeb R, Iturrate I, Perdikis S, Al-Khodairy A, Corbet T, Schnider A, Schmidlin T, Zhang H, Bassolino M, Viceic D, Vuadens P, Guggisberg AG, Millán J d R. Brain-actuated functional electrical stimulation elicits lasting arm motor recovery after stroke. *Nat Commun* 9, 2421(13 pages), 2018.

Biernaskie J, Corbett D. Enriched rehabilitative training promotes improved forelimb motor function and enhanced dendritic growth after focal ischemic injury. *J Neurosci* 21(14), 5272−5280, 2001.

Birbaumer N, Kubler A, Ghanayim N, Hinterberger T, Perelmouter J, Kaiser J, Iversen I, Kotchoubey B, Neumann N, Flor H. The thought translation device (TTD) for completely paralyzed patients. *IEEE Trans Rehabil Eng* 8(2), 190−193, 2000.

Biswal B, Yetkin FZ, Haughton VM, Hyde JS. Functional connectivity in the motor cortex of resting human brain using echo-planar MRI. *Magn Reson Med* 34(4), 537−541, 1995.

Blankertz B, Tangermann M, Vidaurre C, Fazli S, Sannelli C, Haufe S, Maeder C, Ramsey L, Sturm I, Curio G, Müller K-R. The berlin brain-computer interface: Non-medical uses of BCI technology. *Front Neurosci* 4, 198(17 pages), 2010.

Bloom JS, Hynd GW. The role of the corpus callosum in interhemispheric transfer of information: Excitation or inhibition? *Neuropsychol Rev* 15(2), 59−71, 2005.

Bolton DAE, Cauraugh JH, Hausenblas HA. Electromyogram-triggered neuromuscular stimulation and stroke motor recovery of arm/hand functions: A meta-analysis. *J Neurol Sci* 223(2), 121−127, 2004.

Bonmassar G, Purdon PL, Jääskeläinen IP, Chiappa K, Solo V, Brown EN, Belliveau JW. Motion and ballistocardiogram artifact removal for interleaved recording of EEG and EPs during MRI. *NeuroImage* 16(4), 1127−1141, 2002.

Bouton CE, Shaikhouni A, Annetta NV, Bockbrader MA, Friedenberg DA, Nielson DM, Sharma G, Sederberg PB, Glenn BC, Mysiw WJ, Morgan AG, Deogaonkar M, Rezai AR. Restoring cortical control of functional movement in a human with quadriplegia. *Nature* 533(7602), 247−250, 2016.

Bouzit M, Burdea G, Popescu G, Boian R. The Rutgers Master II-new design force-feedback glove. *IEEEASME Trans Mechatron* 7(2), 256−263, 2002.

Boynton GM, Engel SA, Glover GH, Heeger DJ. Linear systems analysis of functional magnetic resonance imaging in human V1. *J Neurosci* 16(13), 4207−4221, 1996.

Braun S, Kleynen M, van Heel T, Kruithof N, Wade D, Beurskens A. The effects of mental practice in neurological rehabilitation; a systematic review and meta-analysis. *Front Hum Neurosci* 7, 390(23 pages), 2013.

Braun SM, Beurskens AJ, Borm PJ, Schack T, Wade DT. The effects of mental practice in stroke rehabilitation: A systematic review. *Arch Phys Med Rehabil* 87(6), 842−852, 2006.

Brogårdh C, Sjölund BH. Constraint-induced movement therapy in patients with stroke: A pilot study on effects of small group training and of extended mitt use. *Clin Rehabil* 20(3), 218−227, 2006.

Brovelli A, Ding M, Ledberg A, Chen Y, Nakamura R, Bressler SL. Beta oscillations in a large-scale sensorimotor cortical network: Directional influences revealed by Granger causality. *Proc Natl Acad Sci U S A* 101(26), 9849−9854, 2004.

Buch E, Weber C, Cohen LG, Braun C, Dimyan MA, Ard T, Mellinger J, Caria A, Soekadar S, Fourkas A, Birbaumer N. Think to move: A neuromagnetic brain-computer interface (BCI) system for chronic. *Stroke* 39(3), 910−917, 2008.

Bundy DT, Souders L, Baranyai K, Leonard L, Schalk G, Coker R, Moran DW, Huskey T, Leuthardt EC. Contralesional brain-computer interface control of a powered exoskeleton for motor recovery in chronic stroke survivors. *Stroke* 48(7), 1908−1915, 2017.

Buzsáki G, Anastassiou CA, Koch C. The origin of extracellular fields and currents--EEG, ECoG, LFP and spikes. *Nat Rev Neurosci* 13(6), 407−420, 2012.

Caporale N, Dan Y. Spike timing-dependent plasticity: A Hebbian learning rule. *Annu Rev Neurosci* 31(1), 25−46, 2008.

Carson RG, Kennedy NC. Modulation of human corticospinal excitability by paired associative stimulation. *Front Hum Neurosci* 7, 823(28 pages), 2013.

Carter AR, Astafiev SV, Lang CE, Connor LT, Rengachary J, Strube MJ, Pope DLW, Shulman GL, Corbetta M. Resting inter-hemispheric fMRI connectivity predicts performance after stroke. *Ann Neurol* 67(3), 365−375, 2010.

Carter AR, Shulman GL, Corbetta M. Why use a connectivity-based approach to study stroke and recovery of function? *NeuroImage* 62(4), 2271−2280, 2012.

Casadio M, Giannoni P, Masia L, Morasso P, Sandini G, Sanguineti V, Squeri V, Vergaro E. A proof of concept study for the integration of robot therapy with physiotherapy in the treatment of stroke patients. *Clin Rehabil* 23(3), 217−228, 2009.

Cauraugh J, Light K, Kim S, Thigpen M, Behrman A. Chronic motor dysfunction after stroke: Recovering wrist and finger extension by electromyography-triggered neuromuscularsStimulation. *Stroke* 31(6), 1360−1364, 2000.

Cervera MA, Soekadar SR, Ushiba J, Millán J del R, Liu M, Birbaumer N, Garipelli G. Brain-computer interfaces for post-stroke motor rehabilitation: A meta-analysis. *Ann Clin Transl Neurol* 5(5), 651−663, 2018.

Chae J, Harley MY, Hisel TZ, Corrigan CM, Demchak JA, Wong Y-T, Fang Z-P. Intramuscular electrical stimulation for upper limb recovery in chronic hemiparesis: An exploratory randomized clinical trial. *Neurorehabil Neural Repair* 23(6), 569−578, 2009.

Chang C, Cunningham JP, Glover GH. Influence of heart rate on the BOLD signal: The cardiac response function. *NeuroImage* 44(3), 857−869, 2009.

Chang WH, Kim Y-H. Robot-assisted therapy in stroke rehabilitation. *J Stroke* 15(3), 174−181, 2013.

Chaudhary U, Birbaumer N, Ramos-Murguialday A. Brain-computer interfaces for communication and rehabilitation. *Nat Rev Neurol* 12(9), 513−525, 2016.

Chen R, Cohen LG, Hallett M. Nervous system reorganization following injury. *Neuroscience* 111(4), 761−773, 2002.

Cheyne D, Gaetz W, Garnero L, Lachaux J-P, Ducorps A, Schwartz D, Varela FJ. Neuromagnetic imaging of cortical oscillations accompanying tactile stimulation. *Cogn Brain Res* 17(3), 599−611, 2003.

Cicinelli P, Marconi B, Zaccagnini M, Pasqualetti P, Filippi MM, Rossini PM. Imagery-induced cortical excitability changes in stroke: A transcranial magnetic stimulation study. *Cereb Cortex* 16(2), 247−253, 2006.

Classen J, Liepert J, Wise SP, Hallett M, Cohen LG. Rapid plasticity of human cortical movement representation induced by practice. *J Neurophysiol* 79(2), 1117−1123, 1998.

Clausen J, Fetz E, Donoghue J, Ushiba J, Spörhase U, Chandler J, Birbaumer N, Soekadar SR. Help, hope, and hype: Ethical dimensions of neuroprosthetics. *Science* 356(6345), 1338−1339, 2017.

Cohen MX. Where does EEG come from and what does it mean? *Trends Neurosci* 40(4), 208−218, 2017.

Conway BA, Halliday DM, Farmer SF, Shahani U, Maas P, Weir AI, Rosenberg JR. Synchronization between motor cortex and spinal motoneuronal pool during the performance of a maintained motor task in man. *J Physiol* 489(3), 917−924, 1995.

Crone NE, Miglioretti DL, Gordon B, Sieracki JM, Wilson MT, Uematsu S, Lesser RP. Functional mapping of human sensorimotor cortex with electrocorticographic spectral analysis. I. Alpha and beta event-related desynchronization. *Brain* 121(12), 2271−2299, 1998.

Daly JJ, Cheng R, Rogers J, Litinas K, Hrovat K, Dohring M. Feasibility of a new application of noninvasive brain computer interface (BCI): A case study of training for recovery of volitional motor control after stroke. *J Neurol Phys Ther* 33(4), 203, 2009.

Daly JJ, Wolpaw JR. Brain-computer interfaces in neurological rehabilitation. *Lancet Neurol* 7(11), 1032−1043, 2008.

Damoiseaux JS, Rombouts S a. RB, Barkhof F, Scheltens P, Stam CJ, Smith SM, Beckmann CF. Consistent resting-state networks across healthy subjects. *Proc Natl Acad Sci* 103(37), 13848−13853, 2006.

Daw ND, O'Doherty JP, Dayan P, Seymour B, Dolan RJ. Cortical substrates for exploratory decisions in humans. *Nature* 441(7095), 876−879, 2006.

Dobkin BH. Strategies for stroke rehabilitation. *Lancet Neurol* 3(9), 528−536, 2004.

Dobkin BH, Plummer-D'Amato P, Elashoff R, Lee J, Group the S. International randomized clinical trial, stroke inpatient rehabilitation with reinforcement of walking speed (SIRROWS), improves outcomes. *Neurorehabil Neural Repair* 24(3), 235−242, 2010.

Dogil G, Ackermann H, Grodd W, Haider H, Kamp H, Mayer J, Riecker A, Wildgruber D. The speaking brain: A tutorial introduction to fMRI experiments in the production of speech, prosody and syntax. *J Neurolinguistics* 15(1), 59−90, 2002.

Drysdale AT, Grosenick L, Downar J, Dunlop K, Mansouri F, Meng Y, Fetcho RN, Zebley B, Oathes DJ, Etkin A, Schatzberg AF, Sudheimer K, Keller J, Mayberg HS, Gunning FM, Alexopoulos GS, Fox MD, Pascual-Leone A, Voss HU, Casey B, Dubin MJ, Liston C. Resting-state connectivity biomarkers define neurophysiological subtypes of depression. *Nat Med* 23(1), 28−38, 2017.

Dubovik S, Pignat J-M, Ptak R, Aboulafia T, Allet L, Gillabert N, Magnin C, Albert F, Momjian-Mayor I, Nahum L, Lascano AM, Michel CM, Schnider A, Guggisberg AG. The behavioral significance of coherent resting-state oscillations after stroke. *NeuroImage* 61(1), 249−257, 2012.

Dubovik S, Ptak R, Aboulafia T, Magnin C, cile, Gillabert N, Allet L, Pignat J-M, Schnider A, Guggisberg AG. EEG alpha band synchrony predicts cognitive and motor performance in patients with ischemic stroke. *Behav Neurol* 26(3), 187−189, 2013.

van Ede F, Lange F de, Jensen O, Maris E. Orienting attention to an upcoming tactile event involves a spatially and temporally specific modulation of sensorimotor alpha- and beta-band oscillations. *J Neurosci* 31(6), 2016−2024, 2011.

van Ede F, Szebényi S, Maris E. Attentional modulations of somatosensory alpha, beta and gamma oscillations dissociate between anticipation and stimulus processing. *NeuroImage* 97(15), 134−141, 2014.

Farzan F, Barr MS, Hoppenbrouwers SS, Fitzgerald PB, Chen R, Pascual-Leone A, Daskalakis ZJ. The EEG correlates of the TMS induced EMG silent period in humans. *NeuroImage* 83, 120−134, 2013.

Fox MD, Raichle ME. Spontaneous fluctuations in brain activity observed with functional magnetic resonance imaging. *Nat Rev Neurosci* 8(9), 700−711, 2007.

Fox MD, Snyder AZ, Vincent JL, Corbetta M, Essen DCV, Raichle ME. The human brain is intrinsically organized into dynamic, anticorrelated functional networks. *Proc Natl Acad Sci U S A* 102(27), 9673−9678, 2005.

Fritz SL, Butts RJ, Wolf SL. Constraint-induced movement therapy: From history to plasticity. *Expert Rev Neurother* 12(2), 191−198, 2012.

Gauthier LV, Taub E, Perkins C, Ortmann M, Mark VW, Uswatte G. Remodeling the brain plastic structural brain changes produced by different motor therapies after stroke. *Stroke* 39(5), 1520−1525, 2008.

Glover GH. Deconvolution of impulse response in event-related BOLD fMRI. *NeuroImage* 9(4), 416−429, 1999.

Goldman RI, Stern JM, Engel J, Cohen MS. Acquiring simultaneous EEG and functional MRI. *Clin Neurophysiol* 111(11), 1974−1980, 2000.

Goldman RI, Stern JM, Engel J, Cohen MS. Simultaneous EEG and fMRI of the alpha rhythm. *Neuroreport* 13(18), 2487−2492, 2002.

Grefkes C, Fink GR. Connectivity-based approaches in stroke and recovery of function. *Lancet Neurol* 13(2), 206−216, 2014.

Guillot A, Collet C, Nguyen VA, Malouin F, Richards C, Doyon J Brain activity during visual versus kinesthetic imagery: An fMRI study. *Hum Brain Mapp* 30(7), 2157−2172, 2009.

Hanakawa T, Dimyan MA, Hallett M. Motor planning, imagery, and execution in the distributed motor network: A time-course study with functional MRI. *Cereb Cortex* 18(12), 2775−2788, 2008.

Handwerker DA, Ollinger JM, D'Esposito M. Variation of BOLD hemodynamic responses across subjects and brain regions and their effects on statistical analyses. *NeuroImage* 21(4), 1639−1651, 2004.

Hari R, Salmelin R. Magnetoencephalography: From SQUIDs to neuroscience: Neuroimage 20th anniversary special edition. *NeuroImage* 61(2), 386−396, 2012.

Hasan MA, Fraser M, Conway BA, Allan DB, Vučković A. Reversed cortical over-activity during movement imagination following neurofeedback treatment for central neuropathic pain. *Clin Neurophysiol* 127(9), 3118−3127, 2016.

Heeger DJ, Ress D. What does fMRI tell us about neuronal activity? *Nat Rev Neurosci* 3(2), 142−151, 2002

Hermann DM, Chopp M. Promoting brain remodelling and plasticity for stroke recovery: Therapeutic promise and potential pitfalls of clinical translation. *Lancet Neurol* 11(4), 369−380, 2012.

Herrero M-T, Barcia C, Navarro J. Functional anatomy of thalamus and basal ganglia. *Child's Nerv Syst* 18(8), 386−404, 2002.

Hess G, Donoghue JP. Long-term potentiation of horizontal connections provides a mechanism to reorganize cortical motor maps. *J Neurophysiol* 71(6), 2543−2547, 1994.

Hesse S. Recovery of gait and other motor functions after stroke: Novel physical and pharmacological treatment strategies. *Restor Neurol Neurosci* 22, 3−5, 2004.

Hindriks R, van Putten MJAM. Thalamo-cortical mechanisms underlying changes in amplitude and frequency of human alpha oscillations. *NeuroImage* 70, 150−163, 2013.

Hirsch S, Reichold J, Schneider M, Székely G, Weber B. Topology and hemodynamics of the cortical cerebrovascular system. *J Cereb Blood Flow Metab* 32(6), 952−967, 2012.

Hjorth B. Principles for transformation of scalp EEG from potential field into source distribution. *J Clin Neurophysiol Off Publ Am Electroencephalogr Soc* 8(4), 391−396, 1991.

Hochberg LR, Bacher D, Jarosiewicz B, Masse NY, Simeral JD, Vogel J, Haddadin S, Liu J, Cash SS, van der Smagt P, Donoghue JP. Reach and grasp by people with tetraplegia using a neurally controlled robotic arm. *Nature* 485(7398), 372−375, 2012.

Honey CJ, Kötter R, Breakspear M, Sporns O. Network structure of cerebral cortex shapes functional connectivity on multiple time scales. *Proc Natl Acad Sci* 104(24), 10240−10245, 2007.

Huber R, Esser SK, Ferrarelli F, Massimini M, Peterson MJ, Tononi G. TMS-induced cortical potentiation during wakefulness locally increases slow wave activity during sleep. *PLoS ONE* 2(3), e276(7 pages), 2007.

Huber R, Ghilardi MF, Massimini M, Tononi G. Local sleep and learning. *Nature* 430(6995), 78−81, 2004.

Hummel F, Andres F, Altenmüller E, Dichgans J, Gerloff C Inhibitory control of acquired motor programmes in the human brain. *Brain* 125(2), 404−420, 2002.

Huster RJ, Debener S, Eichele T, Herrmann CS. Methods for simultaneous EEG-fMRI: An introductory review. *J Neurosci* 32(18), 6053−6060, 2012.

Ietswaart M, Johnston M, Dijkerman HC, Joice S, Scott CL, MacWalter RS, Hamilton SJC. Mental practice with motor imagery in stroke recovery: Randomized controlled trial of efficacy. *Brain* 134(5), 1373−1386, 2011.

IJzerman MJ, Renzenbrink GJ, Geurts AC. Neuromuscular stimulation after stroke: From technology to clinical deployment. *Expert Rev Neurother* 9(4), 541−552, 2009.

Jurcak V, Tsuzuki D, Dan I. 10/20, 10/10, and 10/5 systems revisited: Their validity as relative head-surface-based positioning systems. *NeuroImage* 34(4), 1600−1611, 2007.

Jurkiewicz MT, Gaetz WC, Bostan AC, Cheyne D. Post-movement beta rebound is generated in motor cortex: Evidence from neuromagnetic recordings. *NeuroImage* 32(3), 1281−1289, 2006.

Kaelin-Lang A, Luft AR, Sawaki L, Burstein AH, Sohn YH, Cohen LG. Modulation of human corticomotor excitability by somatosensory input. *J Physiol* 540(2), 623−633, 2002.

Kawakami M, Fujiwara T, Ushiba J, Nishimoto A, Abe K, Honaga K, Nishimura A, Mizuno K, Kodama M, Masakado Y, Liu M. A new therapeutic application of brain-machine interface (BMI) training followed by hybrid assistive neuromuscular dynamic stimulation (HANDS) therapy for patients with severe hemiparetic stroke: A proof of concept study. *Restor Neurol Neurosci* 34(5), 789−797, 2016.

Ketz NA, Jensen O, O'Reilly RC. Thalamic pathways underlying prefrontal cortex-medial temporal lobe oscillatory interactions. *Trends Neurosci* 38(1), 3−12, 2015.

Kimberley TJ, Lewis SM, Auerbach EJ, Dorsey LL, Lojovich JM, Carey JR. Electrical stimulation driving functional improvements and cortical changes in subjects with stroke. *Exp Brain Res* 154(4), 450−460, 2004.

Kirschstein T, Köhling R. What is the source of the EEG? *Clin EEG Neurosci* 40(3), 146−149, 2009.

Klimesch W, Sauseng P, Hanslmayr S. EEG alpha oscillations: The inhibition-timing hypothesis. *Brain Res Rev* 53(1), 63−88, 2007.

Knutson JS, Fu MJ, Sheffler LR, Chae J. Neuromuscular electrical stimulation for motor restoration in hemiplegia. *Phys Med Rehabil Clin N Am* 26(4), 729−745, 2015.

Kottink AI, Hermens HJ, Nene AV, Tenniglo MJ, van der Aa HE, Buschman HP, IJzerman MJ. A randomized controlled trial of an Implantable 2-channel peroneal nerve stimulator on walking speed and activity in poststroke hemiplegia. *Arch Phys Med Rehabil* 88(8), 971−978, 2007.

Kozelka JW, Pedley TA. Beta and mu rhythms. *J Clin Neurophysiol* 7(2), 191−208, 1990.

Krebs et al. Rehabilitation robotics: Pilot trial of a spatial extension for MIT-Manus. *J NeuroEngineering Rehabil* 1, 5(15 pages), 2004.

Krucoff MO, Rahimpour S, Slutzky MW, Edgerton VR, Turner DA. Enhancing nervous system recovery through neurobiologics, neural interface training, and neurorehabilitation. *Front Neurosci* 10, 584(23 pages), 2016.

Kuhlman WN. Functional topography of the human mu rhythm. *Electroencephalogr Clin Neurophysiol* 44(1), 83−93, 1978.

Kuhlman WN, Allison T. EEG feedback training in the treatment of epilepsy: Some questions and some answers. *Pavlov J Biol Sci* 12(2), 112−122, 1977.

Kwakkel G, Kollen BJ, Krebs HI. Effects of robot-assisted therapy on upper limb recovery after stroke: A systematic review. *Neurorehabil Neural Repair* 22(2), 111−121, 2008.

Kwakkel G, Veerbeek JM, van Wegen EEH, Wolf SL. Constraint-induced movement therapy after stroke. *Lancet Neurol* 14(2), 224−234, 2015.

Langhorne P, Coupar F, Pollock A. Motor recovery after stroke: A systematic review. *Lancet Neurol* 8(8), 741−754, 2009.

Laufs H, Krakow K, Sterzer P, Eger E, Beyerle A, Salek-Haddadi A, Kleinschmidt A. Electroencephalographic signatures of attentional and cognitive default modes in spontaneous brain activity fluctuations at rest. *Proc Natl Acad Sci* 100(19), 11053−11058, 2003.

Leeb R, Lee F, Keinrath C, Scherer R, Bischof H, Pfurtscheller G. Brain-computer communication: Motivation, aim, and impact of exploring a virtual apartment. *IEEE Trans Neural Syst Rehabil Eng* 15(4), 473−482, 2007.

Lehéricy S, Bardinet E, Tremblay L, Van de Moortele P-F, Pochon J-B, Dormont D, Kim D-S, Yelnik J, Ugurbil K. Motor control in basal ganglia circuits using fMRI and brain atlas approaches. *Cereb Cortex* 16(2), 149−161, 2006.

Leocani L, Toro C, Manganotti P, Zhuang P, Hallett M. Event-related coherence and event-related desynchronization/ synchronization in the 10 Hz and 20 Hz EEG during self-paced movements. *Electroencephalogr Clin Neurophysiol Potentials Sect* 104(3), 199−206, 1997.

Liepert J, Bauder H, Wolfgang HR, Miltner WH, Taub E, Weiller C. Treatment-induced cortical reorganization after stroke in humans. *Stroke* 31(6), 1210−1216, 2000.

Liepert J, Miltner WHR, Bauder H, Sommer M, Dettmers C, Taub E, Weiller C. Motor cortex plasticity during constraint-induced movement therapy in stroke patients. *Neurosci Lett* 250(1), 5−8, 1998.

Lindquist MA, Wager TD. Validity and power in hemodynamic response modeling: A comparison study and a new approach. *Hum Brain Mapp* 28(8), 764−784, 2007.

Linkenkaer-Hansen K, Nikulin VV, Palva S, Ilmoniemi RJ, Palva JM. Prestimulus oscillations enhance psychophysical performance in humans. *J Neurosci* 24(45), 10186−10190, 2004.

Little CE, Emery C, Black A, Scott SH, Meeuwisse W, Nettel-Aguirre A, Benson B, Dukelow S. Test-retest reliability of KINARM robot sensorimotor and cognitive assessment: In pediatric ice hockey players. *J NeuroEngineering Rehabil* 12, 78(18 pages), 2015.

Liu Z, de Zwart JA, Yao B, van Gelderen P, Kuo L-W, Duyn JH. Finding thalamic BOLD correlates to posterior alpha EEG. *NeuroImage* 63(3), 1060−1069, 2012.

Logothetis NK, Pauls J, Augath M, Trinath T, Oeltermann A. Neurophysiological investigation of the basis of the fMRI signal. *Nature* 412(6843), 150−157, 2001.

Logothetis NK, Wandell BA. Interpreting the BOLD signal. *Annu Rev Physiol* 66, 735−769, 2004.

Lopes da Silva F. Neural mechanisms underlying brain waves: From neural membranes to networks. *Electroencephalogr Clin Neurophysiol* 79(2), 81−93, 1991.

Maffiuletti NA. Physiological and methodological considerations for the use of neuromuscular electrical stimulation. *Eur J Appl Physiol* 110(2), 223−234, 2010.

Maffiuletti NA, Roig M, Karatzanos E, Nanas S. Neuromuscular electrical stimulation for preventing skeletal-muscle weakness and wasting in critically ill patients: A systematic review. *BMC Med* 11, 137(10 pages), 2013.

Mäki H, Ilmoniemi RJ. EEG oscillations and magnetically evoked motor potentials reflect motor system excitability in overlapping neuronal populations. *Clin Neurophysiol* 121(4), 492−501, 2010.

Malhotra S, Rosewilliam S, Hermens H, Roffe C, Jones P, Pandyan AD. A randomized controlled trial of surface neuromuscular electrical stimulation applied early after acute stroke: Effects on wrist pain, spasticity and contractures. *Clin Rehabil* 27(7), 579−590, 2013.

Malmivuo JA, Suihko VE. Effect of skull resistivity on the spatial resolutions of EEG and MEG. *IEEE Trans Biomed Eng* 51(7), 1276−1280, 2004.

Malouin F, Richards CL, Jackson PL, Dumas F, Doyon J. Brain activations during motor imagery of locomotor-related tasks: A PET study. *Hum Brain Mapp* 19(1), 47−62, 2003.

Markand ON. Alpha rhythms. *J Clin Neurophysiol* 7(2), 163−189, 1990.

Massimini M, Tononi G, Huber R. Slow waves, synaptic plasticity and information processing: Insights from transcranial magnetic stimulation and high-density EEG experiments. *Eur J Neurosci* 29(9), 1761−1770, 2009.

McFarland DJ, McCane LM, David SV, Wolpaw JR. Spatial filter selection for EEG-based communication. *Electroencephalogr Clin Neurophysiol* 103(3), 386−394, 1997.

McGregor HR, Gribble PL. Functional connectivity between somatosensory and motor brain areas predicts individual differences in motor learning by observing. *J Neurophysiol* 118(2), 1235−1243, 2017.

van Meer MPA, van der Marel K, Wang K, Otte WM, El Bouazati S, Roeling TAP, Viergever MA, Berkelbach van der Sprenkel JW, Dijkhuizen RM. Recovery of sensorimotor function after experimental stroke correlates with restoration of resting-state interhemispheric functional connectivity. *J Neurosci* 30(11), 3964−3972, 2010.

Meszlényi RJ, Hermann P, Buza K, Gál V, Vidnyánszky Z. Resting state fMRI functional connectivity analysis using dynamic time warping. *Front Neurosci* 11, 75(17 pages), 2017.

Morris SL, Dodd KJ, Morris ME. Outcomes of progressive resistance strength training following stroke: a systematic review. *Clin Rehabil* 18(1), 27−39, 2004.

Mukaino M, Ono T, Shindo K, Fujiwara T, Ota T, Kimura A, Liu M, Ushiba J. Efficacy of brain-computer interface-driven neuromuscular electrical stimulation for chronic paresis after stroke. *J Rehabil Med* 46(4), 378−382, 2014.

Munzert J, Lorey B, Zentgraf K. Cognitive motor processes: The role of motor imagery in the study of motor representations. *Brain Res Rev* 60(2), 306−326, 2009.

Neuper C, Wörtz M, Pfurtscheller G. ERD/ERS patterns reflecting sensorimotor activation and deactivation. *Prog Brain Res* 159, 211−222, 2006.

Niazy RK, Beckmann CF, Iannetti GD, Brady JM, Smith SM. Removal of FMRI environment artifacts from EEG data using optimal basis sets. *NeuroImage* 28(3), 720−737, 2005.

Nishimoto A, Kawakami M, Fujiwara T, Hiramoto M, Honaga K, Abe K, Mizuno K, Ushiba J, Liu M. Feasibility of task-specific brain-machine interface training for

upper-extremity paralysis in patients with chronic hemiparetic stroke. *J Rehabil Med* 50(1), 52−58, 2018.

Norouzi-Gheidari N, Archambault PS, Fung J. Effects of robot-assisted therapy on stroke rehabilitation in upper limbs: Systematic review and meta-analysis of the literature. *J Rehabil Res Dev* 49(4), 479, 2012.

Nudo RJ, Wise BM, SiFuentes F, Milliken GW. Neural Substrates for the effects of rehabilitative training on motor recovery after ischemic infarct. *Science* 272(5269), 1791−1794, 1996.

Ogawa S, Lee TM, Kay AR, Tank DW. Brain magnetic resonance imaging with contrast dependent on blood oxygenation. *Proc Natl Acad Sci U S A* 87(24), 9868−9872, 1990.

Omata K, Hanakawa T, Morimoto M, Honda M. Spontaneous slow fluctuation of EEG alpha rhythm reflects activity in deep-brain structures: A simultaneous EEG-fMRI study. *PLoS ONE* 8(6), e66869(12 pages), 2013.

Ono T, Shindo K, Kawashima K, Ota N, Ito M, Ota T, Mukaino M, Fujiwara T, Kimura A, Liu M, Ushiba J. Brain-computer interface with somatosensory feedback improves functional recovery from severe hemiplegia due to chronic stroke. *Front Neuroengineering* 7, 19(8 pages), 2014a.

Ono T, Tomita Y, Inose M, Ota T, Kimura A, Liu M, Ushiba J. Multimodal sensory feedback associated with motor attempts alters BOLD responses to paralyzed hand movement in chronic stroke patients. *Brain Topogr* 28(2), 340−351, 2014b.

Ostendorf CG, Wolf SL. Effect of forced use of the upper extremity of a hemiplegic patient on changes in function. A single-case design. *Phys Ther* 61(7), 1022−1028, 1981.

Page SJ, Harnish SM, Lamy M, Eliassen JC, Szaflarski JP. Affected arm use and cortical change in stroke patients exhibiting minimal hand movement. *Neurorehabil Neural Repair* 24(2), 195−203, 2010.

Page SJ, Levine P, Leonard AC. Modified constraint-induced therapy in acute stroke: A randomized controlled pilot study. *Neurorehabil Neural Repair* 19(1), 27−32, 2005.

Palmer LM, Schulz JM, Murphy SC, Ledergerber D, Murayama M, Larkum ME. The cellular basis of GABAB-mediated interhemispheric inhibition. *Science* 335(6071), 989−993, 2012.

Palva S, Palva JM. New vistas for α-frequency band oscillations. *Trends Neurosci* 30(4), 150−158, 2007.

Park C, Chang WH, Ohn SH, Kim ST, Bang OY, Pascual-Leone A, Kim Y-H. Longitudinal changes of resting-state functional connectivity during motor recovery after stroke. *Stroke* 42(5), 1357−1362, 2011.

Park S-W, Kim J-H, Yang Y-J. Mental practice for upper limb rehabilitation after stroke: A systematic review and meta-analysis. *Int J Rehabil Res* 41(3), 197, 2018.

Parkes LM, Bastiaansen MCM, Norris DG. Combining EEG and fMRI to investigate the post-movement beta rebound. *NeuroImage* 29(3), 685−696, 2006.

Peters J, Schaal S. Reinforcement learning of motor skills with policy gradients. *Neural Netw* 21(4), 682−697, 2008.

Pfurtscheller G. The cortical activation model (CAM). *Prog Brain Res* 159, 19−27, 2006.

Pfurtscheller G, Brunner C, Schlögl A, Lopes da Silva FH. Mu rhythm (de)synchronization and EEG single-trial classification of different motor imagery tasks. *NeuroImage* 31(1), 153−159, 2006.

Pfurtscheller G, Lopes da Silva FH. Event-related EEG/MEG synchronization and desynchronization: Basic principles. *Clin Neurophysiol* 110(11), 1842−1857, 1999.

Pfurtscheller G, Neuper C. Motor imagery activates primary sensorimotor area in humans. *Neurosci Lett* 239(2−3), 65−68, 1997.

Pfurtscheller G, Neuper C, Krausz G. Functional dissociation of lower and upper frequency mu rhythms in relation to voluntary limb movement. *Clin Neurophysiol* 111, 1873−1879, 2000.

Pfurtscheller G, Stancák Jr. A, Neuper C. Event-related synchronization (ERS) in the alpha band -- an electrophysiological correlate of cortical idling: A review. *Int J Psychophysiol* 24(1−2), 39−46, 1996a.

Pfurtscheller G, Stancák Jr. A, Neuper Ch. Post-movement beta synchronization. A correlate of an idling motor area? *Electroencephalogr Clin Neurophysiol* 98(4), 281−293, 1996b.

Pichiorri F, Morone G, Petti M, Toppi J, Pisotta I, Molinari M, Paolucci S, Inghilleri M, Astolfi L, Cincotti F, Mattia D. Brain-computer interface boosts motor imagery practice during stroke recovery. *Ann Neurol* 77(5), 851−865, 2015.

Power JD, Cohen AL, Nelson SM, Wig GS, Barnes KA, Church JA, Vogel AC, Laumann TO, Miezin FM, Schlaggar BL, Petersen SE. Functional network organization of the human brain. *Neuron* 72(4), 665−678, 2011.

Quattrocchi G, Greenwood R, Rothwell JC, Galea JM, Bestmann S. Reward and punishment enhance motor adaptation in stroke. *J Neurol Neurosurg Psychiatry* 88(9), 730−736, 2017.

Quattrocchi G, Greenwood R, Rothwell JC, Galea JM, Bestmann S. A single session of exercise increases connectivity in sensorimotor-related brain networks: A resting-state fMRI study in young healthy adults. *Front Hum Neurosci* 8, 625(9 pages), 2014.

Ramos-Murguialday A, Broetz D, Rea M, Läer L, Yilmaz Ö, Brasil FL, Liberati G, Curado MR, Garcia-Cossio E, Vyziotis A, Cho W, Agostini M, Soares E, Soekadar S, Caria A, Cohen LG, Birbaumer N. Brain-machine-interface in chronic stroke rehabilitation: A controlled study. *Ann Neurol* 74(1), 100−108, 2013.

Rangaswamy M, Porjesz B, Chorlian DB, Wang K, Jones KA, Bauer LO, Rohrbaugh J, O'Connor SJ, Kuperman S, Reich T, Begleiter H. Beta power in the EEG of alcoholics. *Biol Psychiatry* 52(8), 831−842, 2002.

Rangaswamy M, Porjesz B, Chorlian DB, Wang K, Jones KA, Kuperman S, Rohrbaugh J, O'Connor SJ, Bauer LO, Reich T, Begleiter H. Resting EEG in offspring of male alcoholics: Beta frequencies. *Int J Psychophysiol* 51(3), 239−251, 2004.

Rehme AK, Fink GR, Cramon DY von, Grefkes C. The role of the contralesional motor cortex for motor recovery in the early days after stroke assessed with longitudinal fMRI. *Cereb Cortex* 21(4), 756−768, 2011.

Ridding MC, Taylor JL. Mechanisms of motor-evoked potential facilitation following prolonged dual peripheral and central stimulation in humans. *J Physiol* 537(2), 623−631, 2001.

Rijntjes M, Hamzei F, Glauche V, Saur D, Weiller C. Activation changes in sensorimotor cortex during improvement due to CIMT in chronic stroke. *Restor Neurol Neurosci* 29(5), 299−310, 2011.

Ritter P, Moosmann M, Villringer A. Rolandic alpha and beta EEG rhythms' strengths are inversely related to fMRI-BOLD signal in primary somatosensory and motor cortex. *Hum Brain Mapp* 30(4), 1168−1187, 2009.

Ritter P, Villringer A. Simultaneous EEG-fMRI. *Neurosci Biobehav Rev* 30(6), 823−838, 2006.

Rodriguez E, George N, Lachaux J-P, Martinerie J, Renault B, Varela FJ. Perception's shadow: Long-distance synchronization of human brain activity. *Nature* 397(6718), 430−433, 1999.

Rushton DN. Functional electrical stimulation and rehabilitation--an hypothesis. *Med Eng Phys* 25(1), 75−78, 2003.

Salmelin R, Hámáaláinen M, Kajola M, Hari R. Functional segregation of movement-related rhythmic activity in the human brain. *NeuroImage* 2(4), 237−243, 1995.

Sanes JN, Wang J, Donoghue JP. Immediate and delayed changes of rat motor cortical output representation with new forelimb configurations. *Cereb Cortex* 2(2), 141−152, 1992.

Santucci E, Balconi M. The multicomponential nature of movement-related cortical potentials: Functional generators and psychological factors. *Neuropsychol Trends* 5(1), 59−84, 2009.

Sasai S, Homae F, Watanabe H, Taga G. Frequency-specific functional connectivity in the brain during resting state revealed by NIRS. *Neuroimage* 56(1), 252−257, 2011.

Sauseng P, Gerloff C, Hummel FC. Two brakes are better than one: The neural bases of inhibitory control of motor memory traces. *NeuroImage* 65, 52−58, 2013.

Schultz W. Predictive reward signal of dopamine neurons. *J Neurophysiol* 80(1), 1−27, 1998.

Scott SH. Apparatus for measuring and perturbing shoulder and elbow joint positions and torques during reaching. *J Neurosci Methods* 89(2), 119−127, 1999.

Sharma N, Pomeroy VM, Baron J-C. Motor imagery: A backdoor to the motor system after stroke? *Stroke* 37(7), 1941−1952, 2006.

Sheffler LR, Chae J. Neuromuscular electrical stimulation in neurorehabilitation. *Muscle Nerve* 35(5), 562−590, 2007.

Shindo K, Kawashima K, Ushiba J, Ota N, Ito M, Ota T, Kimura A, Liu M. Effects of neurofeedback training with an electroencephalogram-based brain-computer interface for hand paralysis in patients with chronic stroke: A preliminary case series study. *J Rehabil Med* 43(10), 951−957, 2011.

Sigala R, Haufe S, Roy D, Dinse HR, Ritter P. The role of alpha-rhythm states in perceptual learning: Insights from experiments and computational models. *Front Comput Neurosci* 8, 36(19 pages), 2014.

Simkin DR, Thatcher RW, Lubar J. Quantitative EEG and neurofeedback in children and adolescents: anxiety disorders, depressive disorders, comorbid addiction and attention-

deficit/hyperactivity disorder, and brain injury. *Child Adolesc Psychiatr Clin N Am*, 23(3), 427−464, 2014.

Sitaram R, Ros T, Stoeckel L, Haller S, Scharnowski F, Lewis-Peacock J, Weiskopf N, Blefari ML, Rana M, Oblak E, Birbaumer N, Sulzer J. Closed-loop brain training: The science of neurofeedback. *Nat Rev Neurosci* 18(2), 86−100, 2017.

Soekadar SR, Birbaumer N, Slutzky MW, Cohen LG. Brain-machine interfaces in neurorehabilitation of stroke. *Neurobiol Dis* 83, 172−179, 2015.

Sporns O. Structure and function of complex brain networks. *Dialogues Clin Neurosci* 15(3), 247−262, 2013.

Srivastava G, Crottaz-Herbette S, Lau KM, Glover GH, Menon V. ICA-based procedures for removing ballistocardiogram artifacts from EEG data acquired in the MRI scanner. *NeuroImage* 24(1), 50−60, 2005.

Stefan K, Kunesch E, Cohen LG, Benecke R, Classen J. Induction of plasticity in the human motor cortex by paired associative stimulation. *Brain* 123(3), 572−584, 2000.

Sun FT, Miller LM, D'Esposito M. Measuring interregional functional connectivity using coherence and partial coherence analyses of fMRI data. *NeuroImage* 21(2), 647−658, 2004.

Takeda K, Tanino G, Miyasaka H. Review of devices used in neuromuscular electrical stimulation for stroke rehabilitation. *Med Devices (Auckl)* 10, 207−213, 2017.

Takemi M, Masakado Y, Liu M, Ushiba J. Event-related desynchronization reflects downregulation of intracortical inhibition in human primary motor cortex. *J Neurophysiol* 110(5), 1158−1166, 2013.

Takemi M, Masakado Y, Liu M, Ushiba J. Sensorimotor event-related desynchronization represents the excitability of human spinal motoneurons. *Neuroscience* 297, 58−67, 2015.

Taub E, Uswatte G, Mark VW, Morris DMM. The learned nonuse phenomenon: Implications for rehabilitation. *Eur Medicophysica* 42(3), 241−256, 2006.

Taub E, Uswatte G, Pidikiti R. Constraint-induced movement therapy: A new family of techniques with broad application to physical rehabilitation--a clinical review. *J Rehabil Res Dev* 36(3), 237−251, 1999.

Teo W-P, Chew E. Is motor-imagery brain-computer interface feasible in stroke rehabilitation? *PM R* 6(8), 723−728, 2014.

Turrigiano GG, Nelson SB. Homeostatic plasticity in the developing nervous system. *Nat Rev Neurosci* 5(2), 97−107, 2004.

Tzagarakis C, West S, Pellizzer G. Brain oscillatory activity during motor preparation: Effect of directional uncertainty on beta, but not alpha, frequency band. *Front Neurosci* 9, 246(13 pages), 2015.

Tzourio-Mazoyer N, Landeau B, Papathanassiou D, Crivello F, Etard O, Delcroix N, Mazoyer B, Joliot M. Automated anatomical labeling of activations in SPM using a macroscopic anatomical parcellation of the MNI MRI single-subject brain. *Neuroimage* 15(1), 273−289, 2002.

Uehara T, Yamasaki T, Okamoto T, Koike T, Kan S, Miyauchi S, Kira J, Tobimatsu S. Efficiency of a "small-world" brain network depends on consciousness level: A resting-state fMRI study. *Cereb Cortex*, 24(6), 1529−1539, 2014.

Ushiba J, Soekadar SR. Brain-machine interfaces for rehabilitation of poststroke hemiplegia. *Prog Brain Res* 228, 163−183, 2016.

Uswatte G, Taub E. Implications of the learned nonuse formulation for measuring rehabilitation outcomes: Lessons from constraint-induced movement therapy. *Rehabil Psychol* 50(1), 34−42, 2005.

Vahdat S, Darainy M, Milner TE, Ostry DJ. Functionally specific changes in resting-state sensorimotor networks following motor learning. *J Neurosci* 31(47), 16907−16915, 2011.

Viswanathan A, Freeman RD. Neurometabolic coupling in cerebral cortex reflects synaptic more than spiking activity. *Nat Neurosci* 10(10), 1308−1312, 2007.

Volz LJ, Sarfeld A-S, Diekhoff S, Rehme AK, Pool E-M, Eickhoff SB, Fink GR, Grefkes C. Motor cortex excitability and connectivity in chronic stroke: A multimodal model of functional reorganization. *Brain Struct Funct* 220(2), 1093−1107, 2015.

Vukelić M, Bauer R, Naros G, Naros I, Braun C, Gharabaghi A. Lateralized alpha-band cortical networks regulate volitional modulation of beta-band sensorimotor oscillations. *NeuroImage* 87, 147−153, 2014.

Wang L, Yu C, Chen H, Qin W, He Y, Fan F, Zhang Y, Wang M, Li K, Zang Y, Woodward TS, Zhu C. Dynamic functional reorganization of the motor execution network after stroke. *Brain* 133(4), 1224−1238, 2010.

Westlake KP, Nagarajan SS. Functional connectivity in relation to motor performance and recovery after stroke. *Front Syst Neurosci* 5, 8(12 pages), 2011.

Wolpaw JR, Birbaumer N, McFarland DJ, Pfurtscheller G, Vaughan TM. Brain-computer interfaces for communication and control. *Clin Neurophysiol* 113(6), 767−791, 2002.

Woo C-W, Krishnan A, Wager TD. Cluster-extent based thresholding in fMRI analyses: Pitfalls and recommendations. *NeuroImage* 91, 412−419, 2014.

Worsley KJ, Evans AC, Marrett S, Neelin P. A three-dimensional statistical analysis for CBF activation studies in human brain. *J Cereb Blood Flow Metab* 12(6), 900−918, 1992.

Wu C, Lin K, Chen H, Chen I, Hong W. Effects of modified constraint-induced movement therapy on movement kinematics and daily function in patients with stroke: A kinematic study of motor control mechanisms. *Neurorehabil Neural Repair* 21(5), 460−466, 2007.

Wu G-R, Marinazzo D. Sensitivity of the resting-state haemodynamic response function estimation to autonomic nervous system fluctuations. *Philos Trans A Math Phys Eng Sci* 274(2067), 20150190(16pages), 2016.

Yin HH, Knowlton BJ. The role of the basal ganglia in habit formation. *Nat Rev Neurosci* 7(6), 464−476, 2006.

Yin S, Liu Y, Ding M. Amplitude of sensorimotor mu rhythm Is correlated with BOLD from multiple brain regions: A simultaneous EEG-fMRI study. *Front Hum Neurosci* 10, 364(12 pages), 2016.

Yokoi A, Arbuckle SA, Diedrichsen J. The role of human primary motor cortex in the production of skilled finger sequences. *J Neurosci* 38(6), 1430−1442, 2018.

Young BM, Nigogosyan Z, Walton LM, Remsik A, Song J, Nair VA, Tyler ME, Edwards DF, Caldera K, Sattin JA, Williams JC, Prabhakaran V. Dose-response relationships using brain-computer interface technology impact stroke rehabilitation. *Front Hum Neurosci* 9, 2015.

Young BM, Nigogosyan Z, Walton LM, Song J, Nair VA, Grogan SW, Tyler ME, Edwards DF, Caldera K, Sattin JA, Williams JC, Prabhakaran V. Changes in functional brain organization and behavioral correlations after rehabilitative therapy using a brain-computer interface. *Front Neuroengineering* 7, 26(15 pages), 2014.

Young KD, Siegle GJ, Misaki M, Zotev V, Phillips R, Drevets WC, Bodurka J. Altered task-based and resting-state amygdala functional connectivity following real-time fMRI amygdala neurofeedback training in major depressive disorder. *NeuroImage Clin* 17, 691−703, 2017.

Yuan H, Liu T, Szarkowski R, Rios C, Ashe J, He B. Negative covariation between task-related responses in alpha/beta-band activity and BOLD in human sensorimotor cortex: An EEG and fMRI study of motor imagery and movements. *NeuroImage* 49(3), 2596−2606, 2010.

Zhang R, Xu P, Chen R, Li F, Guo L, Li P, Zhang T, Yao D. Predicting inter-session performance of SMR-based brain-computer interface using the spectral entropy of resting-state EEG. *Brain Topogr* 28(5), 680−690, 2015.

Zhang Y, Ding M. Detection of a weak somatosensory stimulus: Role of the prestimulus mu rhythm and its top-down modulation. *J Cogn Neurosci* 22(2), 307−322, 2009.

Zimmermann-Schlatter A, Schuster C, Puhan MA, Siekierka E, Steurer J. Efficacy of motor imagery in post-stroke rehabilitation: A systematic review. *J NeuroEngineering Rehabil* 5, 8(10 pages), 2008.